Title
miR290-5p and miR292-5p Activate the Immunoglobulin kappa Locus

Author
Garcia, Patty Bertha

Publication Date
2012

Peer reviewed|Thesis/dissertation

miR290-5p and miR292-5p Activate the Immunoglobulin *kappa* Locus

By

Patty Bertha Garcia

A dissertation submitted in partial satisfaction of the

Requirements for the degree of

Doctor of Philosophy

In Molecular and Cell Biology

in the

Graduate Division

of the

University of California, Berkeley

Committee in charge:

Professor Mark S. Schlissel, Chair
Professor Lin He
Professor G. Steven Martin
Professor Daniela Kaufer

Spring 2012

Abstract

miR290-5p and miR292-5p Activate the Immunoglobulin *kappa* Locus

by

Patty Bertha Garcia

Doctor of Philosophy in Molecular and Cell Biology

University of California, Berkeley

Professor Mark S. Schlissel, Chair

Regulated expression of miRNAs influences development in a wide variety of contexts. We report here that miR290-5p and miR292-5p are induced at the pre-B stage of murine B cell development and that they influence assembly of the Igκ light chain gene by contributing to the activation of germline Igκ transcription (κGT). We found that upon forced over-expression of miR290-5p/292-5p in Abelson Murine Leukemia Virus (AMuLV) transformed pro-B cells two known activators of κGT, E2A and NF-κB, show increased DNA binding activity. E2A shows increased binding specific to the *kappa* intronic enhancer *in vivo*. Conversely, knockdown of miR290-5p/292-5p in AMuLV pro-B cells blunted drug-induced activation of κGT. Furthermore, miR290-5p/292-5p knockdown also blunted κGT activation, but not Rag1/2 expression, in an IL-7 dependent primary pro-B cell culture system. In addition, we identified a deficiency in κGT induction in miR290 cluster knockout mice. We hypothesize that increased expression of miR290-5p and miR292-5p contributes to the induction of κGT at the pre-B stage of B cell development through increased DNA binding activity of NF-κB and E2A and to *kappa* locus regulatory sequences. To identify the pathway(s) through which miR290-5p/292-5p are acting, we observed that inhibitors of both NF-κB and E2A, IκBα and Id2 respectively are indirectly regulated. In attempts to identify the direct targets of miR290-5p/292-5p we found that Pim1 and Blimp1 may be direct targets. In addition, miR290-5p/292-5p regulation of Blimp1 differs in a cell-context dependent manner. In conclusion, we report here that miR290-5p and miR292-5p play a role in regulating B cell developmental pathways at the pre-B stage.

I dedicate this work to my parents, Carlos and Adelina Garcia. Their hard work and struggles inspire me to be the best I can be. I also dedicate this work to my brother Carlos S. Garcia, and my niece Maliah Garcia for being my motivation to keep going every day.

Table of Contents

List of Figures and Tables

Acknowledgements

I would first like to acknowledge Mark Schlissel for being a wonderful and patient mentor to me over the years, and for giving me the best graduate training I could have asked for. I also want to acknowledge Angel Islas for continuing to be a mentor to me in science and in life. I want to thank Tracy Kuo, Jamie Geier Bates, and Emily Cadera for teaching me a lot about science and for pushing me to have a thicker skin. A special thanks to Kwan Chow for being my lab buddy from beginning to end, and for being a true friend outside of lab. I want to especially acknowledge the SACNAS community at Berkeley including Jose Estrada and Galo Garcia for keeping me grounded. Last but definitely not least, I want to thank my Marias, Tokuyama and Mouchess, for making graduate school unforgettable. Your friendship was crucial on a day-to-day basis and helped me push through.

Chapter 1: Introduction
An Introduction to miRNAs, B Cell Development and miRNAs in Lymphocyte Development.

microRNAs (miRNAs)

microRNAs (miRNAs) are small non-coding RNAs, usually 20-25 nucleotides in length (He et al., 2004; Filipowicz et al., 2008). miRNAs post-transcriptionally regulate their target transcripts, thereby regulating various biological processes, including in development and oncogenesis.

miRNAs have widely been reported to affect these various pathways by postranscriptionally inhibiting their mRNA target by directly interacting with the 3'UTR. Because of the rapid processing of effector miRNAs, it makes sense that these small RNAs are actively involved in various biological processes that may require swift signaling changes, such as in developmental processes. For this reason, the original hypothesis of my thesis examined the involvement of miRNAs in B cell development.

miRNA Processing

miRNAs are gene products, transcribed most often from their own promoters (He et al 2004). Some miRNAs are generated as splice products of spliced gene transcripts, and are known as miRtrons. miRtrons are under the transcriptional and control of the host gene from which they derive (He et al. 2004). A miRNA, as it is transcribed in the nucleus, folds onto itself to form a hairpin loop called pri-miRNA (Fig. 1.1). These pri-miRNAs are initially processed into smaller hairpin loops, pre-miRNAs, by an enzyme found in the nucleus, Drosha. This protein is a member of the RNAse III family of proteins. These proteins process double-stranded RNA to leave a 5' overhang with a phosphate group and a 3' end with 2-nucleotide overhang and a hydroxyl group (Czech et al. 2011). Pre-miRNAs are exported into the cytoplasm by Exportin for further processing by another RNAse III protein, Dicer (Fig. 1.1). Dicer nicks open the hairpin loop generating a miRNA:miRNA* duplex from which one miRNA strand is then selected by Dicer to become the mature miRNA and is stabilized. The other strand that is not stabilized, miRNA*, is known as the passenger strand and is degraded and not used in further steps. The mature miRNA, known as the guide strand is taken up by an Argonaute protein, a critical component of the RISC complex (RNA Induced Silencing Complex) (Fig. 1.1). The mature miRNA then guides the RISC complex to bind the 3'UTR of the target transcript, as described above, to confer post-transcriptional regulation of the target mRNA (Fig. 1.1).

Post-transcriptional Regulation by miRNAs

As mentioned above, miRNAs postranscriptionally regulate their mRNA transcript target by directly interacting with the 3'UTR (Fig. 1.1). Generally, this posttranscriptional regulation happens in the form of inhibition (Filipowicz et al. 2008). The direct

interactions to target a 3'UTR occur through homologous binding of the miRNA seed regions with binding sites found in the 3'UTR of the target (Fig. 1.1). Generally, the miRNAs and their binding sites are evolutionarily conserved across species. The main seed sequence in the miRNAs is found between the 2^{nd}-8^{th} nucleotide of the small RNA (Filipowicz et al. 2008). Once there is interaction of the miRNA with the target mRNA, the expression of the target mRNA is inhibited by either translational inhibition or degradation of the transcript mRNA.

As described above, the RISC complex is the effector complex that guides miRNA-mRNA posttranscriptional regulation. The RISC complex is composed of the mature miRNA, an Argonaute protein, and other additional supporting proteins. Mammals have four Argonaute proteins while *Drosophila* has 2 Argonaute proteins, and *C. elegans* has as many as 27 Argonaute genes (Yigit et al. 2006). Argonaute2 is considered to be the *Slicer* Argonaute protein that is used in siRNA effector pathways. The siRNA pathway differs in that it requires small RNA-target interaction with perfect homology and the target transcript is then degraded. Argonaute2 contains an RNaseH-like PIWI domain that other Argonaute proteins do not, allowing it to degrade the target (Filipowicz et al. 2008).

There is also evidence that Argonaute1 may play a role in degradation of target transcripts by deadenylation. This is possible by Argonaute association with GW182, a regulatory miRNP. GW182 is believed to associate or recruit CCR4-NOT for the deadenylation action. Upon depletion of CCR4-NOT, GW182's deadenylation activity is ablated (Filipowicz et al. 2008).

Argonaute proteins may also inhibit their targets translationally. The Argonaute-associated proteins in the RISC complex may dictate the mode of repression of the target (He et al. 2004; Filipowicz et al. 2008). One model states that Argonaute can associate with the m7G cap of the mRNA. This interaction blocks eIF4e of the translation initiation complex, from binding the m7G cap, thereby blocking initiation (Filipowicz et al. 2008). The RISC complex then helps guide the targeted transcript to P-bodies for degradation. Another model posits the RISC complex causes 'ribosome drop-off.' In this model, translation of the target transcript is slowed down or stopped all together by the RISC complex.

Inhibition by miRNAs is not the only proposed mode of target transcript regulation. Recent evidence supports that miRNAs posttranscriptionally activate gene expression of the target mRNA, in some uncommon cases. Posttranscriptional activation has been observed under certain cell-cycle conditions (Mortensen et al. 2011; Vasudevan et al. 2007). Cells that are quiescent, G0 or G0-like states, seem to upregulate expression of their seed-matched target transcripts by a 3'UTR-binding, sequence-specific mechanism, similar to the one described above that is involved in miRNA mediated inhibition.

The mechanism by which posttranscriptional activation is selected over posttranscriptional repression is not completely understood. As in posttranscriptional

repression, it is thought that the Argonaute proteins may associate with different regulatory proteins in the posttranscriptional activation mechanism. In one model, there is evidence that the Argonaute protein recruits an alternative modulating protein, Fragile X Mental Retardation Gene 1 (FXR1) (Vasudevan et al. 2007). FXR1 has been shown to be involved in activating translation of mRNA transcripts. The association of Argonaute to FXR1 is thought to happen only under cell-cycle conditions similar to a G0-like state as described above, causing miRNA regulated activation of the target.

Regardless of the post-transcriptional regulation mechanism that miRNAs may use, this thesis is motivated by the hypothesis that miRNAs may regulate the critical transition of pro-B to pre-B stage in B cell development.

B-Cell Development

A critical component of the adaptive immune response is antibody-generating B cells (Cooper et al. 2006). Antibodies, also known as immunoglobulins exist in two forms, either secreted or membrane associated. The latter form is also known as the B-cell receptor (BCR). Immunoglobulins contain both a heavy chain and a light chain. The genes encoding immunoglobulins are generated through a highly intricate and regulated process, V(D)J Recombination (Schatz et al. 2011), that occurs as B cells develop.

B cell development occurs in the bone marrow of mice and humans. There they develop from hematopoietic stem cells (HSCs) (Fig. 1.2). HSCs through different signals and cues, also generate other cell types of the immune system including T cells, NK Cells, macrophages, etc(Hardy et al. 2007; Nutt et al. 2007). HSCs must differentiate to common lymphoid progenitors to generate B and T cells. At this stage, RAG1/2 expression is activated and B cells become responsive to IL-7 through expression of the IL-7 receptor (Hardy et al. 2007; Johnson et al. 2008). At this stage, the cells are committed to the B cell lineage in what is known as the early-pro-B stage (Fig. 1.2). Here the cells express the surface protein B220, or CD45R, which is often used as a marker of B cells in mice (Hardy et al. 2007; Geier et al. 2006).

Cells committed to the B cell lineage commence V(D)J Recombination to generate the genes encoding a BCR (Schatz et al. 2011)(Fig. 1.2). Expression of the Rag proteins helps catalyze V(D)J recombination, generating the heavy chain gene encoding part of the eventual immunoglobulin (Nutt et al. 2007). Although the heavy chain has two alleles, only one allele is rearranged at a time, in a process called allelic exclusion. A productive rearrangement at one allele must occur to generate a functional immunoglobulin heavy chain, μHC, that signals to the cell to refrain rearrangement at the second allele. If the first allele does not generate a productive rearrangement, the second allele is then recombined. If neither allele generates a functional μHC, then the cell dies. Once a functional μHC is generated, at the pro-B (B220+CD43+IgM-) stage (Fig. 1.2), it pairs with a surrogate light chain to form a pre-BCR. The pre-BCR signals the cell to go through a proliferative burst, clonally expand, and continue to the pre-B (B220+CD43-IgM-) stage in B cell development (Hardy et al. 2007). At the pre-B stage the cell

commences V(D)J recombination at the light chain loci, *kappa* and *lambda* (Geier et al. 2006) (Fig. 1.2). V(D)J recombination of the light chain loci is also allelically excluded. V(D)J recombination at the light chain loci first exhausts both copies of the *kappa* locus in search of a successful rearrangement. If neither *kappa* locus allele results in a successful rearrangement, rearrangement proceeds at the *lambda* locus (Geier et al. 2006). Once a successful light chain is paired to the heavy chain, the immature B cell (B220+CD43-IgM+) is then ready to encounter antigen.

Activating the *kappa* Locus for Rearrangement

A hallmark of B cell development at the pre-B stage is activation of the light chain locus for rearrangement. Concomitant Pre-BCR signaling and attenuation of IL-7 signaling are known to activate the light chain loci (Johnson et al. 2008; Ochiai et al. 2012). Repressive cues are lost and positive cues gained, from these two signaling pathways, in order for light chain rearrangement to occur. The two regions of the immunoglobulin *kappa* locus that receive these cues and that are essential for *kappa* locus activation are the *kappa* intronic enhancer (Eκi) and the 3' *kappa* enhancer (3'Eκ) (Geier et al. 2006) (Fig. 1.3).

One indication that the light chain locus is ready for rearrangement is the expression of *kappa* germline transcripts (κGT) (Schlissel et al. 1989; Schlissel et al. 1994). The Accessibility Hypothesis posits that the expression of germline transcripts is an indication that the locus is in an open confirmation poised for recombination to occur. This occurs when both Eκi and 3'Eκ are bound by activating transcription factors and activate the light chain locus for rearrangement.

Eκi is located in DNA encoding intronic sequences between the variable domain exon and the constant domain exon (Fig. 1.3). Eκi accessibility is repressed by the transcription factor Stat5 (Fig. 1.4). Stat5 directly represses Eκi by sterically inhibiting binding of positive transcription factors to the locus. Stat5 also recruits repressive marks to the locus upon continued IL-7 signaling (Mandal et al. 2011; Johnson et al. 2008). When the IL-7 signal is attenuated, the locus acquires activating marks and the transcription factor E2A binds Eκi (Fig. 1.4). Eκi is positively regulated by both E2A and NFkB (Geier et al. 2006; Shaffer et al. 1997).

3'Eκ is located 3' of the Constant Region Exon (Fig. 1.3). 3'Eκ is positively regulated through pre-BCR signaling as well (Fig. 1.4). The positive signaling cascade, described below, that emanates from pre-BCR signaling induces the transcription factor IRF4 to directly bind 3'Eκ (Fig. 1.4). It is regulated by E2A, IRF4, PAX5, PU.1, and SPIB (Shaffer et al. 1997; Geier et al. 2006). These factors at 3'Eκ, along with E2A and NFkB on Eκi, all coordinately act on the enhancers of the *kappa* light chain locus to activate transcription, eventually leading to recombination of the locus by the Rag proteins (Geier et al. 2006).

Pre-BCR and IL-7 Receptor Signaling

Activation of the *kappa* locus for rearrangement at the pro-B to pre-B transition is guided by a delicate interplay between preBCR and the IL7 receptor signaling (Johnson et al. 2008; Ochiai et al. 2012) (Fig. 1.4). Pre-BCR signaling is believed to initiate immunoglobulin light chain rearrangement.

Pre-BCR signaling occurs at the pro-B to pre-B transition, upon confirmation that an in-frame rearrangement has occurred at the heavy chain locus and a functional heavy chain protein is made (Geier et al. 2006; Schlissel et al. 1994). The rearranged heavy chain locus product, μHC, is paired with a surrogate light chain composed of VpreB and λ5. The paired μHC-surrogate light chain is tested for expression on the surface of the cell as a pre-BCR along with the transmembrane proteins Igα and Igβ. If a functional pre-BCR has been generated, it signals the cells to refrain from rearranging the heavy chain locus any further and the cell continues development to the next stage, the pre-B cell stage. The pro-B to pre-B transition is a critical checkpoint in B cell development and the cells must have a functional pre-BCR before continuing (Geier et al. 2006).

The pro-B to pre-B checkpoint is successfully passed when the pre-BCR signals, causing a cascade of events downstream. In this process, members of the Syk and Src family kinases along with the adapter protein BLNK, dock at the transmembrane proteins, Igα and Igβ (Geier et al. 2006). Phosphorylation of these kinases causes calcium to flux downstream of this signal. The MAP kinase pathway is activated leading the cell to go through a proliferative burst producing numerous cells of clonal origin. Through this process, a clone of cells is generated that all share the same functional pre-BCR before each cell progresses to the pre-B cell stage (Schatz et al. 2011). This clonal expansion allows a proven functional heavy chain protein many opportunities to pair with a successful light chain rearrangement product. Each cell in the clone goes through the next round of rearrangement of the light chain locus, amplifying immunoglobulin diversity.

V(D)J recombination at the light chain locus occurs at the pre-B stage (Fig. 1.2). Once a successful light chain has been produced, it is paired with the heavy chain product to generate the surface immunoglobulin of the B cell (Schatz et al. 2011; Schlissel et al. 1994). The surface immunoglobulin, because of the nature of the rearrangement process, has a high range of diversity of antigen-specificty. Therefore, some surface immunoglobulins can recognize self-antigen and be autoreactive. The self-reactive immature B cell can be rescued by further performing gene rearrangements, through a process called receptor editing (Fig. 1.2). Successive rearrangements continue at the light-chain loci until the rearrangement product is no longer autoreactive. If the cells exhaust rearrangement opportunities and those rearrangements remain self-reactive, then the self-reactive cell apoptoses.

The IL-7 signaling pathway is the counterpart to the pre-BCR involved in regulating light chain rearrangement (Johnson et al. 2008; Ochiai et al. 2012). The IL-7 cytokine

emanates from the bone marrow niche to regulate IL-7 receptor positive developing pro-B cells. IL-7 signals, together with pre-BCR signals, promote continued cell-cycling of pro-B cells, repression of Rag1/2 signaling and maintain Stat5, an inhibitor, bound to Eκi (Mandal et al. 2011) (Fig. 1.4).

Attenuation of the IL-7 signal occurs, possibly because the developing cell migrates away from its source or downmuodulates the IL-7 receptor. This halts the cell-cycling cue, arresting the cells, and the cells proceed to the pre-B cell stage (Johnson et al. 2008). Attenuation of the IL-7 signal relieves repression of the Rag proteins. The Rag proteins then target the light chain loci for recombination. Through binding of positive transcription factors, such as E2A, and loss of negative transcription factors, such as Stat5 (Fig. 1.4), the immunoglobulin *kappa* locus is activated and an open chromatin confirmation is marked by *kappa* germline transcripts (Johnson et al. 2008; Geier et al. 2006).

miRNAs in B Cell Development

miRNAs regulate various biological processes including the development of different tissues (Carrington et al. 2003). During the course of my thesis work, several groups published works that show roles for miRNAs in B cell development as well, particularly the pro-B to pre-B transition (Ventura et al. 2008; Xiao et al. 2007; Koralov et al. 2008). High-throughput sequencing in the forms of miRNA-Seq and mRNA-Seq during lymphopoiesis has highlighted the fluidity of miRNA expression during B cell development (Kuchen et al. 2010). It has also allowed more knowledge as to the expression and possible roles of hundreds of individual miRNAs and miRNA families at different stages of B cell development.

There are hundreds of miRNAs with changing expression patterns during B cell development; most of them have yet to be explored for important roles in regulating B cell development pathways. However, a few miRNAs that robustly regulate several target transcripts have been described in B cell development. A few miRNAs important for the pro-B to pre-B transition include the miR17-92 family, and individual miRNAs such as miR150, miR155, miR142-3p, among others (He et al. 2004; He et al. 2005; Xiao et al. 2007; Ventura et al. 2008). Among the miRNAs not yet described in the literature, it is believed that many of them are more modulatory, causing modest effects in their target regulation. These modulatory miRNAs do not cause such robust effects as the ones described above.

The first publication to describe the potential role of the miRNA machinery in developing B cells was *Koralov et al* (Koralov et al. 2008). They examined the miRNA signature in Dicer deficient and sufficient pro-B cells. Mice that were Dicer deficient had a block in B cell development at the pro-B cell stage. They were able to identify several target transcripts that were upregulated in the absence of Dicer that had the miR17-92 seed sequence signature in the 3'UTR. Bcl2, Bim, and PTEN were all found to be targets of

miR17-92 in this system. This seminal publication supports our original hypothesis that miRNAs regulate stages of B cell development.

Abelson Transformed Pro-B Cells

The Abelson Murine Leukemia Virus (AMuLV)-transformed pro-B cell serves as a model system for studying the pro-B to pre-B cell transition of B cell development. AMuLV transformation immortalizes developing B cells at the pro-B to large pre-B stages of B cell development (Chen et al. 1994; Klug et al. 1994). The immortalized cells are blocked in differentiation and receive survival signals from constitutive v-Abl kinase activity, independent of IL7 cytokine signals (Muljo et al. 2003). Studies by our lab and others have shown that inactivation of the constitutive Abl kinase activity, by STI571 (also known as Gleevec), in AMuLV cell lines results in G1 cell cycle arrest, progression to a pre-B-like stage, and eventual apoptosis (Muljo et al. 2003). The transcripts induced upon STI571 treatment include pre-B stage-specific genes such as SpiB, IRF4, Rag1/2, and κGT, confirming that Abl kinase activity blocks B cell differentiation. This system is therefore frequently used as a model system for in-vitro studies of the pro-B to pre-B transition.

Purpose

As described briefly above, our lab is interested in identifying and characterizing the mechanisms and pathways that govern the pro-B to pre-B stage transition in B cell development. I hypothesized that the small non-coding RNAs, miRNAs, may be involved in regulating pathways in this transition. In order to identify potential miRNA candidates I used the Abelson (AMuLV) transformed pro-B cell as a model system to screen for miRNAs induced at the pro-B to pre-B cell transition. Eventually, the candidate miRNAs obtained from the screen were further characterized in the AMuLV pro-B cells to determine pathways affected by their expression. Their effects were confirmed *in vivo* in cultured primary pro-B cells from the bone marrow of wild type mice. Finally we validated our *in vitro* results in knockout mice for the miRNAs of interest. In those mice we confirmed our *in vitro* observations and determined physiological relevance.

The experiments that comprise this thesis are geared towards: 1) identifying miRNAs that change in expression at the pro-B to pre-B cell stage in B cell development, 2) characterizing the pathways and downstream effects if any of these miRNAs, 3) and characterizing the targets as well as identifying the mode of regulation of the miRNAs on their targets.

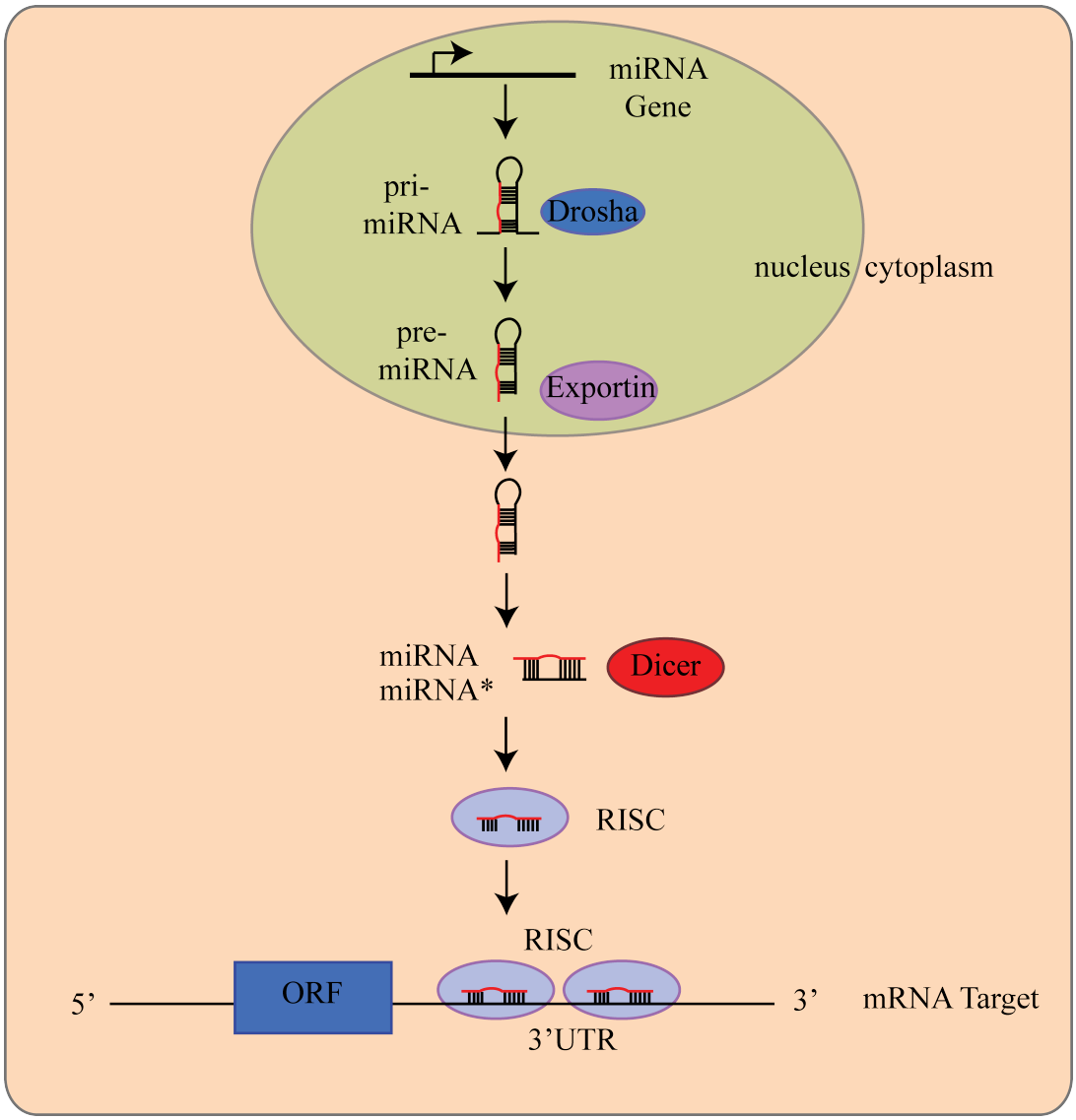

Figure 1.1. **Diagram of miRNA processing.**
Adapted from He et al. (He et al. 2004). miRNAs are transcribed in the nucleus and processed by Drosha into a pre-miRNA. The pre-miRNA is exported to the cytoplasm by Exportin for further processing by Dicer. The processed mature miRNA is incorporated into the RISC complex to post-transcriptionally regulate the target mRNA.

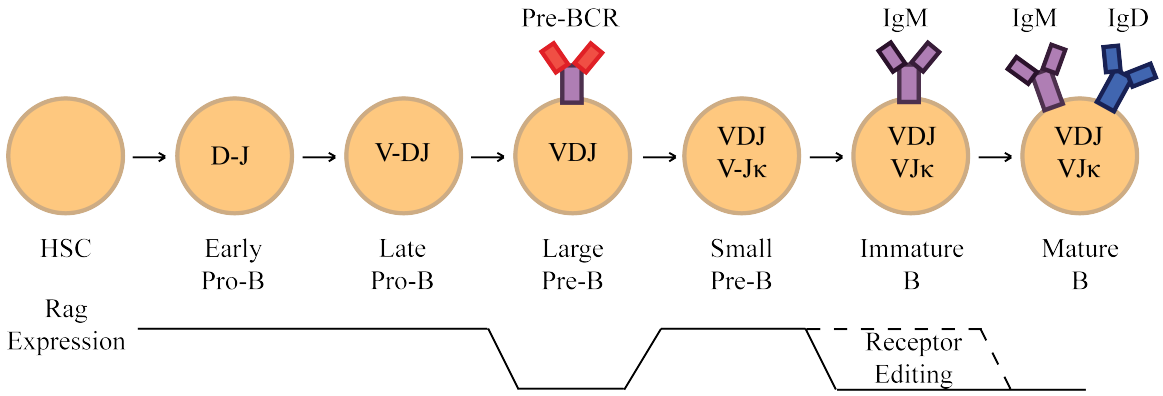

Figure 1.2. **Diagram of B cell development.**
B cells develop from hematopoietic stem cells (HSC) and are committed to the B cell lineage at the early pro-B stage (Hardy et al. 2007). V(D)J recombination at the heavy chain locus occurs in the pro-B stages, while V(D)J recombination at the light chain loci occurs at the pre-B stage. Expression of Rag1/2 is delineated at the bottom.

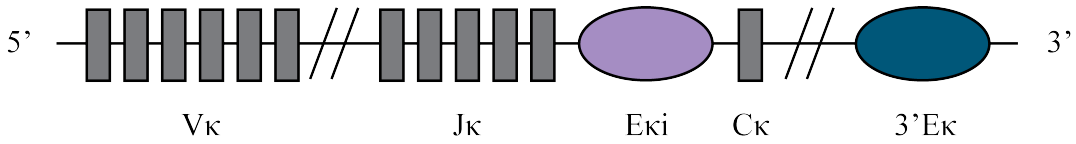

Figure 1.3 **Diagram of the immunoglobulin *kappa* locus.**
Adapted from Geier et al. (Geier et al. 2006). The immunoglobulin *kappa* locus has two enhancers, Eκi and 3'Eκ. Vκ= variable genes; Jκ= joining genes; Cκ= constant region. Diagram not drawn to scale.

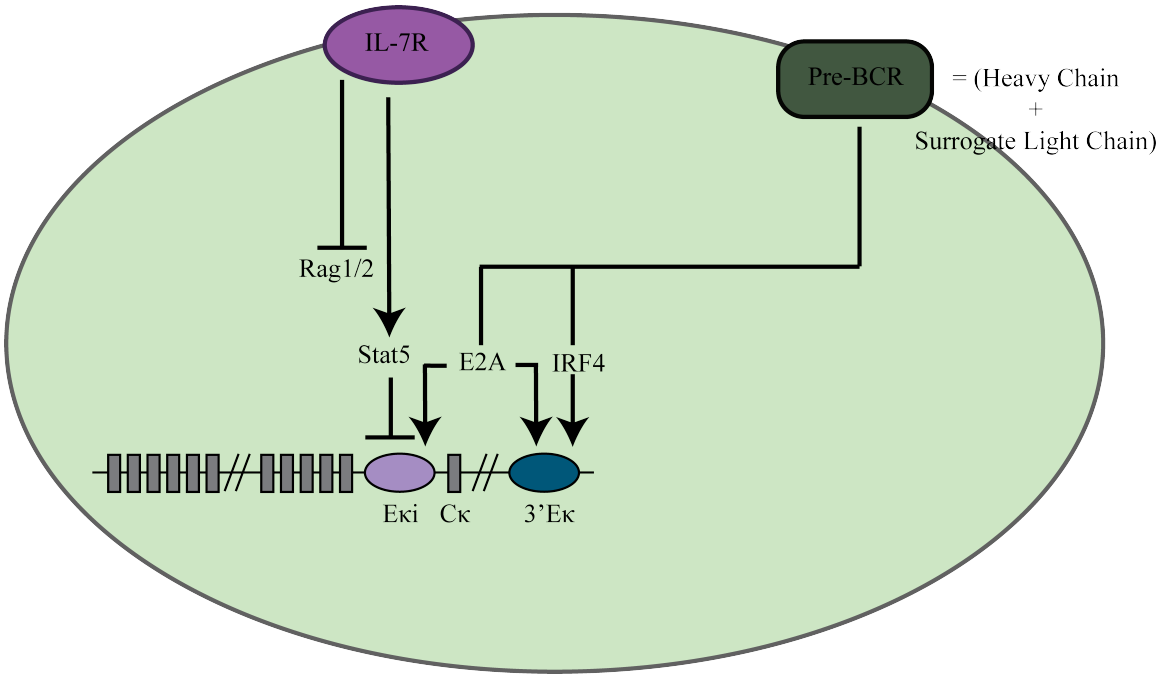

Figure 1.4 **Diagram of IL-7R and Pre-BCR signaling on the *kappa* locus.**
Signaling of the IL-7R inhibits Rag1/2 and Eκi through Stat5. Signaling of a functionally rearranged heavy chain, paired with a surrogate light chain activates transcription factors that activate the *kappa* locus through both enhancers. Adapted from Johnson et al (Johnson et al. 2008).

Chapter 2: Identification of miRNAs that Regulate the Pro-B to Pre-B Transition

Background:

Recent work implicates microRNAs (miRNAs) in the regulation of B cell development (Koralov et al. 2008; Xiao et al. 2007; Ventura et al. 2008). Mice with B cell lineage-specific deletion of Dicer exhibit a developmental block at the pro-B stage of development (Koralov et al. 2008). This finding implicates the miRNA pathway and its effector members as playing an essential role at this stage. Although some miRNAs and their functions have been described (Xiao et al. 2007; Ventura et al. 2008), further studies are needed to thoroughly identify miRNAs regulating important hallmarks in B cell development.

A hallmark of the pre-B stage is rearrangement of the light chain immunoglobulin loci, *kappa* or *lambda* (Constantinescu et al. 1997; Schlissel et al. 1994). Prior to rearrangement, transcription occurs across the unrearranged *kappa* locus generating what are known as germline *kappa* transcripts (κGT) (Schlissel et al. 1989). The appearance of these transcripts indicates a *kappa* locus that is in an open chromatin state, available for access by the V(D)J recombinase proteins, Rag1 and Rag2 (McDevit et al. 2005). *Kappa* locus activation is tightly regulated during B cell development, however it is not known if miRNAs may regulate this process.

We sought to identify miRNAs that play a role in the pro-B to pre-B transition using AMuLV-transformed pro-B cells as a model system (Chen et al. 1994; Klug et al. 1994). The drug STI571, also known as Gleevec, targets the Abelson kinase, and seemingly untransforms the cells. The cells then exit the cell cycle and progress to a pre-B-like stage of B cell development. Studies by our group (Muljo et al. 2003) have shown that STI571-treated AMuLV cells, have a similar gene expression profile to cells in the pro-B to pre-B transition of B cell development. Two examples of critical B cell-lineage genes with similar patterns in both systems include Rag1/2 and κGT expression (Muljo et al. 2003). This system is therefore frequently used as a model system for *in vitro* studies of the pro-B to pre-B transition. While pre-B stage-specific genes have been identified in this system, miRNAs specific to this stage have yet to be described.

In this study, we screened for miRNAs that are upregulated in STI571-treated AMuLV-transformed pro-B cells and that promote B cell differentiation. Our screen identified two miRNAs, miR290-5p and miR292-5p, that originate from the miR290 Cluster transcript and share an identical seed-sequence. miR290-5p and miR292-5p are independently able to induce expression of κGT upon over-expression in AMuLV pro-B cells and primary B cells. We propose a novel role for miR290-5p and miR292-5p in the activation of the *kappa* locus during B cell development.

Materials and Methods

Mice

miR290 Cluster -/- mice, on a C57BL/6 and 129 mixed background, were a gift from the Sharp and Jaenisch Labs at the Koch Institute (MIT). C57BL/6 mice were purchased from Jackson Laboratories. All mouse experimentation was approved by the Animal Care and Use Committee of the University of California at Berkeley.

Cell Culture and Retroviral Infections

Phoenix cells (Swift et al. 2001) were grown in Dulbecco's modified Eagle's medium (DMEM) supplemented with heat-inactivated 10% fetal calf serum, and sodium pyruvate (800μM). AMuLV cell lines E2A+/+, 220-8, and 63-12 were cultured in RPMI supplemented with heat-inactivated 5% fetal calf serum, penicillin (100μg/ml), 2mM L-Glutamine, and 2-mercaptoethanol (50μM).

MSCV-iRES-hCD2-miR30 was previously described (Amin et al. 2008). The miR30 cassette was replaced with either miR129-2_3p, miR290-5p, or miR292-5p. The corresponding miRNAs* were mutated for each pre-miRNA. Primers used for miRNA cloning were as follows:
miR129-2_3p 5' ACTGCTCGACCCCCTTCGAGCTACCCTTAT
miR129-2_3P 3' ACTGGCGGCCGCTCCCCCTGTGGTACAAAGTC
miR290-5p 5' ATCGGGATCCTCTGGGCGCGAGTGA
miR290-5p 3' ATCGGTCGACGCTCAAGAGAGGG
miR292-5p 5' ATCGGGATCCGTGGAGGCCCTCTCT
miR292-5p 3' ATCGGTCGACCCAAGCCGCGGAG.

Sponges were generated from long oligos with imperfect binding sites for miRNAs and were annealed and cloned into V26-MSCV-PIG. Long oligos used to generate each miRNA sponge contain three consecutive copies of binding sites for the corresponding miRNA with each binding site separated by a CCGG stuffer sequence. A bulge for imperfect binding was created corresponding to positions 9-12 of the miRNA. Binding sites were as follows:
miR129-2_3p: ATGCTTTTTGTTTGAAGGGCTT
miR290-5p: AAAGTGCCCCACCCGTTTGAGT
miR292-5p: CAAAAGAGCCAAACGTTTGAGT.

Phoenix cells were transduced with above retroviral plasmids and 3μg of a vector expressing vesicular stomatitis virus G, using Lipofectamine 2000 according to the manufacturer's instructions (Invitrogen). Two days after transfection, E2A+/+, HF4 AMuLV cells or primary bone marrow cells were transduced with the viral supernatant.

qRT-PCR

Total RNA was isolated with Trizol Reagent (Invitrogen) and reverse transcription was performed with random hexamers and Moloney MLV reverse Transcriptase (MMLV) (Invitrogen). Quantitative reverse transcription PCR (qRT-PCR) was performed with

Jumpstart *Taq* (Sigma), EvaGreen (Biotium), on an ABI 7300 Thermocycler (Applied Biosystems). PCR amplification was as follows: 95C 3min, 95C 30sec, 60C 30 sec, 72C 30 sec (data collection), for 40 cycles. Primers used in this study were previously described (Amin et al. 2009).
Kappa 5': GGA CGT TCG GTG GAG GC
Kappa 3': GGA AGA TGG ATA CAG TTG GT
miRNA reverse transcription was conducted as previously described (Chen et al. 2005), using 50ng of total RNA and miRNA-specific reverse-transcription primer (Assay IDs 001184, 002590, 001055, ABI) . miRNA qRT-PCR was conducted as previously described (Chen et al. 2005), using miRNA-specific Taqman primer sets included in miRNA-specific assays.

Flow Cytometry and FACS Sorting Analysis
Total bone marrow was harvested from mice and red blood cells were depleted with EryLyse Buffer (0.14M NH4Cl, 20mM Hepes). Cells were stained with anti-CD19 MACS microbeads (Miltenyi Biotec) and were CD19+ enriched using MACS MS columns (Miltenyi Biotec). CD19+ cells were then stained using the following antibodies: B220-PeCy5 (clone RA3-6B2, BD), CD43-Pe (clone S7, BD), IgM-FITC (clone II/41, eBiosciences), IgD-Biotin (clone 11-26, eBiosciences), Streptavidin-PeCy7 (BD). Stained cells were resuspended in FACS buffer (5% BSA, 10mM Hepes) for cell sorting.

Results

microRNA Screen in AMuLV proB cells

To identify miRNAs that may be of importance at the pro-to-pre-B cell transition of B cell development we analyzed RNA purified from AMuLV-transformed pro-B cell lines. When AMuLV-transformed pro-B cells are treated with STI571 (Gleevec), they progress to a pre-B-like state of development (Muljo et al. 2003). To broadly identify miRNAs that change in expression levels upon the addition of STI571, we used the Exiqon microarray platform to screen for such miRNA populations in three independent AMuLV transformants (E2A+/+, 220-8, 63-12). We cultured each line in the presence or absence of STI571 for 12hrs (2.5μM), purified total RNA from these samples, and subjected them to microarray analysis.

The general trend observed was an increase in expression of miRNAs upon STI571 treatment. However, there were a few miRNAs that decreased in expression upon STI571 treatment (Fig. 2.5). Two of the miRNAs identified in the screen as having expression consistently and significantly increased across all three independently transformed AMuLV-transformed pro-B cell lines (Fig. 2.5) were miR290-5p and miR292-5p. These miRNAs are members of the murine miR290 polycistronic cluster, previously reported to be expressed only in gonads of both sexes, but not in other tissues examined (Medeiros et al. 2011). They share the same seed sequence (Fig. 2.6) indicating a possible functional redundancy within pre-B cells.

To validate the results of the microarray, we cultured E2A+/+ AMuLV cells in the presence or absence of STI571 for 12hrs (2.5μM). Using specific Taqman qPCR assays, we confirmed that both miR290-5p and miR292-5p increase in expression upon STI571 treatment (Fig. 2.7).

We next asked whether these miRNAs displayed a similar pattern of regulated expression in wild-type primary developing pro- and pre-B cells. We sorted pro-B (B220+, CD43+, IgM-) and pre-B (B220+, CD43-, IgM-) cells from wild-type mouse bone marrow by flow cytometry, purified total RNA, and performed qPCR for quantification of miR290-5p and miR292-5p. We found that the increase in expression we observed in STI571 treated AMuLV-transformed pro-B cells, was mirrored in primary pro-B and pre-B cells (Fig. 2.8). A third member of the miR290 polycistronic cluster, miR291-5p is also induced, however other members of the miR290 cluster did not increase upon STI571 treatment (Fig. 2.9).

Over-expression of miR290-5p or miR292-5p induces germline Igκ transcription in AMuLV cells

Previous studies have shown that the addition of STI571 to AMuLV-transformed pro-B cells induces expression of genes characteristic of the pre-B cell stage in development (Muljo et al. 2003). Since these miRNAs increase in expression upon STI571 treatment,

we hypothesized that they may play a role in regulating developmental progression at the pre-B cell stage. In order to probe the role that these miRNAs might play at this drug-induced developmental transition, we cloned each miRNA in its genomic context into an MSCV-based IRES-CD2 marked retroviral expression vector. We transduced the E2A+/+ AMuLV cell line with each miRNA vector or an empty vector control and asked whether the miRNA-overexpressing cells activate transcription of the germline Igκ locus transcript, κGT. The activation of the Igκ locus is a hallmark of the pre-B stage of development that is tightly correlated with the activation of V-to-Jκ rearrangement (Schlissel et al. 1989). Upon stable over-expression of either miR290-5p or mir292-5p, we observed an induction in κGT (Fig. 2.10), but not to the levels seen in wild-type AMuLV-transformed pro-B cells treated with STI571. However, when we treated the miRNA-transduced cell lines with STI571 (12hrs, 2.5μM), we saw a super-induction of κGT (Fig. 2.10). These data indicate that either miRNA is able to independently act upon a pathway that results in activation of the germline Igκ locus. In contrast, neither miRNA altered the induced or basal levels of *Rag1* transcription in these same cells (Fig. 2.11).

miRNAs knockdown partially blunts the induction of κGT upon v-Abl inhibition

To confirm that the apparent role of miR290-5p and miR292-5p in the activation of κGT observed in these experiments was not an artifact of over-expression, we generated miRNA sponge constructs to perform knockdown experiments. These sponge constructs were generated by independently cloning three imperfect miRNA binding sites for each miRNA into the 3'UTR of a GFP cDNA (Ebert et al. 2007). We also cloned a sponge construct for a different miRNA, miR129-2_3p, to use as a negative control. miR129-2_3p is expressed at similar levels as miR290-5p and miR292-5p at the pro-B stage, but is not induced at the pre-B stage in primary B cells or upon STI571 treatment of AMuLV-transformed pro-B cells (Table 1). We generated stable AMuLV-transformed cell lines transduced with retroviral vectors expressing these sponge constructs to examine their effects on κGT expression.

To first confirm that the sponge constructs were engaging with the target miRNA, we stably transduced AMuLV cells with GFP miRNA-sponge constructs marked with a dual tomato red cDNA. The expression of the tandem tomato red cDNA was independent of miRNA sponge regulation and serves for normalization against the variable GFP expression. Upon STI treatment (42hrs, 1μM) we observed a decrease in GFP expression relative to tomato red expression, in the miR290-5p or miR292-5p sponges, suggesting that the sponges were engaging with the target miRNAs (Fig. 2.12).

We then examined the sponge effects on κGT expression. We cultured the stable GFP sponge cell lines with STI571 (12hrs, 2.5μM) and observed a normal induction of κGT in the negative control sponge cell line (Fig. 2.13). However, we observed a blunting of normal κGT induction in the miR290-5p or miR292-5p sponge lines (Fig. 2.13). This blunting of κGT induction upon knockdown of endogenous drug-induced miR290-5p or miR292-5p indicates that these miRNAs partially contribute to the activation of the *kappa* locus upon STI571 treatment of AMuLV-transformed cells.

miRNA knockdown partially blunts κGT induction in primary cell culture

To further test the role of miR290-5p and miR292-5p in the activation of the *kappa* locus observed in our AMuLV model system, we performed similar sponge knockdown experiments in a primary developing B cell culture system. Cultured primary pro-B cells proliferate in the presence of high concentrations of rIL7 but do not differentiate, while at low concentrations of rIL7, the cells exit the cell cycle and progress to the pre-B cell stage of development (Johnson et al. 2008). We harvested bone marrow from wild-type mice and cultured cells in 2ng/ml rIL7 for 5 days to expand the pro-B cell population. We then retrovirally transduced the expanded pro-B cell culture with either the negative control, miR290-5p, or miR292-5p sponges. After an additional 24 hours in rIL7 culture, we harvested a portion of each population as a "0 hour" time-point. We then washed the remaining cells and re-cultured them in the absence of rIL7 for 24hr.

In cells transduced with the negative control sponge, there was normal induction of κGT upon IL-7 withdrawal as expected (Fig. 2.14). However, in the presence of the miR290-5p or miR292-5p sponges, IL7 withdrawal resulted in a significantly diminished induction of κGT expression (Fig. 2.14). We observed indistinguishable induction of Rag1 gene expression upon IL7 withdrawals in miR292-5p as compared to miR129-2_3p negative control sponge cultures (Fig. 2.15). Together these data indicate that miR290-5p and miR292-5p independently contribute to the induction of κGT expression in primary pre-B cells.

The miR290 cluster in B Cell Development

To confirm whether miR290-5p, miR292-5p, and more broadly the miR290 cluster are involved in B cell development, we analyzed B cell development in a miR290 cluster knockout as compared to wild-type mice (Medeiros et al. 2011). We analyzed total bone marrow by flow cytometry focusing on pro-B (B220+, CD43+, IgM-), pre-B (B220+, CD43-, IgM-), large pre-B (B220+, CD43-, IgM- FSC-Hi), small pre-B (B220+, CD43-, IgM- FSC-Lo), and immature B (B220+, CD43-, IgM-Lo) populations. We found a moderate increase in the percentage of pre-B cells in the homozygous miR290 knockout mice, as compared to the wild-type mice ($p=0.05$) (Fig. 2.16, 2.17).

To confirm our miRNA knockdown results that implicated both miR290-5p and miR292-5p as playing a role in activating the *kappa* locus, we used the miR290 cluster knockout mice to analyze κGT expression in pro-B, small pre-B, and large pre-B cell populations. We observed a blunted κGT induction in the small pre-B population of miR290 cluster knockout mice (Fig. 2.18). Interestingly, we also observed a blunted Rag1 induction in the small pre-B population of miR290 cluster knockout mice (Fig. 2.19). This was unexpected since we did not observe an effect on Rag1 in the pro-B culture experiments. This difference could be a result of the transformation process of the AMuLV cell lines.

Together, these data indicate that members of the miR290 polycistronic cluster, miR290-5p and miR292-5p are involved in the activation of the *kappa* locus as indicated by expression of κGT.

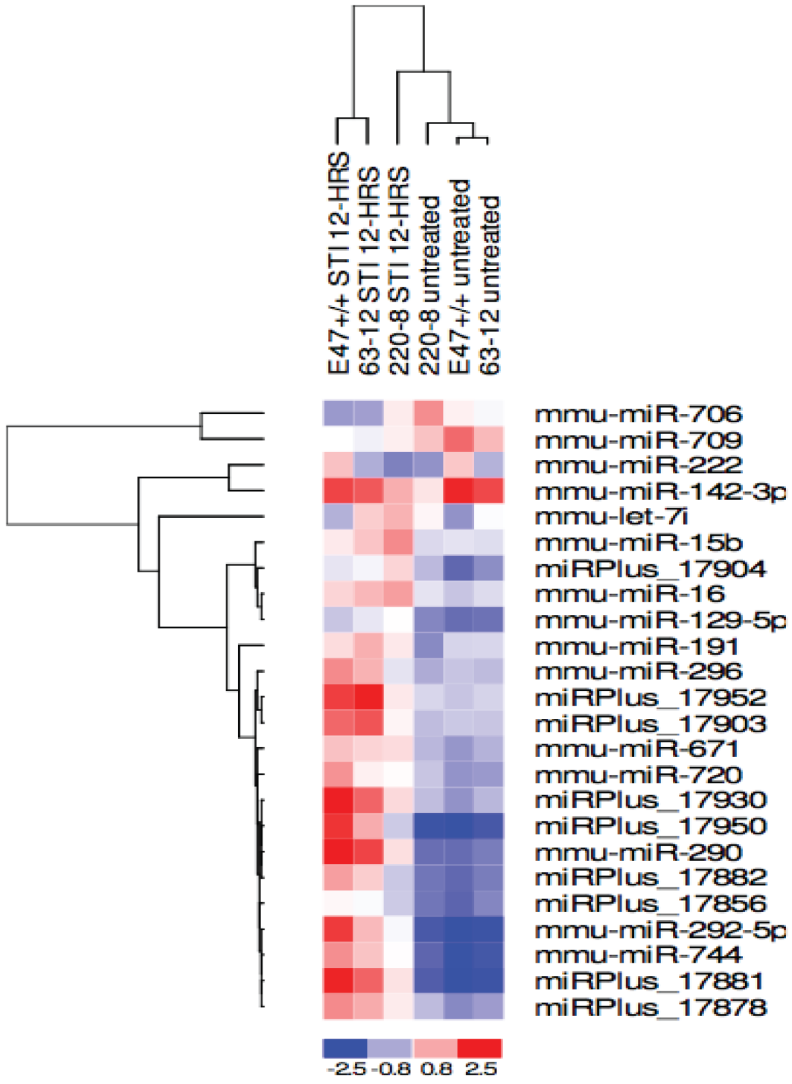

Figure 2.5. **miRNA microarray screen for differentially expressed miRNAs in AMuLV Cells Upon STI571 Treatment.** Heat-map of miRNA microarray of AMuLV cell lines with or without STI571 (2.5μM, 12hr). Performed once in three independently transformed cell lines: E2A+/+ (also known as E47+/+), 63-12, 220-8. miRNA individual expression was compared to its average expression across all six samples.

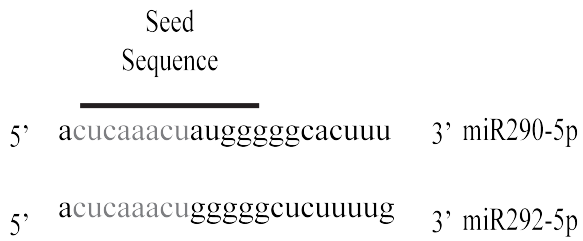

Figure 2.6. **miR290-5p and miR292-5p Seed Sequence.** Schematic depiction of the shared seed sequence, CUCAAACU, of the mature miR290-5p and miR292-5p microRNAs

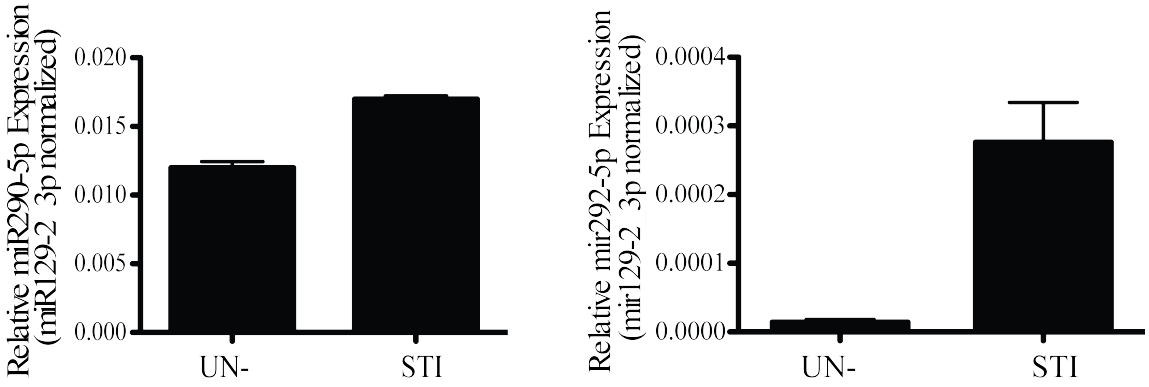

Figure 2.7. **miR290-5p and miR292-5p are induced in AMuLV cells upon STI571 treatment.** qPCR analysis of miR290-5p or miR292-5p in E2A+/+ AMuLV cells treated with STI571 (2.5μM, 12hr). Normalization gene was miR129-2_3p. Error bars represent range for replicate qPCR reactions. qPCR was performed for each miRNA from three biological replicates.

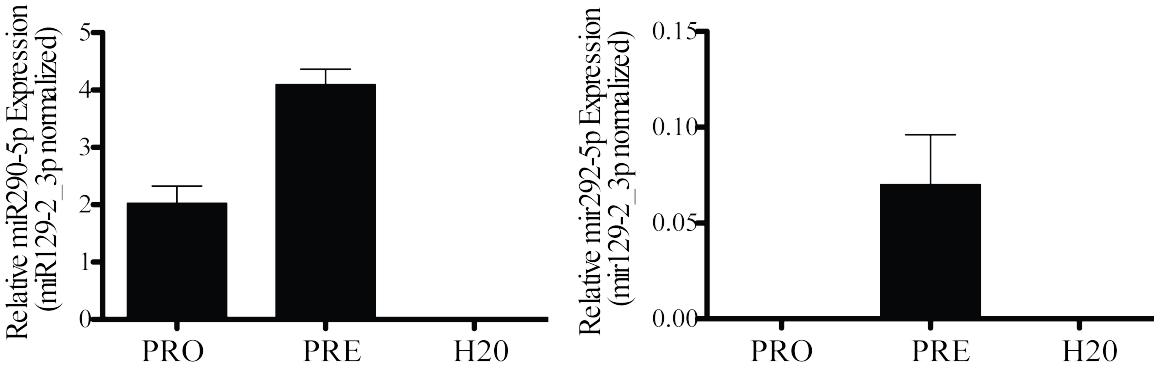

Figure 2.8. **miR290-5p and miR292-5p are induced in primary pro-B to pre-B cells.** qPCR analysis of miR290-5p or miR292-5p in primary wild-type pro-B (B220+, CD43+, IgM-) cells or pre-B (B220+, CD43-, IgM-) cells. Normalization gene was miR129-2_3p. Error bars represent range for replicate qPCR reactions. qPCR was performed for each miRNA from sorted lymphocyte populations of at least three different mice.

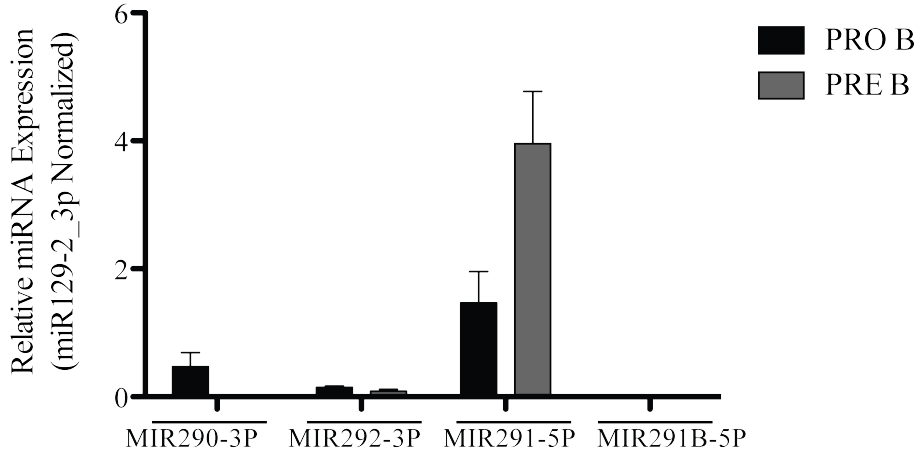

Figure 2.9. **Expression of alternative miR290 cluster members.**
qPCR analysis of miR291-5p, miR290-3p, and miR292-3p expression levels in RNA purified from primary wild-type pro-B (B220+, CD43+, IgM-) or pre-B (B220+, CD43-, IgM-) cells. Data was normalized to the expression of miR129-2_3p. Error bars represent range for replicate qPCR reactions. Data represents at least three independent experiments.

MIRNA	220-8 UNT.	220-8 STI 12hr	E2A+/+ UNT.	E2A+/+ STI 12hr	63-12 UNT.	63-12 STI 12hr
mmu-miR-129-3p	1.36	1.51	1.66	1.50	1.63	1.48
mmu-miR-292-5p	-1.93	-0.09	-2.59	1.97	-2.30	0.67
mmu-miR-290	-1.37	0.32	-1.41	2.50	-1.24	1.87

Table 1. **miR129-2_3p, miR290-5p, miR292-5p microarray Log Median ratios.**

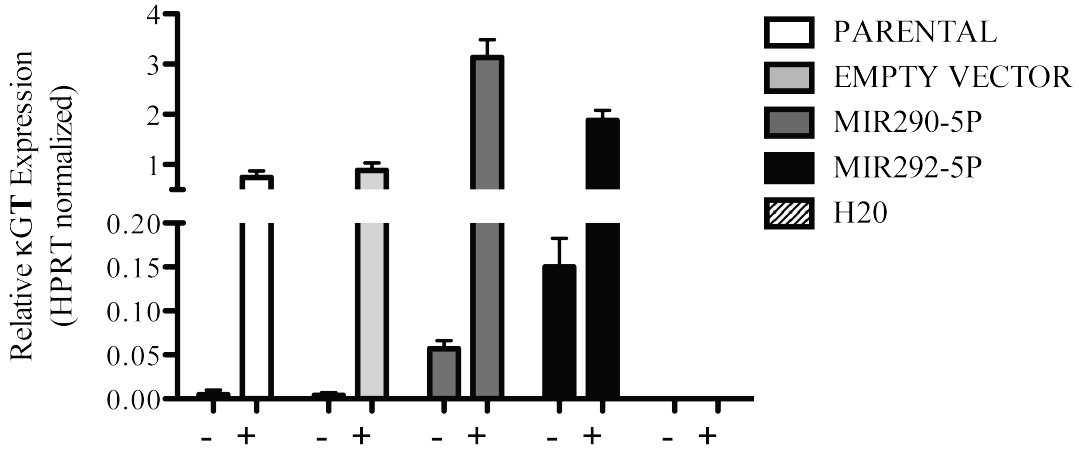

Figure 2.10. **Over-expression of miR290-5p or miR292-5p induces κGT expression in AMuLV cells.** qPCR analysis of κGT expression in E2A+/+ AMuLV cells over-expressing miR290-5p or miR292-5p, with or without STI571 (2.5μM, 12hr). Normalization gene was HPRT. Error bars represent range for replicate qPCR reactions. Data represents at least four individual experiments.

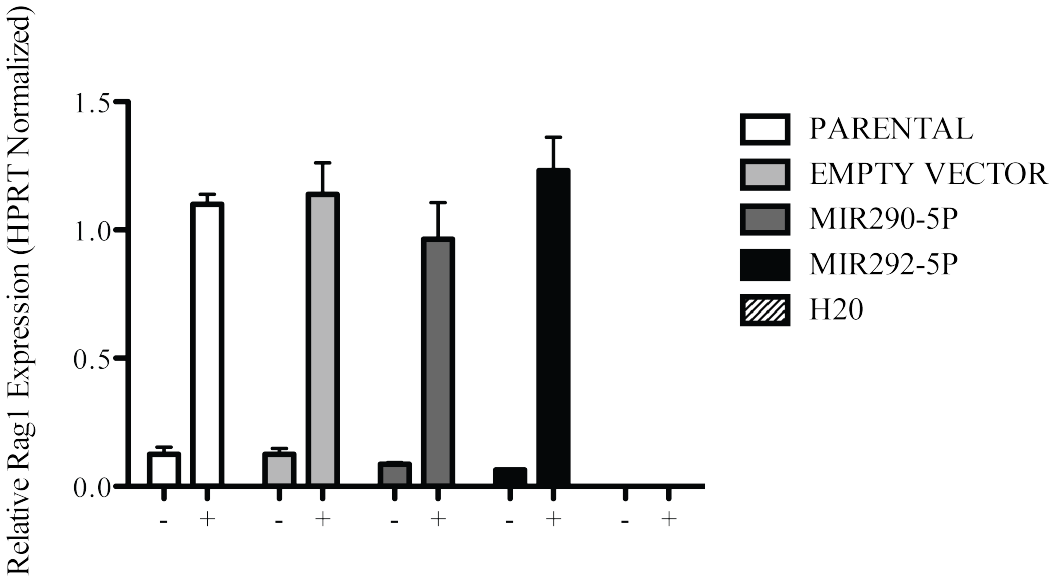

Figure 2.11. **Over-expression of miR290-5p or miR292-5p does not induce Rag1 expression in AMuLV cells.** qPCR analysis of Rag1 expression in E2A+/+ AMuLV cells over-expressing miR290-5p or miR292-5p, with or without STI571 (2.5μM, 12hr). Normalization gene was HPRT. Error bars represent range for replicate qPCR reactions. Data represents at least four individual experiments.

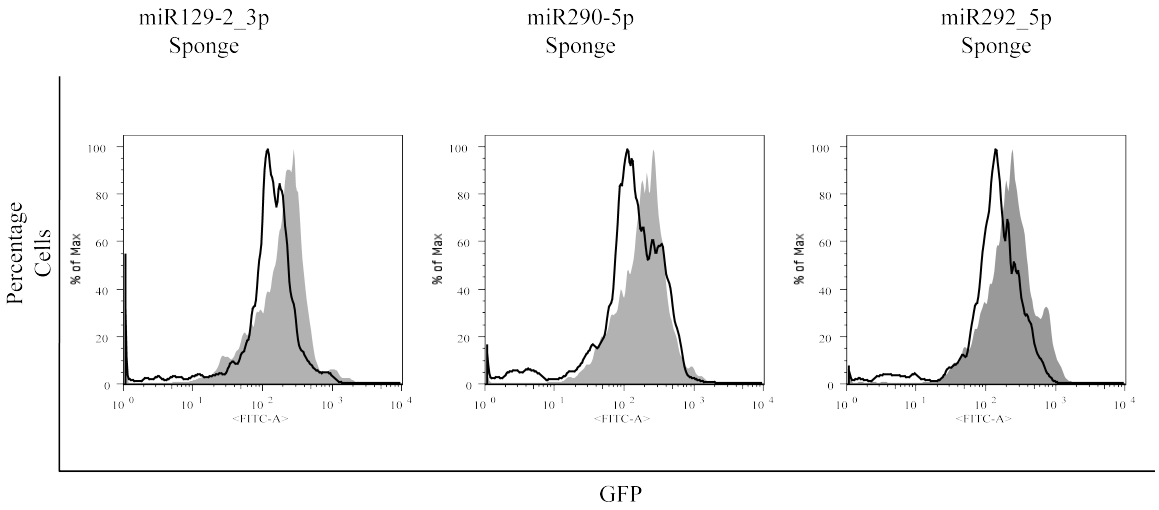

Figure 2.12. **miRNAs engage with knockdown-sponge construct.** FACS analysis of sponge marker, GFP, expression upon STI571 (1μM, 42hr) induction of miRNAs. E2A+/+ AMuLV cells were stably transduced with tandem tomato marked sponge constructs for miR129-2_3p, mir290-5p, or miR292-5p. Cells were gated on the tomato positive population and were analyzed for GFP expression upon STI571 treatment. (grey-filled, untreated cell line; Black line, STI-treated cell line).

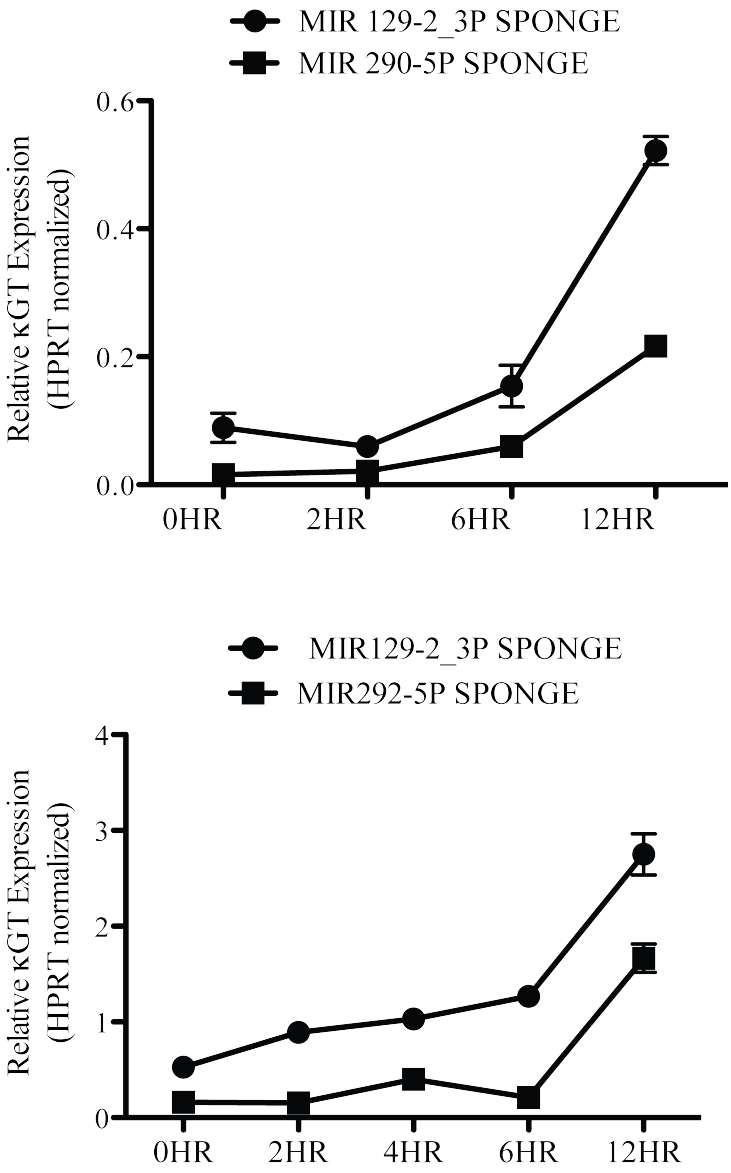

Figure 2.13. **κGT induction is blunted upon knockdown of miR290-5p or miR292-5p in AMuLV cells.** qPCR analysis of κGT expression in E2A+/+ AMuLV cells expressing a miR290-5p or miR292-5p sponge knockdown construct, and treated with STI571 (2.5μM) at the time points indicated. Normalization gene was HPRT. Error bars represent range for replicate qPCR reactions. These data derive from at least four independently performed experiments.

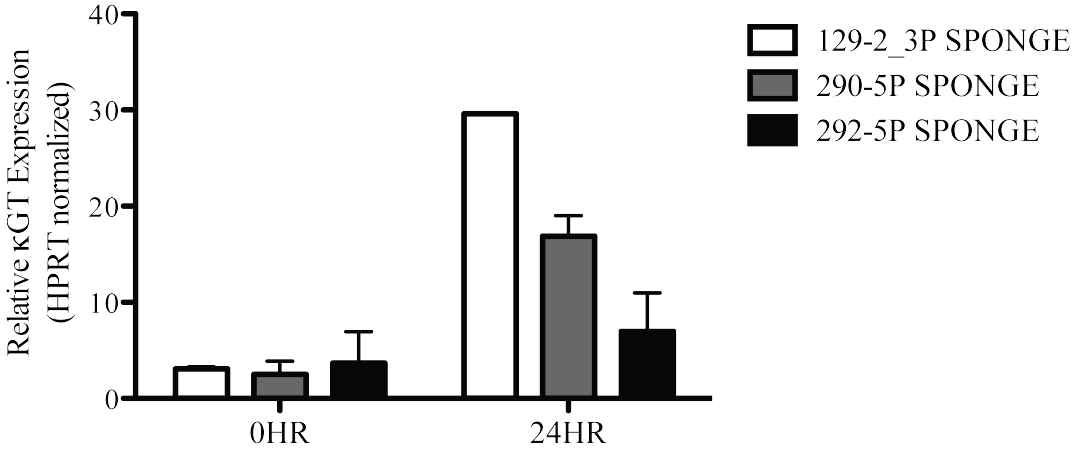

Figure 2.14. **κGT induction is blunted upon knockdown of miR290-5p or miR292-5p upon IL-7 withdrawal of primary pro-B cells.** qPCR analysis of κGT expression in wild-type primary B cells transduced with either a miR129-2_3p control knockdown sponge, or a miR290-5p or miR292-5p knockdown sponge. Wild-type primary B cells were cultured in IL7 (2ng/ml) for 5 days and then transduced with indicated sponge construct. Marker positive cells were then sorted and IL7 withdrawn from culture for 24hrs and RNA was harvested. qPCR measures κGT expression in IL7 proficient and IL7 withdrawn cells. Normalization gene was HPRT. Error bars represent range for replicate qPCR reactions. These data derive from at least four independently performed experiments.

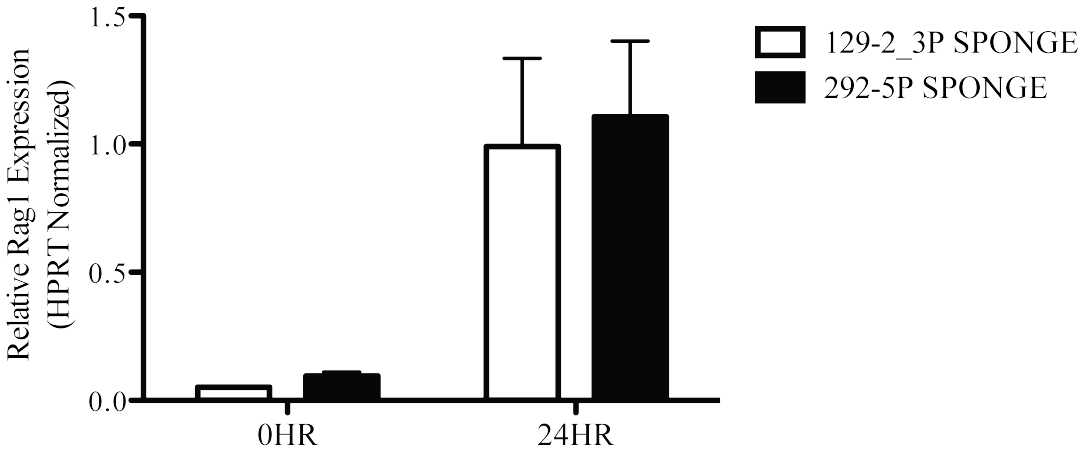

Figure 2.15. **Rag1 induction is normally induced upon knockdown of miR290-5p or miR292-5p upon IL-7 withdrawal of primary pro-B cells.** qPCR analysis of Rag1 expression in wild-type primary B cells transduced with either a miR129-2_3p control knockdown sponge, or a miR290-5p or miR292-5p knockdown sponge. Wild-type primary B cells were cultured in IL7 (2ng/ml) for 5 days and then transduced with indicated sponge construct. Marker positive cells were then sorted and IL7 withdrawn from culture for 24hrs and RNA was harvested. qPCR measures Rag1 expression in IL7 proficient and IL7 withdrawn cells. Normalization gene was HPRT. Error bars represent range for replicate qPCR reactions. These data derive from at least four independently performed experiments.

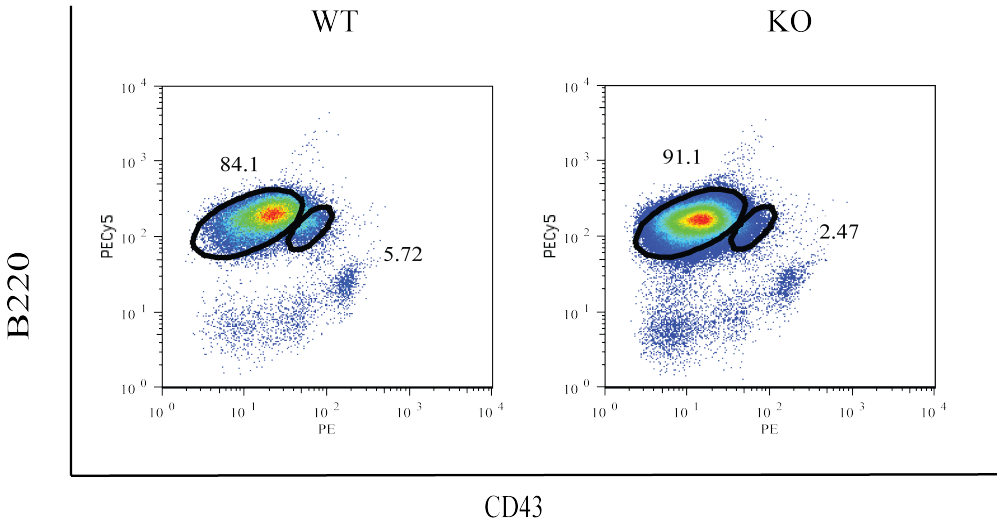

Figure 2.16. **Germline knockout of the miR290 cluster affects the pre-B cell population.** FACS analysis of 6 week old miR290 cluster knockout or wild-type mice. FACS plot reflects CD19 enriched cells gated on IgM negative cells. This experiment is representative of four independent experiment. Each experiment was with at least one mouse per genotype.

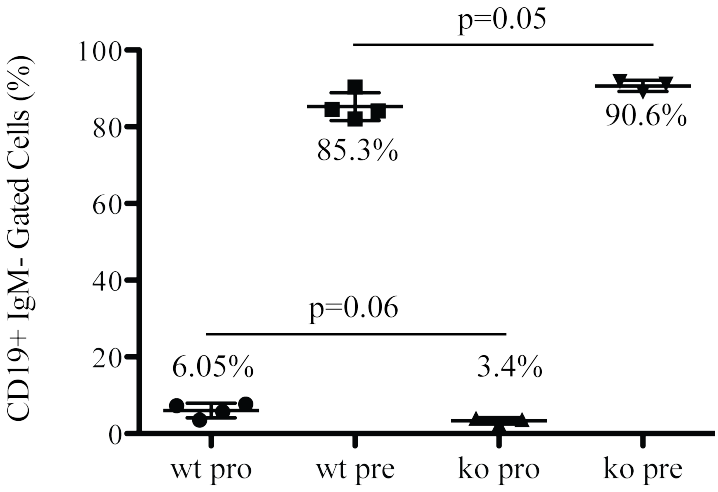

Figure 2.17. **Germline knockout of the miR290 cluster affects the pre-B cell population.** Percent CD19+, IgM- pro-B (B220+, CD43+) and pre-B (B220+, CD43-) cell data for each independent knockout and wild-type mouse analyzed as in Figure 1.12. Line represents the average percentage for each population and the P value was derived by the Student's T test. This experiment is derived from at least four mice per genotype.

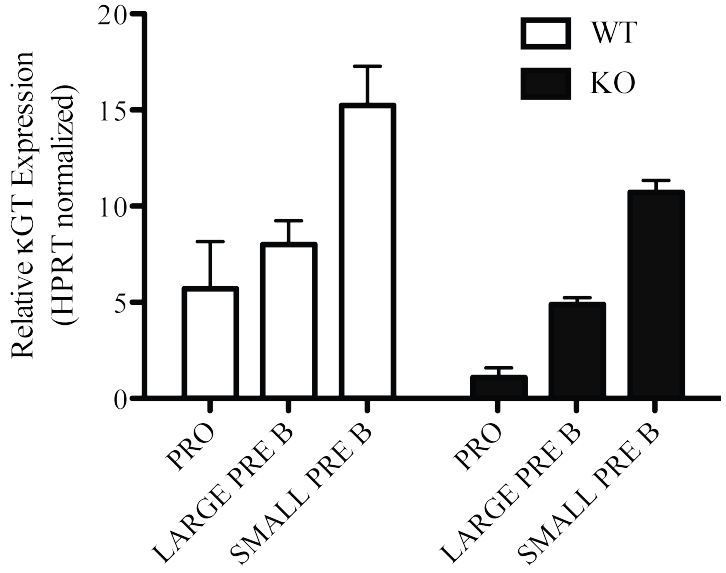

Figure 2.18. **κGT expression is blunted in the small pre-B population in miR290 cluster knockout mice.** qPCR analysis of κGT from sorted pro-B (B220+, CD43+, IgM-), large pre-B (B220+, CD43-, IgM-, FSC-Hi), and small pre-B (B220+, CD43-, IgM-, FSC-Lo) cells sorted by FACS. Mice were 6 week old miR290 cluster knockout, heterozygote, or wild-type mice. Normalization gene was HPRT. This experiment has been repeated with at least four mice per genotype.

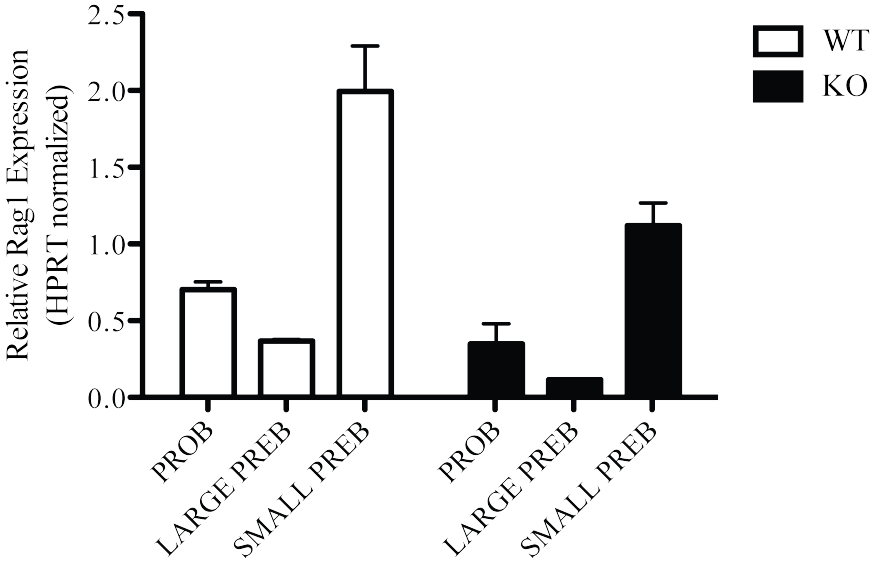

Figure 2.19. **Rag1 expression is blunted in the small pre-B population in miR290 cluster knockout mice.** qPCR analysis of Rag1 from sorted pro-B (B220+, CD43+, IgM-), large pre-B (B220+, CD43-, IgM-, FSC-Hi), and small pre-B (B220+, CD43-, IgM-, FSC-Lo) cells sorted by FACS. Mice were 6 week old miR290 cluster knockout, heterozygote, or wild-type mice. Normalization gene was HPRT. This experiment has been repeated with at least four mice per genotype.

Discussion

This study demonstrates that developing B cells induce expression of miR290-5p and miR292-5p at the pre-B stage to fully activate the germline Igκ locus, a critical event in the pro-to-pre-B cell transition. Induction of miR290-5p/292-5p occurs in response to STI571-inhibition of v-abl in transformed pro-B cell cultures, as well as in response to IL-7 attenuation in primary B cell cultures. Over-expression supported that miR290-5p/292-5p are involved in full activation of κGT. Knockdown strategies confirmed this and showed that miR290-5p/292-5p are necessary for full activation of κGT. Additional pre-B stage signals, such as other miRNAs, may be required to induce full expression of κGT. This system serves as an example of the well-supported notion that multiple miRNAs work cooperatively to target individual transcripts and elicit fully repressive effects (Filipowicz et al. 2008).

V-abl inhibition or IL-7 attenuation induce additional signaling pathways, aside from miRNAs, that are complementary to miR290-5p/292-5p, and necessary for full κGT induction and *kappa* locus rearrangement (Johnson et al. 2008; Muljo et al. 2003; Ochiai et al. 2012). Previous studies by our group have shown that v-abl inhibition induces factors such as Spi-b and Irf4 (Muljo et al. 2003). Both are transcription factors that bind 3'Eκ and activate κGT. Recent studies have also shown that IL-7 signaling regulates PI3K/AKT signaling (Ochiai et al. 2012). Attenuation of the IL-7 signal, and thereby PI3K/AKT, releases inhibition of Rag1/2 as well as induces factors such as Foxo1 and Pax5. We therefore propose that miR290-5p/292-5p expression partially contributes to κGT induction in parallel with transcripton factors induced by v-abl inhibition or IL-7 attenuation. Together they achieve full κGT induction and *kappa* locus rearrangement.

Previous work has shown that κGT correlate with the activation of Igκ LC rearrangement (Schlissel et al. 1989), and may be required for progression from pre-B to immature B cells. Therefore, cells that are defective in full κGT induction may accumulate at the pre-B stage of development. We observed a deficiency in κGT induction in knockdown experiments from AMuLV-transformed pro-B cells and primary B cell cultures. In the miR290 cluster knockout mice we observed a modest accumulation of pre-B cells and a blunting of κGT at the small pre-B stage. These observations support our conclusion that members of the miR290 polycistronic cluster play a role at the pre-B stage.

A miRNA-regulated pathway for the activation of the Igκ*appa* locus.

In our study, we have identified a pathway at the pre-B stage of B cell development that is regulated by miR290-5p/miR292-5p, and is induced upon the attenuation of IL-7 signaling in primary B cell cultures. Previous work showed that IL-7 attenuation allows for both expression of Rag1/2 as well as induction of κGT. We note that miR290-5p/292-5p does not regulate Rag1/2 expression in cell culture systems. Rag1 induction remained intact in both the AMuLV pro-B cells as well as the IL-7-dependent primary B cell cultures, upon knockdown of miR290-5p or mir292-5p, while κGT induction was blunted. We did not observe *kappa* locus rearrangements, despite κGT induction in

miR290-5p/292-5p over-expressing cell lines. This may be explained by the lack of Rag1/2 activation when miR290-5p/292-5p are over-expressed in AMuLV pro-B cells. However, in the miR290 cluster knockout mice we observe a blunting of Rag1 induction at the small pre-B stage. This difference may be attributed to the transformed state of AMuLV-transformed pro-B cells. It is unclear why we did not observe an effect on Rag1 induction in the primary cell miRNA knockdown experiments. Therefore, loss of IL-7 signaling activates miR290-5p/292-5p, which leads to induction of κGT and Rag1.

miRNAs in B Cell development.

In this study, we show a role for miRNAs at the pre-B stage in B cell development. Several groups have shown that miRNAs are essential for the pro-to-pre-B transition, supporting our postulate that miRNAs regulate different stages of B cell development. Notably, Koralov (Koralov et al. 2008) and colleagues deleted Dicer, an essential miRNA processing enzyme, in AMuLV-transformed pro-B cells and identified a set of upregulated transcripts. They also identified several miRNAs necessary for regulating the pro-B stage of B cell development. One such example, Bim, a pro-apoptotic gene, was identified as a target of miR17-92 at the pro-B stage (Koralov et al. 2008; Ventura et al. 2008; Xiao et al. 2008). These studies provide a foundation in support of the AMuLV-transformed pro-B cell model system for identifying miRNAs. They also support that miRNAs may regulate other transitions in B cell development such as the pre-B to immature-B transition that we observe.

Many miRNAs, including those expressed at the pro-to-pre-B transition, are described as being master regulators of key pathways. For example, miR150, in both loss of function and gain of function mouse model studies, was identified as a robust regulator at the pro-to-pre-B transition (Xiao et al. 2007; Zhou et al. 2007). B lineage-specific miR150 transgenic mice display a block at the pro-to-pre-B transition. Additionally, the miR17-92 polycistronic cluster knockout mouse has a block at the pro-to-pre-B transition in B cell development (Ventura et al. 2008). Conversely, the gain of function miR17-92 transgenic mouse manifests lymphoproliferative disease (Xiao et al. 2008), and also serves as an example of master regulatory miRNA potential in B cell development.

Germline-deletion of the miR290 cluster in mice and miR290-5p/292-5p knockdown, in either STI571-treated AMuLV-transformed pro-B cells or in an IL-7 regulated primary B cell culture system, result in blunting of κGT induction. These miRNAs contribute to, but are not essential for, this process as indicated by blunting rather than ablation of κGT induction. Coordinate action of additional factors, some of which may include other miRNAs, must also occur. This is different than the robust effect of miR150 described above. The modest effect on κGT induction, together with the accumulation of the pre-B population in the miR290 cluster knockout mouse, underscores the potential of low-expressing miRNAs, such as miR290-5p/292-5p, that behave as modulators of pathways in developmental systems.

miR290 Cluster and its members.

miR290-5p and miR292-5p are members of the miR290 polycistronic cluster (Houbaviy et al. 2005). The miR290 cluster is expressed as a single transcript encoding seven miRNAs. The miR290 cluster germline knockout has a partially penetrant embryonic lethality in which homozygotes survive gestation at only 7% of the predicted Mendelian ratio (Medeiros et al. 2011). Medeiros et al. hypothesize that the phenotype is partially penetrant in part due to the mixed background in their studies (129/C57BL6). Additionally, they point out that other miRNA deletions result in partially penetrant phenotypes, possibly due to random fluctuations of gene levels in the absence of the miRNAs. They further speculate that this is the case in the miR290 cluster deletion.

Homozygous knockout mice that die in-utero have two major abnormal phenotypes. At E.10.5, 16% of homozygous knockouts develop outside of the yolk sac, while 40% of homozygotes have severe developmental defects including reduced somite number and delayed chorioallantoic attachment, among other things (Medeiros et al. 2011). These defects are obvious contributors to the reduced survival potential of homozygotes, and emphasize the importance of the miR290 cluster in development. Our studies are the first to describe a phenotype in lymphoid cells in the miR290 cluster knockout mice.

In summary, we identified two miRNAs, miR290-5p and miR292-5p, that are induced in pre-B cells. They modulate induction of κGT expression upon IL7 attenuation. κGT expression is critical to activation of the *kappa* locus for rearrangement of a functional immunoglobulin light chain. Our studies have uncovered a novel role for miR290-5p and miR292-5p in this key developmental process.

Chapter 3: Pathway Analysis for κGT Induction by miR290-5p and miR292-5p

Background:

The activation and rearrangement of the *kappa* locus is a highly regulated process at the pre-B stage of B cell development. Activation of the *kappa* locus requires two *kappa* locus enhancers, the kappa intronic enhancer (Eκi) and the 3' kappa enhancer (3'Eκ) (Inlay et al. 2002). Signaling through the IL-7 receptor and pre-B Cell Receptor (pre-BCR) concomitantly direct transcription factors to bind either enhancer, thereby activating κGT and *kappa* rearrangements (Johnson et al. 2008; Mandal et al. 2011). While much is known about signaling through these pathways, nothing is known about the role miRNAs play in *kappa* locus activation at the pre-B stage.

Several transcription factors have been described to bind the two *kappa* locus enhancers driven by IL-7 receptor and pre-BCR signaling. Some of these transcription factors include E2A, which binds to both enhancers (Inlay 2004), NF-κB, which binds Eκi (Shaffer et al. 1997; Sen et al. 1986), and Pax5, which binds 3'Eκ and has been shown to be necessary for *kappa* rearrangements (Geier et al. 2006). Binding of each of these transcription factors to the *kappa* locus enhancers is differentially regulated as cells develop in the bone marrow.

The transcription factor NF-κB is made up of homo- and heterodimerized Rel family members (Geier et al. 2006). NF-κB exclusively binds Eκi and not 3'Eκ. At the pre-B stage, NF-κB is highly expressed, as shown by our group and others (Cadera et al. 2009; Derudder et al. 2009). Additionally, NF-κB has been shown to be involved in *kappa* locus activation, however it is not essential, as seen by targeted mutation of the κB binding site (Inlay 2004). NF-κB is negatively regulated by the inhibitor, IκBα (Chiao et al. 1994). IκBα sequesters NF-κB in the cytoplasm, blocking it from exerting transcriptional activity on its targets in the nucleus. Interestingly, IκBα is in a negative feed-back loop with NF-κB (Cadera et al. 2009). Together, NF-κB and IκBα expression correlate with κGT and light chain gene rearrangements in pre-B cells.

NF-κB has been shown to regulate expression of several miRNAs (Boldin et al. 2012). NF-κB expression can also be modulated by miRNAs induced by alternative signaling pathways. Specifically, miRNAs directly target kinases that activate NF-κB expression. For example, Ikk2, a known activator of NF-κB, has been shown to be directly targeted by miRNAs such as miR199a and miR218 in epithelial ovarian cells and glial cells respectively (Boldin et al. 2012). Since NF-κB has also been shown to directly regulate expression of miRNAs, it is no surprise that NF-κB may be involved in NF-κB-miRNA feedback loops (Boldin et al. 2012).

The transcription factor E2A binds both Eκi and 3'Eκ. Two E2A binding sites in Eκi are essential for V-to-Jκ rearrangements. The E2A gene can be alternatively spliced to encode two different proteins, E12 and E47 (Kee et al. 2009). These two proteins are highly similar and both contain the protein dimerization domain known as the helix-loop-

helix (HLH) domain. E2A transcriptionally activates its targets by acting as a homodimer and binding to DNA.

The inhibitors of differentiation (Id) proteins are direct inhibitors of E2A binding activity. The Id proteins have an HLH domain (Kee et al. 2009), however they lack the DNA binding domain. Therefore, by heterodimerizing with E2A proteins through the HLH domain, Id proteins block E2A protein DNA binding activity. Id2 and Id3 have both been shown to interact with E2A proteins in the B and T cell lineages (Kee et al. 2009; Ji et al. 2011).

Stat5 has recently been shown to bind Eκi and directly repress the *kappa* locus. Stat5 binds to Eκi upon IL-7R signaling and with it recruits Ezh2. Ezh2 targets repressive histone methylation marks to the locus. Together, Stat5 and Ezh2 block the overlapping E2A binding sites in Eκi (Mandal et al. 2009; Mandal et al. 2011; Johnson et al. 2008). Stat5 activity is repressed upon attenuation of the IL-7 signal leading to loss of the methylation marks on the locus, allowing for E2A to bind Eκi.

In these studies we attempt to elucidate the pathways by which miR290-5p and miR292-5p act to regulate *kappa* locus activation. By EMSA analysis we determined that miR290-5p/292-5p expression enhances E2A and NF-κB DNA binding activity. We further determined that inhibitors of both transcription factors were regulated by the miR290-5p/292-5p pathway. We propose that miR290-5p and miR292-5p activate the *kappa* locus through both the E2A and NF-κB pathways.

Materials and Methods

EMSA

EMSA was conducted as previously described (Kuo et al. 2011). Probes were generated from annealed oligonucleotides, labeled with ^{32}P. Reactions included 10μg nuclear extracts from HF4 AMuLV cells incubated with ^{32}P-labeled probe.

ChIP

Chromatin Immunoprecipitation (ChIP) was conducted as previously described (Kuo et al. 2011). Recovered DNA was resuspended in 100μl water. Primers used for PCR analysis of recovered DNA were as follows:
Eκi F' TTAAGGCCTGTCCATACAGT;
Eκi R' ATGTTTGGGAGTCTGAACAC.

qRT-PCR

Total RNA was isolated with Trizol Reagent (Invitrogen) and reverse transcription was performed with random hexamers and Moloney MLV reverse Transcriptase (MMLV) (Invitrogen). Quantitative reverse transcription PCR (qRT-PCR) was performed with Jumpstart *Taq* (Sigma), EvaGreen (Biotium), on an ABI 7300 Thermocycler (Applied Biosystems). PCR amplification was as follows: 95C 3min, 95C 30sec, 60C 30 sec, 72C 30 sec (data collection), for 40 cycles. Primers used in this study were previously described (Amin et al. 2009); Id3 primers were designed by John Curry: Id3 271F and Id3 526R. Id3-specific PCR amplification was as follows: 95C 3min, 95C 30sec, 60C 30 sec, 72C 30 sec, 82C 28sec (data collection), for 40 cycles.

Immunoblot

Total protein lysate was isolated with RIPA buffer (1XPBS, 1% NP-40, 0.5% Sodium Deoxycholate, 0.1% SDS, 1mM DTT, Protease Inhibitors). Antibodies used were as follows: anti-IκBα, Santa Cruz (sc-371); anti-Id2, Santa Cruz (sc-489); anti-Tubulin, Calbiochem (cp06); anti-Actin, Santa Cruz (sc-1615).

Luciferase Assay

Dual luciferase assay with the Psicheck2 vector (Fig. 3.25). IκBα wild-type and mutant 3'UTRs were cloned into the XhoI and NotI sites downstream of the renilla luciferase gene in the psicheck2 vector. miR290-5p/miR292-5p binding site was mutated by introducing a SacI restriction enzyme site. IκBα 3'UTR wild-type sequence:
TCGAGTCGACAGTGGAAAGTGGCAAAAAGAATGTGGACTTGTATATTTGTAC
AAATAGAGTTTTATTTTTCTGC;
IκBα 3'UTR mutant sequence:
TCGAGTCGACAGTGGAAAGTGGCAAAAAGAATGTGGACTTGTATATTTGTAC
AAATAGAGAGCTCTTTTTCTGC.
miRNA mimcs used were as follows:
scramble miRNA: Allstars negative control miRNA (Qiagen, 1027281);
miR290-5p mimic: SYN-MMU-MIR290-5P MISCRIPT MIRNA MIMIC (Qiagen, MSY0000366);

miR292-5p mimic: SYN-MMU-MIR292-5P MISCRIPT MIRNA MIMIC (Qiagen, MSY0000369).

Transient transfections of reporter constructs were performed using Lipofectamine 2000 according to the manufacturer's instructions (Invitrogen).

Dual luciferase assays were performed using the Dual-Luciferase Reporter Assay System (Promega). Substrate for Firefly luciferase was first added and quantified followed by addition of Dual-Glo Stop & Glo (Promega) to quench the firefly reaction while adding substrate for the *Renilla* luciferase reaction, at which point it was quantified.

Mutagenesis

Mutagenesis reactions for each 3'UTR was performed in the corresponding wild-type 3'UTR cloned into the psicheck2 vector. 100ng of vector was used as substrate for mutagenesis reactions along with 100ng primer.

Id2 3'UTR mutagenesis (SalI): GGG TTC AGT TAT AAC ATA GCA TAA AAA AAA TCA GTC GAC TGG TTG TCT G

Each mutagenesis reaction was performed using the Quikchange mutagenesis kit (Agilent). Mutagenesis PCR conditions were as follows:

Results

miR290-5p and miR292-5p enhance DNA binding activity of E2A and NF-κB

In an effort to elucidate the pathway through which miR290-5p or miR292-5p induce κGT, we examined transcription factors known to be involved in the induction of κGT by direct binding to either the 3' *kappa* enhancer (3'Eκ) or the *kappa* intronic enhancer (Eκi). Among them, E2A and NF-κB bind Eκi while E2A and Pax5 can bind 3'Eκ (Inlay 2004; Shaffer et al. 1997; Geier et al. 2006). To determine if the induction of κGT by miR290-5p and miR292-5p involves any of these transcription factors we performed electrophoretic mobility shift assays (EMSA). Equal loading of nuclear extracts was determined by Oct1 EMSA (Fig. 3.20).

It was previously reported that upon IL7 withdrawal, the amount of bound E2A increases at Eκi (Johnson et al. 2008) and knockdown of miR290-5p or mir292-5p upon IL7 withdrawal blunts κGT induction, as shown above. So we asked if miR290-5p or miR292-5p expression enhances activation of E2A DNA binding. To address this question we purified nuclear extracts from the E2A+/+ cell lines stably over-expressing either miR290-5p or miR292-5p and performed EMSA using an E2A binding site probe from 3'Eκ. Specificity of the probe for E2A was confirmed by incubating lysates with either anti-E2A antibody or a control IgG antibody ("super-shift" assays). The lysates from cells over-expressing either miR290-5p or miR292-5p alone induced a DNA-protein complex with an intensity comparable to that seen with STI571-treated E2A+/+ cells (Fig. 3.21). When we used extracts from the miR290-5p or miR292-5p stable cell lines treated with STI571 (12hrs, 2.5μM), we saw an even greater increase in the intensity of this protein-DNA complex (Fig. 3.21). These data indicate that induction of miR290-5p and miR292-5p result in increased E2A DNA binding activity.

To determine if the induction of E2A DNA binding activity upon over-expression of miR290-5p or miR292-5p results in its binding to the endogenous Eκi enhancer, we performed Chromatin Immunoprecipitation (ChIP). We made use of the HF4 AMuLV-transformed pro-B cell line generated from a mouse that has a FLAG-tagged E2A knocked into the E2A locus (Kuo et al. 2011; Greenbaum et al. 2002). We stably expressed miR290-5p or miR292-5p in this cell line and performed ChIP with anti-FLAG or anti-IgG antibodies. Using qPCR, we observed increased E2A-FLAG binding to Eκi in both miR290-5p and miR292-5p over-expressing cells (Fig. 3.22). These data indicate that miR290-5p or miR292-5p expression induces binding of E2A to Eκi of the *kappa* locus.

NF-κB, like E2A, binds Eκi within the *kappa* locus (Shaffer et al. 1997). Since miR290-5p or miR292-5p over-expression enhances E2A DNA binding activity, we examined whether NF-κB binding activity increases when these two miRNAs are expressed in E2A+/+ AMuLV lines. We performed an EMSA using the same lysates described above, using an Eκi probe with an NF-κB binding site. Specificity of the probe for NF-κB was confirmed by incubating lysates with either anti-NF-κB antibody or an IgG control. We

did not observe an increase in the amount of the specific NF-κB-DNA complex using lysates from miR290-5p or miR292-5p over-expressing AMuLV-transformed cells (Fig. 3.23). However, when we performed the binding reaction using nuclear extracts from the miR290-5p or miR292-5p transduced cell line treated with STI571 (12hrs, 2.5μM), we saw an enhanced increase in the amount of protein-DNA complex (Fig. 3.23). This suggests that either miR290-5p or miR292-5p expression alone are not enough to induce NF-κB DNA binding to the Eκi probe. Enhanced DNA binding of NF-κB to the Eκi probe requires a second signal such as that from STI571. The binding of E2A and NF-κB to probes for enhancers of the *kappa* locus as seen by EMSA was specific to these two transcription factors, as another transcription factor known to bind the *kappa* locus at this stage, Pax5 (Shaffer et al. 1997; Geier et al. 2006), did not produce a gel shift complex under the conditions described above (Fig. 3.24).

The transcription factor, Stat5 directly binds a site within Eκi (Mandal et al. 2009; Mandal et al. 2011; Johnson et al. 2008). Although, Stat5 transcript levels have not been described as changing in the pro-B to pre-B transition, this does not discard the possibility that miRNAs may be curtailing a potential induction of Stat5 at the pre-B stage. To account for this possibility, we performed a luciferase assay with the Stat5a 3'UTR using a dual luciferase vector in the presence of the miRNAs. Stat5a has binding sites for miR290-5p/miR292-5p in the 3'UTR. We therefore cloned the wild-type Stat5a 3'UTR downstream of the Renilla luciferase gene to use renilla expression as a readout for Stat5a 3'UTR stability (Fig. 3.25). As a negative control, we separately cloned in the Stat5a 3'UTR that was mutated at the miR290-5p/miR292-5p binding site. We transiently transfected either reporter construct into E2A+/+ cells stably over-expressing miR129-2_3p, miR290-5p or miR292-5p (Fig. 3.26). We then used lysates from these cells, 24 hours post-transfection, to perform luciferase assays for both the renilla reporter and the firefly transfection control. We did not observe an effect on the Stat5a 3'UTR by miR290-5p or miR292-5p, as measured by renilla luciferase activity (Fig. 3.27).

Elucidation of E2A and NF-κB pathway components regulated by miR290-5p/miR292-5p

We determined that both E2A and NF-κB had increased DNA binding activity upon miR290-5p/miR292-5p over-expression. To elucidate the pathway through which miR290-5p and miR292-5p induce DNA binding of E2A and NF-κB, we examined factors upstream of them. We sought to determine whether the upstream factors may be direct targets of the miRNAs or regulated indirectly by the miRNAs.

To examine upstream pathway components of NF-κB, we first focused on a known inhibitor, IκBα (Chiao et al. 1994). To address if IκBα is regulated by miR290-5p/miR292-5p we harvested total cell lysates from the E2A+/+ cell lines stably over-expressing either miR290-5p or miR292-5p in the absence or presence of STI571 (2.5μM, 12hr). We used these lysates to perform immunoblot analysis using anti-IκBα and anti-Tubulin antibodies. We observed that IκBα protein levels are repressed upon

miR290-5p or miR292-5p over-expression (Fig. 3.28). These data support that members of this pathway may be regulated by miR290-5p/292-5p.

To confirm that IκBα repression by miR290-5p/miR292-5p was not an artifact of over-expression, we analyzed IκBα protein levels upon miR290-5p/miR292-5p knockdown using the sponge constructs described above. We used the E2A+/+ cell lines stably expressing sponges specific to miR129-2_3p (negative control), miR290-5p, or miR292-5p and performed STI571 (2.5μM) time course experiments. We used these lysates to perform immunoblot analysis using anti-IκBα and anti-Tubulin antibodies. We observed that IκBα protein levels are repressed between 4-6 hours of STI571 treatment in the miR129-2_3p negative control and then increase again by 12 hours (Fig. 3.29). However, we observed that protein levels for IκBα are not repressed upon miR290-5p or miR292-5p knockdown at the 4-6 hour time points (Fig. 3.29). This data, together with the over-expression immunoblot data, indicate that IκBα expression is regulated by miR290-5p/miR292-5p.

To consider IκBα as a direct target of miR290-5p/miR292-5p we performed luciferase assays with the IκBα 3'UTR using a dual luciferase vector in the presence of the miRNAs. IκBα has binding sites for miR290-5p/miR292-5p in exon 4 of the IκBα mRNA as well as in the 3'UTR. As previously noted, miRNAs conventionally target the 3'UTR of the target transcripts (Filipowicz et al. 2008). We therefore cloned the wild-type IκBα 3'UTR downstream of the Renilla luciferase gene to use renilla expression as a readout for IκBα 3'UTR stability. As a negative control, we separately cloned in the IκBα 3'UTR that was mutated at the miR290-5p/miR292-5p binding site. We transiently transfected either reporter construct along with a scramble miRNA, miR290-5p or miR292-5p into HEK293 cells (Fig. 3.26). We then used lysates from these cells, 24 hours post-transfection, to perform luciferase assays for both the renilla reporter and the firefly transfection control. We did not observe an effect on the IκBα 3'UTR by miR290-5p or miR292-5p (Fig. 3.30), as measured by renilla luciferase activity. Interestingly, there is a predicted binding site for miR290-5p/miR292-5p in exon 4 of the IκBα mRNA that we have not explored.

To examine upstream pathway components of E2A, we first examined known inhibitors Id2 and Id3 (Kee et al. 2009). To address if Id2 and Id3 are regulated by miR290-5p/miR292-5p we harvested total cell lysates from the E2A+/+ cell lines stably over-expressing either miR290-5p or miR292-5p in the absence or presence of STI571 (2.5μM, 14hr). We used these lysates to perform immunoblot analysis using anti-Id2, anti-Id3, and anti-Actin antibodies. We observed repression of Id2 protein levels upon miR290-5p or miR292-5p over-expression (Fig. 3.31), indicating that members of this pathway are regulated by miR290-5p/292-5p. Id3 protein levels were not readily detectable by immunoblot.

To address if Id3 is regulated by miR290-5p/miR292-5p we harvested RNA from the E2A+/+ cell lines stably over-expressing either miR290-5p or miR292-5p in the absence

or presence of STI571 (2.5μM, 14hr). We then generated cDNA to perform qPCR analysis using Id3 primers and Hprt primers for normalization. The effect of miR290-5p/miR292-5p over-expression on Id3 transcripts was inconsistent (Fig. 3.32). In two out of the three biological replicates performed, there was no effect observed (Fig. 3.25 Bottom Panel), while in the third replicate Id3 was repressed upon miR290-5p/miR292-5p over-expression (Fig. 3.32 Top Panel). This indicates that indirect regulation of Id3 by miR290-5p/miR292-5p may exist.

To consider Id2 as a direct target of miR290-5p/miR292-5p we performed luciferase assays with the Id2 3'UTR using a dual luciferase vector in the presence of the miRNAs. Id2 has binding sites for miR290-5p/miR292-5p in the 3'UTR. We therefore cloned the wild-type Id2 3'UTR downstream of the Renilla luciferase gene to use renilla expression as a readout for Id2 3'UTR stability. As a negative control, we separately cloned in the Id2 3'UTR that was mutated at the miR290-5p/miR292-5p binding site. We transiently transfected either reporter construct along with a scramble miRNA, miR290-5p or miR292-5p into HEK293 cells. We then used lysates from these cells, 24 hours post-transfection, to perform luciferase assays for both the renilla reporter and the firefly transfection control. We did not observe an effect on the Id2 3'UTR by miR290-5p or miR292-5p (Fig. 3.33), as measured by renilla luciferase activity.

Together these data indicate that miR290-5p/292-5p-regulated *kappa* locus activation occurs through activation of the E2A and NF-κB pathways.

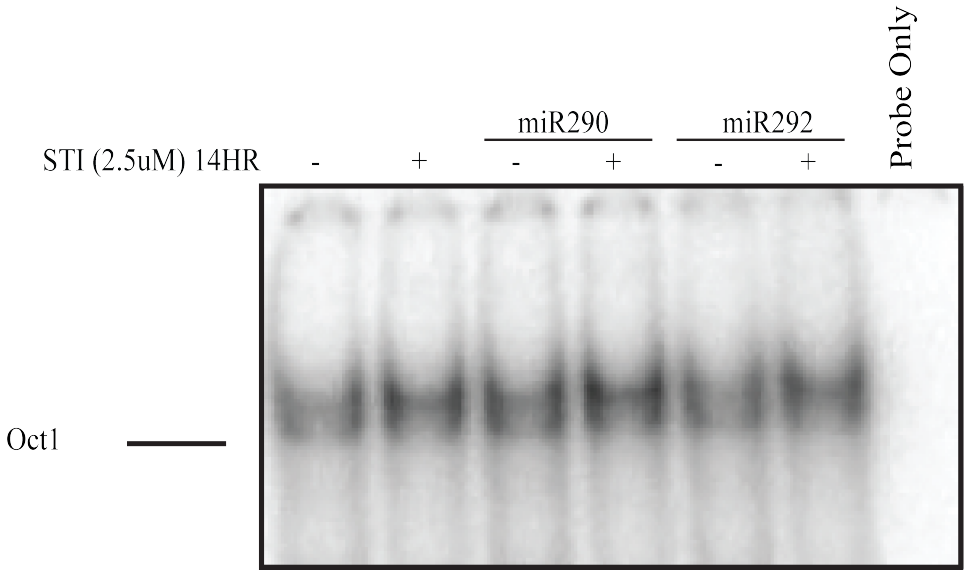

Figure 3.20. **miR290-5p and miR292-5p Over-expression do not enhance Oct1 DNA binding activity.** EMSA analysis of nuclear extracts from E2A+/+ AMuLV cells expressing either miR290-5p or miR292-5p and cultured in either the absence or presence of STI571 (2.5mM, 12hr). Lysates were incubated with ^{32}P-labeled Oct1 probe, and analyzed on EMSA. The line indicates the specific Oct1-DNA complex.

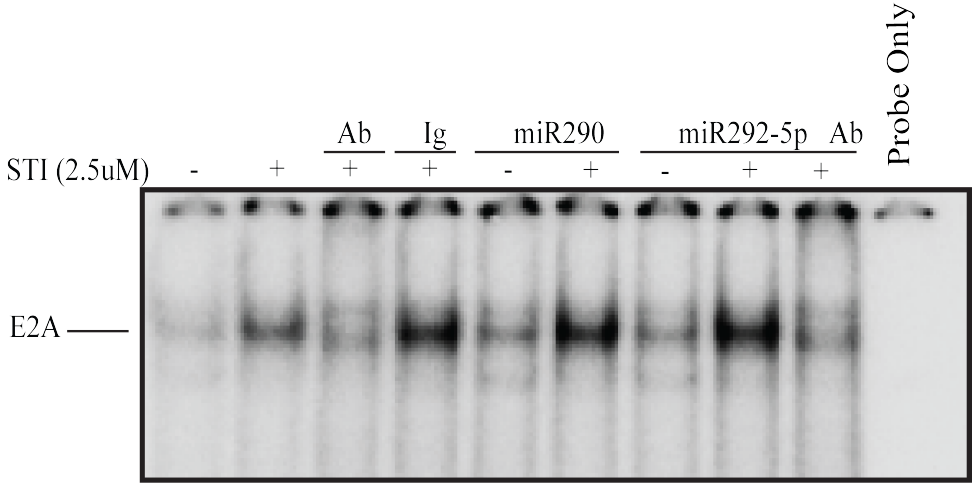

Figure 3.21. **Over-expression of miR290-5p or miR292-5p induces DNA binding activity of E2A.** EMSA analysis of nuclear extracts from E2A+/+ AMuLV cells expressing miR290-5p or miR292-5p and cultured in either the absence or presence of STI571 (2.5mM, 12hr). Lysates were incubated with ^{32}P-labeled 3'Eκ probe with an E2A binding site, and analyzed on EMSA. Lysates were incubated with an anti-E2A antibody (Ab) or a control IgG antibody (IgG), to confirm complex specificity. The line indicates the specific E2A-DNA complex. This experiment is representative of two independent experiments.

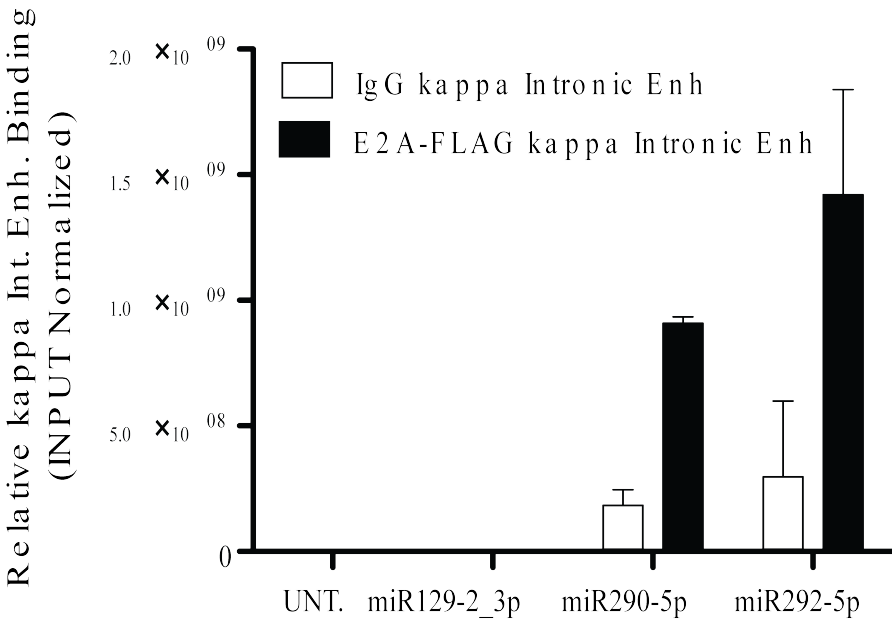

Figure 3.22. **Over-expression of miR290-5p or miR292-5p induces E2A binding to Eκi.** ChIP analysis of HF4 AMuLV cells expressing His-FLAG-E2A, at endogenous levels, and over-expressing either miR129-2_3p, miR290-5p, or mir292-5p. Chromatin samples were immunoprecipitated with anti-FLAG or IgG control antibody. Relative enrichment of bound DNA over Input was determined by subjecting precipitates to qPCR with primers specific to the Eκi binding region for E2A. This experiment is representative of two independent experiments.

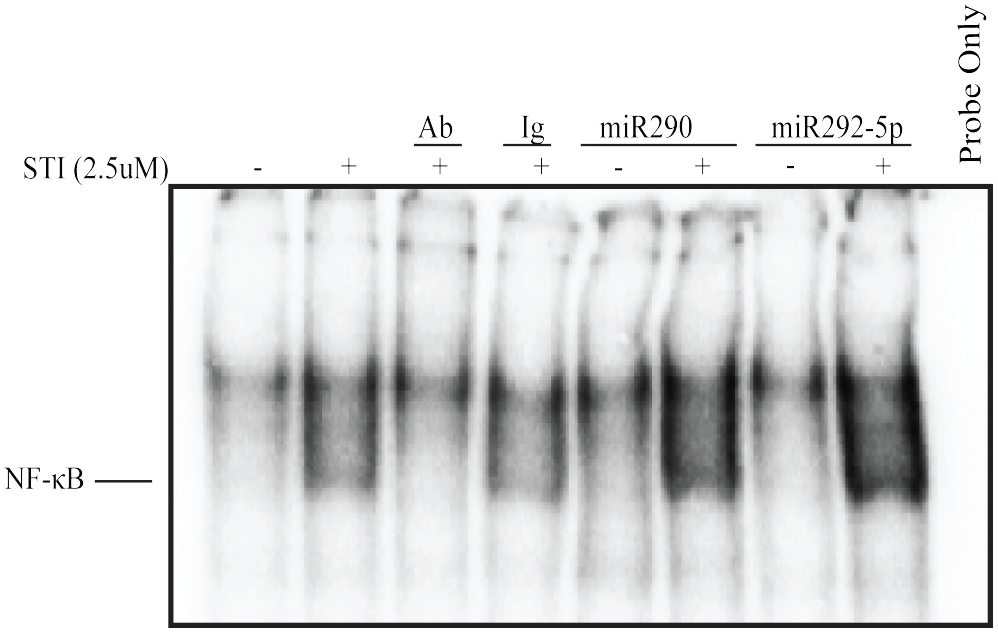

Figure 3.23. **Over-expression of miR290-5p or miR292-5p induces DNA binding activity of NF-κB.** EMSA analysis of nuclear extracts from E2A+/+ AMuLV cells expressing either miR290-5p or miR292-5p and cultured in either the absence or presence of STI571 (2.5μM, 12hr). Lysates were incubated with a ^{32}P-labeled Eκi probe containing an NF-κB binding site, and analyzed on EMSA. Lysates were incubated with an anti-p65 antibody (Ab) or a control IgG antibody (IgG), to confirm complex specificity. The line indicates the specific NF-κB-DNA complex. This experiment is representative of two independent experiments.

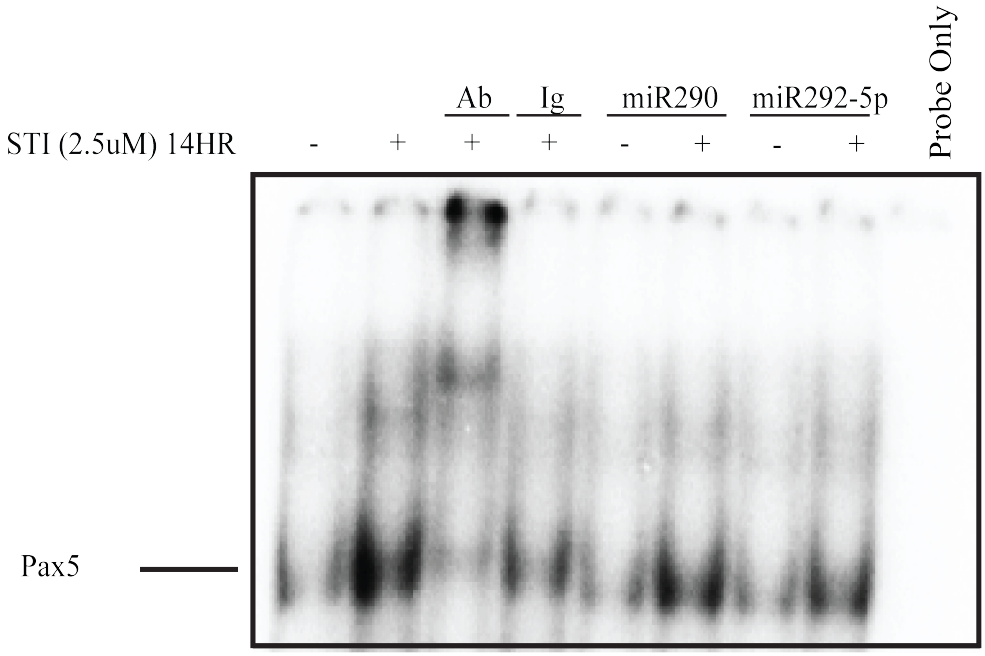

Figure 3.24. **Over-expression of miR290-5p or miR292-5p do not induce Pax5 DNA binding activity.** EMSA analysis of nuclear extracts from E2A+/+ AMuLV cells expressing either miR290-5p or miR292-5p and cultured in either the absence or presence of STI571 (2.5μM, 12hr). Lysates were incubated with a ^{32}P-labeled Pax5 binding site probe, and analyzed on EMSA. Lysates were incubated with an anti-Pax5 antibody (Ab) or a control IgG antibody (IgG), to confirm complex specificity. The line indicates the specific Pax5-DNA complex.

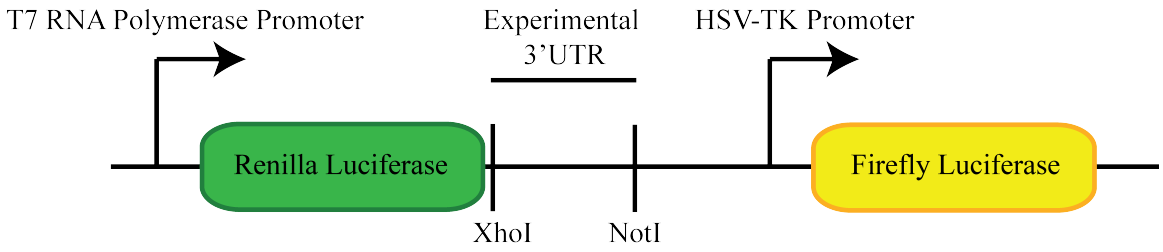

Figure 3.25. **Diagram of the dual luciferase vector.** Wild-type or mutant experimental 3'UTR is cloned downstream of the Renilla luciferase gene. Firefly luciferase is transient transfection normalization control.

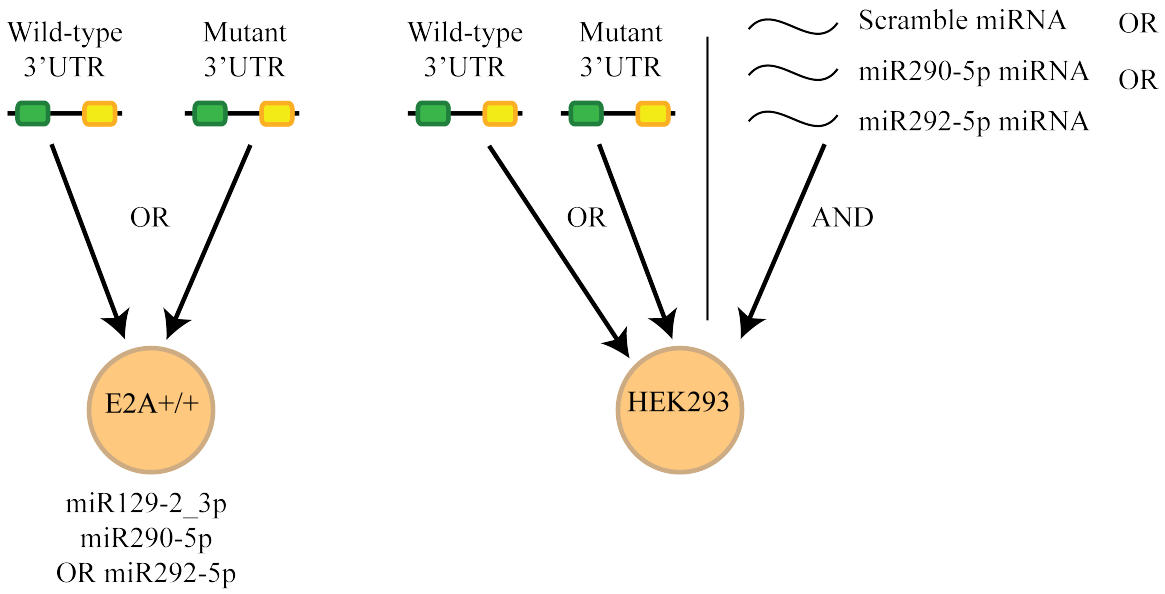

Figure 3.26. **Diagram of the Dual Luciferase assay.**
On the left side, the wild-type or mutant 3'UTR of interest cloned into the dual luciferase reporter is transiently transfected into E2A+/+ AMuLV cells stably over-expressing miR129-2_3p, miR290-5p, or miR292-5p. On the right side, the wild-type or mutant 3'UTR of interest cloned into the dual luciferase reporter is transiently transfected with either a scramble miRNA, miR290-5p or miR292-5p mimic into HEK293 cells.

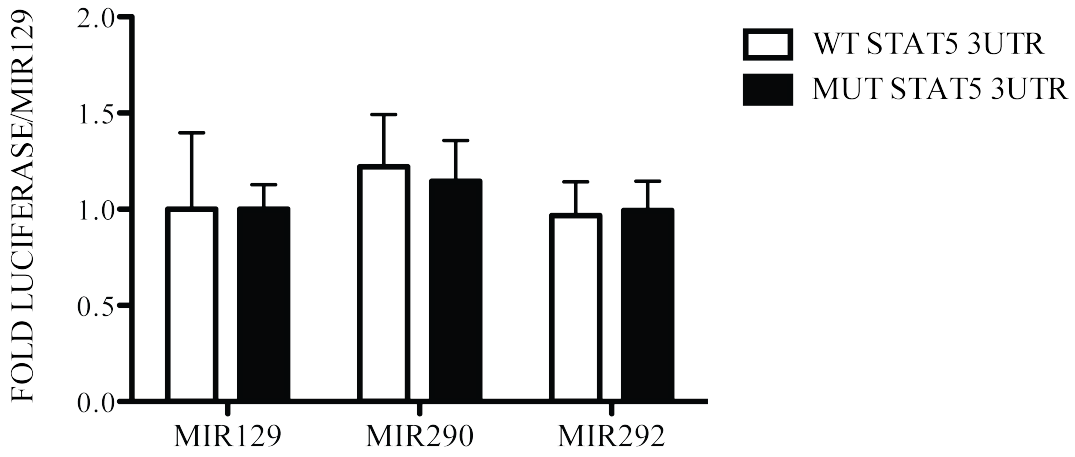

Figure 3.27. **miR290-5p and miR292-5p do not directly target the Stat5 3'UTR.** Luciferase assay of total cell lysates from E2A+/+ cells stably over-expressing miR129-2_3p, miR290-5p or miR292-5p and transiently transduced with either a wild-type STAT5 3'UTR reporter or a mutant STAT5 3'UTR reporter. Error bars represent range for biological replicate luciferase reactions. Data represents at least three independent experiments.

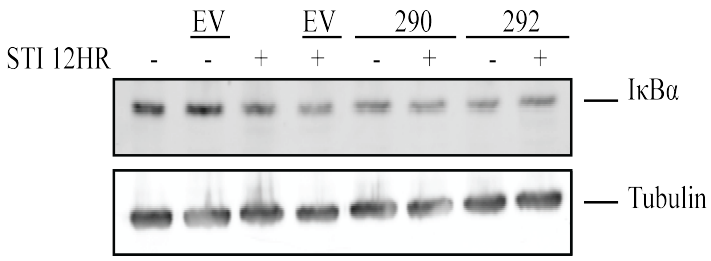

Figure 3.28. **IκBα protein levels are repressed upon miR290-5p or miR292-5p over-expression.** Immunoblot analysis of E2A+/+ AMuLV cells expressing either an empty vector control, miR290-5p, or miR292-5p and cultured in either the absence or presence of STI571 (2.5mM, 12hr). Immunoblot was probed with anti-IκBα and anti-Tubulin antibodies.

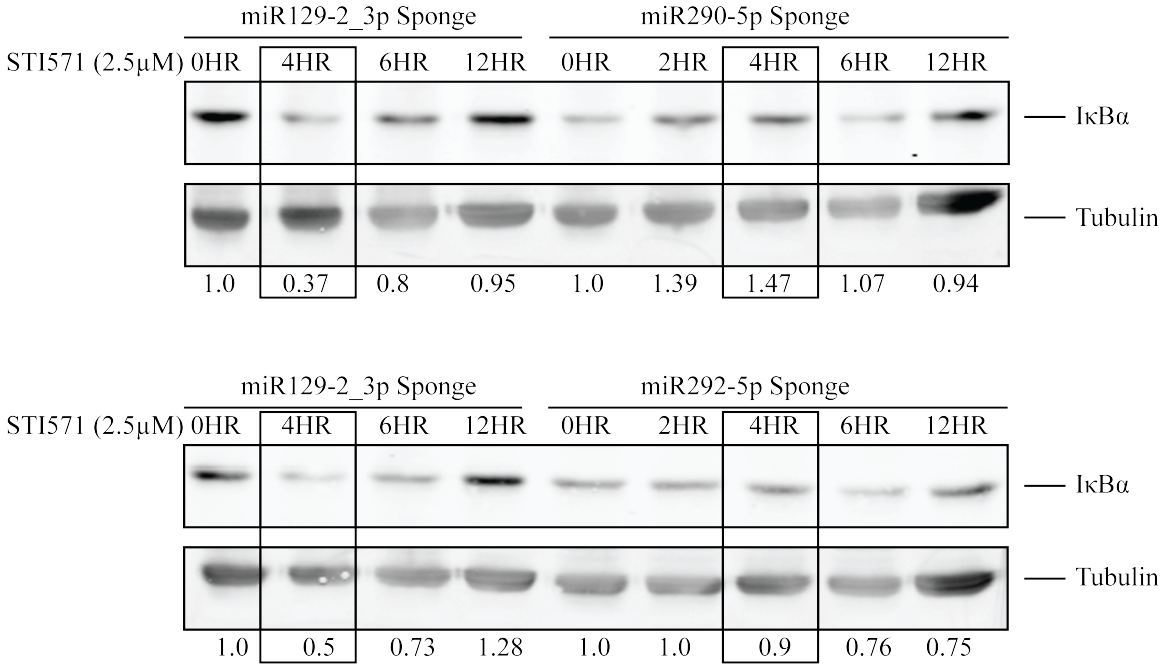

Figure 3.29. **IκBα protein levels are not repressed upon STI571 treatment under knockdown of miR290-5p or miR292-5p.** Immunoblot analysis of E2A+/+ AMuLV cells expressing a miR290-5p or miR292-5p sponge knockdown construct, and cultured in the presence of STI571 (2.5μM) for the indicated lengths of time. Immunoblot was probed with anti-IκBα and anti-Tubulin antibodies. IκBα band intensity was normalized to corresponding Tubulin band intensity. The untreated (time-point '0HR') was set to a value 1.0 and all other values are relative to this sample. These data represent at least two independently performed experiments.

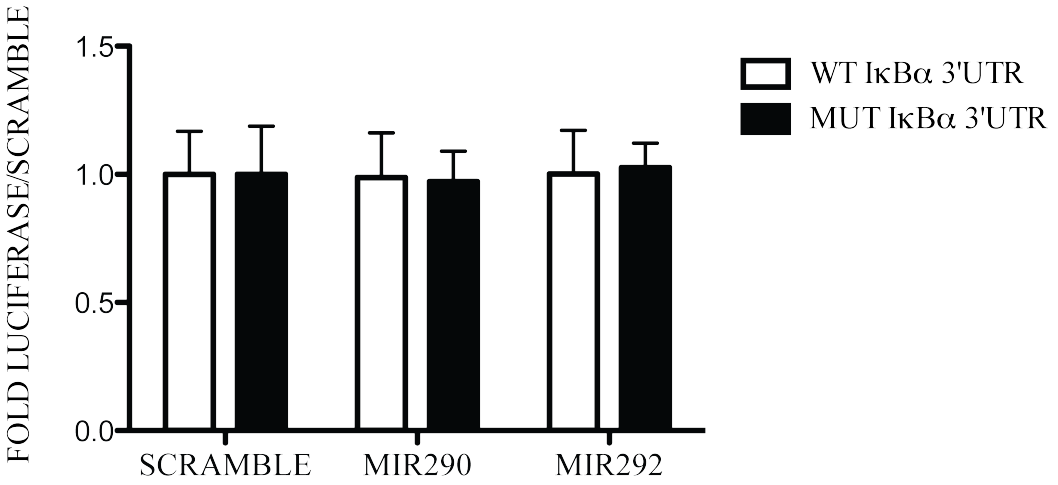

Figure 3.30. **miR290-5p and miR292-5p do not directly target the IκBα 3'UTR.** Luciferase assay of total cell lysates from HEK293 cells transiently transfected with either a wild-type IκBα 3'UTR reporter or a mutant IκBα 3'UTR reporter along with a scramble miRNA, mir290-5p or miR292-5p. Error bars represent range for biological replicate luciferase reactions. Data represents at least three independent experiments.

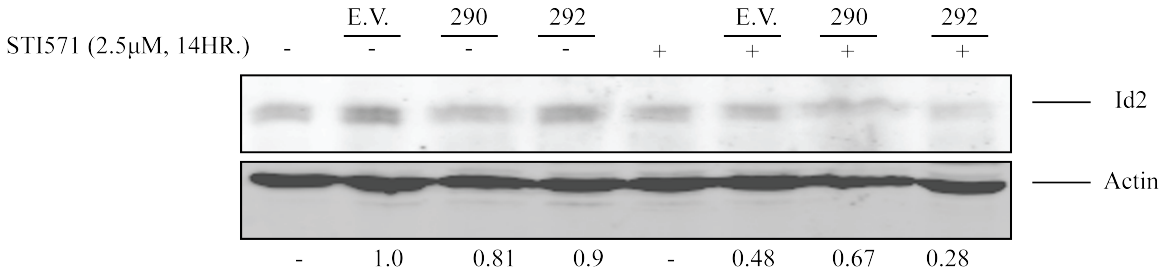

Figure 3.31. **Id2 protein levels are repressed upon miR290-5p or miR292-5p over-expression.** Immunoblot analysis of E2A+/+ AMuLV cells expressing either an empty vector control, miR290-5p, or miR292-5p and cultured in either the absence or presence of STI571 (2.5mM, 12hr). Immunoblot was probed with anti-Id2 and anti-Tubulin antibodies.

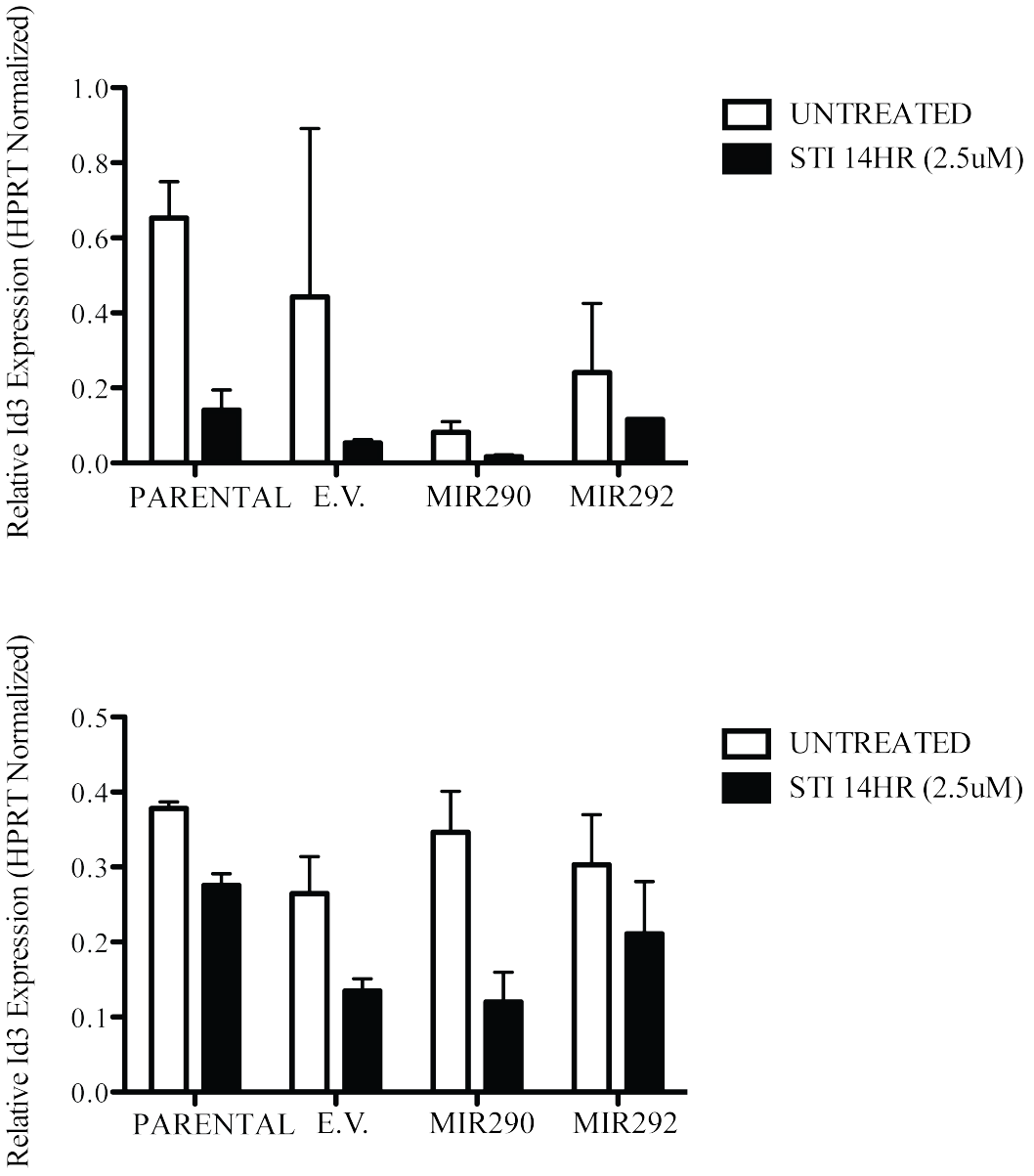

Figure 3.32. **miR290-5p and miR292-5p over-expression inconsistently repressed Id3 expression.** qPCR analysis of Id2 expression in RNA purified from E2A+/+ AMuLV cells over-expressing either miR290-5p or miR292-5p, cultured in the absence or presence of STI571 (2.5μM, 12hr). Data was normalized to the expression of HPRT. Top panel represents an example of Id3 repression. Bottom panel represents an example of "no effect" on Id3 expression. Error bars represent range for replicate qPCR reactions. Data represents at least four individual experiments.

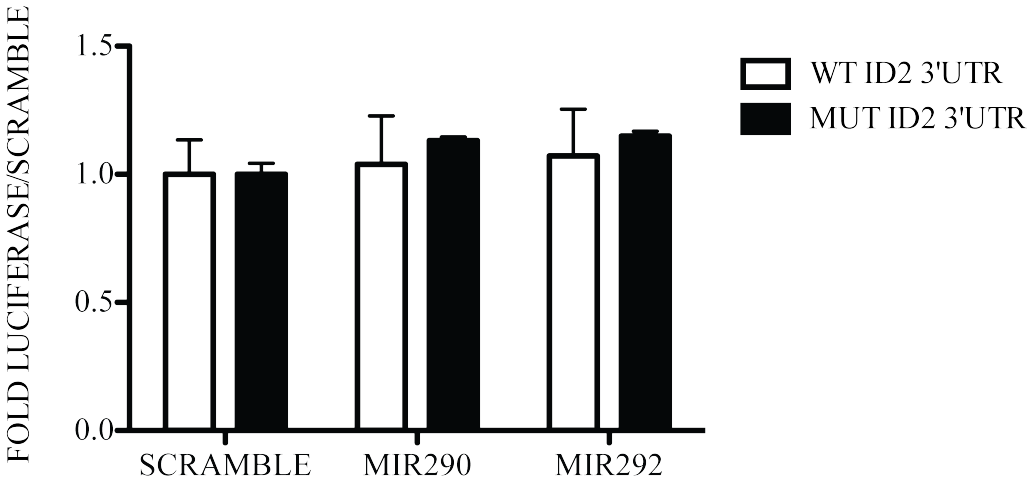

Figure 3.33. **miR290-5p and miR292-5p do not directly target the Id2 3'UTR.** Luciferase assay of total cell lysates from HEK293 cells transiently transfected with either a wild-type Id2 3'UTR reporter or a mutant Id2 3'UTR reporter along with a scramble miRNA, miR290-5p or miR292-5p. Error bars represent range for biological replicate luciferase reactions. Data represents at least three independent experiments.

Discussion

Previous work showed that IL-7 attenuation allows for induction of κGT by relieving Stat5 inhibition of E2A binding to Eκi (Johnson et al. 2008). Here, we propose that E2A activation, upon IL-7 attenuation, is regulated through miR290-5p/292-5p expression. We observed that over-expression of miR290-5p or miR292-5p in E2A+/+ AMuLV cells induced DNA binding activity of the E2A transcription factor. We also noted that over-expression of miR290-5p or miR292-5p in the same cells enhanced *in vivo* binding of E2A to Eκi. Therefore, we propose that miR290-5p/292-5p expression, upon loss of IL-7 signaling leads to increased E2A DNA binding activity and increased κGT.

The E2A inhibitors, Id2 and Id3 (Kee et al. 2009), are interesting candidates for direct targeting by miR290-5p/292-5p. In our studies we observed a decrease in Id2 protein expression upon miR290-5p/292-5p over-expression. When we combined miR292-5p over-expression with STI571 treatment the decrease was enhanced, indicating that this protein is in the miR290-5p/292-5p pathway. However, when we quantified Id3 expression upon miR290-5p or miR292-5p over-expression, the results were inconsistent. This could indicate that Id2 is the relevant protein regulated by the miR290-5p/292-5p pathway to activate E2A DNA binding activity. Despite having predicted miR290-5p/292-5p binding sites in its 3'UTR, the mRNA encoding Id2 was not directly repressed by these miRNAs in 3'UTR dual-luciferase studies. This points to an upstream component being directly regulated by miR290-5p/miR292-5p.

NF-κB, has been shown, by our group and others, to be highly expressed at the pre-B stage (Cadera et al. 2009; Derudder et al. 2009). We reported a correlation between the expression of both NF-κB and its inhibitor, IκBα, with κGT and light chain gene rearrangements. Here we propose that NF-κB activation is regulated through miR290-5p/292-5p expression at the pre-B stage. We observed that over-expression of miR290-5p or miR292-5p in E2A+/+ AMuLV cells induced DNA binding activity of NF-κB to an Eκi probe. We have already established that miR290-5p/292-5p expression is induced upon IL-7 attenuation, implicating that the NF-κB pathway is possibly regulated through this signaling as well.

The NF-κB inhibitor, IκBα (Chiao et al. 1994), is another interesting candidate for direct targeting by miR290-5p/292-5p. In our studies we observed a decrease in IκBα protein expression upon miR290-5p/292-5p over-expression. Interestingly, in miR290-5p/292-5 knockdown experiments, we observed that at 4hr STI IκBα protein expression was not as repressed as in the negative control knockdown experiment. This indicates that IκBα expression is regulated by miR290-5p/292-5p induction. However, it is interesting to note that at a longer STI-treatment time-point, IκBα protein levels increase again. The fluctuating expression of IκBα observed is expected, as it is in a feed-back loop with NF-κB. Yet, from this data, we propose that miR290-5p/292-5p induction by STI571 regulates IκBα at an initial early step in this loop. This makes IκBα an interesting candidate for direct targeting, since miRNAs are notorious for having immediate effects to induce a transition in development.

Given these observations, we considered IκBα as a logical direct target of miR290-5p/292-5p. Despite having predicted miR290-5p/miR292-5p binding sites in its 3'UTR, mRNA encoding IκBα was not directly repressed by these miRNAs in 3'UTR dual-luciferase studies. Likewise, E2A inhibitor, Id2 (Kee et al. 2009), was not repressed by the miRNAs in dual-luciferase studies as described above. It is possible that the target of miR290-5p/miR292-5p is an unknown inhibitor of one or both of these transcription factors, or a factor that is further upstream in the pathway. In the case for IκBα, there is an additional predicted binding site for miR290-5p/292-5p in exon 4 of the IκBα mRNA. Although, there have been a few reports supporting that miRNAs may regulate their targets through exonic interactions, we have not yet pursued this possibility. In conclusion, additional studies are necessary to identify the relevant direct targets of these miRNAs in pre-B cells.

Chapter 4: Exploring miR290-5p and miR292-5p direct targets at the pre-B stage of B cell Development.

Background:

miRNAs traditionally regulate their direct target transcripts by repressing their partially sequence-matched 3'UTRs (Filipowicz et al. 2008). However, one group has reported that miRNAs can posttranscriptionally activate expression of their target mRNAs, by the same miRNA-mRNA mediated sequence-matched rules (Mortensen et al. 2011; Vasudevan et al. 2007). This proposed method of miRNA-target regulation has been controversial in the field and there have only been a few reports to support it.

In these reports, Vasudevan et al (Vasudevan et al. 2007; Mortensen et al. 2011) describe miRNA-mediated target activation as occurring in cells that are in cell-cycle arrest. They describe Let-7 and miRcxcr4, which had previously been reported to repress their target transcripts in other systems, as activating the same target mRNA transcripts in cell-cycle arrested instances. They further report that the mechanism by which this switch in regulation occurs, from repression to activation, is through AU-rich elements (ARE) in the 3'UTR.

At the pro-B to pre-B transition, developing B cells arrest at a G0-like state in order to rearrange the immunoglobulin light chain loci. Therefore, we take into consideration the possibility that miR290-5p and miR292-5p may be activating their target transcripts at the pre-B stage. We consider this without discarding consideration for the canonical miRNA repression mechanism that miR290-5p/miR292-5p may be acting through.

Blimp1/Prdm1

Blimp1 (Prdm1), a zinc finger transcription factor, has been well characterized as a repressive factor in many systems, including mature B cells (Ji et al. 2011; Shaffer et al. 2002). Specifically, it has been described as a master regulator of terminal B-cell differentiation. In mature B cells, Blimp1 expression drives mature B cells to plasma cells by repressing the transcription factor Bcl6 as well as targeting c-myc (Lin et al. 2000), Id3 (Ji et al. 2011), Pax5 (Lin et al. 2002) and Spi-B (Shaffer et al. 2002).

Recently, Blimp1 has also been implicated in the E2A-Id axis (Ji et al. 2011). Blimp1 binds to and represses the Id3 promoter in CD8+ T cells, allowing E2A to help drive the cells into short-lived effector T cells (SLECs). While Blimp1 expression has been shown to regulate differentiation in many systems, its role in the pro-B to pre-B transition of B cell development is not known.

Pim1

As described above, IL-7 signaling at the pro-B stage promotes proliferation and survival. Upon attenuation of that signal, the cells stops proliferating to prepare for further

recombination at the light chain loci. Pim1 acts at the pro-B stage through IL-7 signaling to promote survival, and upon IL-7 attenuation Pim1 expression decreases (Bednarski et al. 2012). Pim1 expression is critical to proliferation and survival at the pro-B stage. Pim1 knockout mice show a block in B cell development at the pro-B to pre-B transition. However, the block is not as dramatic as the pro-B to pre-B block observed in IL-7 receptor knockout mice (Milne et al. 2004). This indicates that other pathways and mechanisms exist to compensate for the loss of Pim1 at this stage.

In these studies we attempt to elucidate the direct targets by which miR290-5p and miR292-5p act to regulate *kappa* locus activation. We first observed Blimp1 translationally activated in a collaboration to identify translationally regulated genes, in AMuLV cells treated with STI (see Appendix Gradient Encoding). We examined the role of Blimp1 at the pre-B stage of B cell development and found that it may be regulating the E2A-Id3 axis in our system. We also consider upregulated Blimp1 as a direct target of miR292-5p, contrary to the conventional wisdom that miRNAs repress their targets (Vasudevan et al. 2007). We observed that the survival factor Pim1 has miR290-5p/292-5p predicted binding sites and has an expression pattern at the pro-B to pre-B transition that conforms to conventional miRNA-repression regulation. We, therefore, examine the survival factor Pim1 as a potential repressed target of miR290-5p/292-5p at the pre-B stage.

Materials and Methods

qRT-PCR

Total RNA was isolated with Trizol Reagent (Invitrogen) and reverse transcription was performed with random hexamers and Moloney MLV reverse Transcriptase (MMLV) (Invitrogen). Quantitative reverse transcription PCR (qRT-PCR) was performed with Jumpstart *Taq* (Sigma), EvaGreen (Biotium), on an ABI 7300 Thermocycler (Applied Biosystems). PCR amplification was as follows: 95C 3min, 95C 30sec, 60C 30 sec, 72C 30 sec (data collection), for 40 cycles. Primers used in this study are as follows:
Pim1 F1': CTG GAG TCG CAG TAC CAG G;
Pim1 R1': CAG TTC TCC CCA ATC GGA AAT C;
Pim1 F2': TGT CCA AGA TCA ACT CCC TGG;
Pim1 R2': CCA CCT GGT ACT GCG ACT C

Doxycycline Experiments

pFG12-TRE-UbC-rtTA-Thy1.1 vector was used to clone in the Blimp1 cDNA for inducible experiments. E2A+/+ AMuLV cell lines were treated with 1:5000 dilution of 5mg/ml stock doxycycline or 1:5000 dilution of EtOH.

Luciferase Assay

Dual luciferase assay was performed using the Psicheck2 vector. Wild-type and mutant 3'UTRs were cloned into the XhoI and NotI sites downstream of the renilla luciferase gene in the psicheck2 vector. Primers for cloning wild-type 3'UTRs are as follows:
Pim1 3'UTR F: ATC GCT CGA GGG GAC AGC AAT GAC AAC TCA
Pim1 3'UTR R: ATC GGC GGC CGC GTT GTG CGT TCT GTG TGA GG
Blimp1 3'UTR F: ACT GCT CGA GTG AAT CAG GGT GCC TTT AGC
Blimp1 3'UTR R: ACT GGC GGC CGC CTT TTG CAA TGC CCT TTC AT

miRNA mimcs used were the following:
scramble miRNA: Allstars negative control miRNA (Qiagen, 1027281);
miR290-5p mimic: SYN-MMU-MIR290-5P MISCRIPT MIRNA MIMIC (Qiagen, MSY0000366);
miR292-5p mimic: SYN-MMU-MIR292-5P MISCRIPT MIRNA MIMIC (Qiagen, MSY0000369).

Transient transfections of reporter constructs were performed using Lipofectamine 2000 according to the manufacturer's instructions (Invitrogen).

Dual luciferase assays were performed using the Dual-Luciferase Reporter Assay System (Promega). Substrate for Firefly luciferase was first added and quantified followed by addition of Dual-Glo Stop & Glo (Promega) to quench the firefly reaction while adding substrate for the *Renilla* luciferase reaction, at which point it was quantified.

Mutagenesis

Mutagenesis reactions for each 3'UTR was performed in the corresponding wild-type 3'UTR cloned into the psicheck2 vector. 100ng of vector was used as substrate for mutagenesis reactions along with 100ng primer.

Blimp1 3'UTR mutagenesis site1 primer (ClaI): GCT TTA AAA TGA GGT ATC GAT ATT GCC AAA GTC ATG TGG TTG GTG
Blimp1 3'UTR mutagenesis site2 primer (SacI): GTG TGT GTG TGT GGG TTG GGG GGA GCT CGT CTG GCT GTC ATT TTG CTG TTG
Blimp1 3'UTR mutagenesis site3 primer (SpeI): GCT GGT GCC CTA CCA AGA AGG AAC TAG TAT AGA AAG GCT CAG GCC
Blimp1 3'UTR mutagenesis site4 primer (SalI): GAC TGA CAT TTC TGG ATG CAT CTG TAG TCG ACA AAA ATA CTC AC
PIM1 3'UTR mutagenesis (PacI): TGT CGA TGG AAC TTT AGT CAC CAT GGA GAT TAA TTA ACC AAG ATG GGC CGG GG

Each mutagenesis reaction was performed using the Quikchange mutagenesis kit (Agilent). Mutagenesis PCR conditions were as follows:

Results:

Blimp1, the repressive transcription factor first described in plasma cell differentiation, has recently been implicated in regulating the E2A-Id3 axis in SLECs (Ji et al. 2011). To determine if Blimp1 may play a novel role in the pro-B to pre-B transition, we first determined its pattern of expression at this transition. We harvested RNA from E2A+/+ AMuLV cell lines in the absence or presence of STI571 (2.5μM, 14hr). We then generated cDNA to perform qPCR analysis using Blimp1 primers and Hprt primers for normalization. We observed that Blimp1 expression increases upon STI571 treatment (Figure 4.34, Bottom Panel).

To determine if Blimp1 is in the miR290-5p/292-5p pathway at the pre-B stage, we harvested RNA from the E2A+/+ AMuLV cell lines stably over-expressing either an empty vector control, miR290-5p, or miR292-5p in the absence or presence of STI571 (2.5μM, 14hr). We then generated cDNA to perform qPCR analysis for Blimp1 and observed that miR290-5p/miR292-5p over-expression alone induces Blimp1 expression in the AMuLV cells (Figure 4.34, Top Panel). This induction is further increased when miR290-5p/miR292-5p over-expression is combined with STI571 treatment (Figure 4.34, Bottom Panel). These results indicate that Blimp1 expression is induced in AMuLV cells upon STI571-treatment and that it is regulated by the miR290-5p/miR292-5p pathway at the pre-B-like stage.

As mentioned above, Blimp1 has been shown to directly repress the Id3 promoter, thereby activating E2A activity in SLECs (Ji et al. 2011). This same pathway activates κGT in pre-B cells. To consider the possibility that Blimp1 may be acting by way of this pathway, upstream of κGT activation at the pre-B stage of development, we stably over-expressed Blimp1 cDNA in E2A+/+ AMuLV cell lines. We harvested total RNA from E2A+/+ cells over-expressing Blimp1 in the absence or presence of STI571 (2.5μM, 14hr). We then generated cDNA to perform qPCR analysis for κGT. We observed that Blimp1 over-expression alone modestly increased κGT (Figure 4.35). Combined Blimp1 over-expression with STI571 treatment also had a modest increase in κGT over STI571 alone treatment (Figure 4.35). These results were observed in two out of three biological replicates.

To determine if Blimp1 is essential for κGT expression upon STI571 treatment, we stably expressed a dominant-negative version of Blimp1 in E2A+/+ AMuLV cell lines. The dominant-negative Blimp1 (tBlimpDN) consists only of the minimal zinc finger DNA-binding domain (Sciammas et al. 2004). We harvested total RNA from E2A+/+ cells stably expressing tBlimpDN in the absence or presence of STI571 (2.5μM, 14hr). In two out of three biological replicates we observed a blunting of κGT induction upon STI571 treatment in the presence of tBlimpDN (Figure 4.36). Combined with the Blimp1 over-expression results above, this indicates that Blimp1 may be indirectly upstream of κGT activation.

We sought to determine if Blimp1 expression represses Id3 expression in our system, as previously observed in SLECs (Ji et al. 2011). To consider this possibility we cloned Blimp1 cDNA into a Doxycycline-inducible construct. We stably expressed the Dox-inducible Blimp1 cDNA or an empty vector control in E2A+/+ AMuLV cell lines. We harvested total RNA from these cells in the absence or presence of Dox or EtOH (1ug/ml, 16hrs). We observed a decrease in Id3 expression upon Blimp1 induction with Doxycycline (Figure 4.37), but not in the empty vector control. This indicates that Blimp1 may be acting to repress Id3 expression in AMuLV pro-B cells.

To determine how Blimp1 may be regulated by miR290-5p/miR292-5p in AMuLV pro-B cells we considered the possibility that miR290-5p/miR292-5p may be directly regulating the 3'UTR of Blimp1. A few controversial publications have described miRNAs as activating expression of their target transcripts (Mortensen et al. 2011; Vasudevan et al. 2007). We therefore examined the Blimp1 3'UTR for predicted binding sites for miR290-5p/miR292-5p using the Targetscan algorithm. We observed that the Blimp1 3'UTR has two 7mer-1A binding sites for miR290-5p/mir292-5p as well as two less-favorable 5mer binding sites. We mutagenized the wild-type Blimp1 3'UTR for all four predicted binding sites to conduct dual-luciferase assays. We transiently transfected the wild-type or mutagenized reporter construct into E2A+/+ cells stably over-expressing miR129-2_3p or miR292-5p. We then used lysates from these cells, 24 hours post-transfection, to perform luciferase assays for both the renilla reporter and the firefly transfection control. Interestingly, we observed a consistent increase in luciferase expression with the wild-type Blimp1 3'UTR reporter upon miR292-5p over-expression ($p=0.0003$) (Fig. 4.38). This increase was not observed in the mutagenized Blimp1 3'UTR reporter (Fig. 4.38). This indicates that the intact miR290-5p/292-5p binding site in the Blimp1 3'UTR is required to upregulate Blimp1 expression upon miR292-5p expression in AMuLV pro-B cells.

To determine if this observation was a cell-type specific phenomenon, we performed dual luciferase assays for the Blimp1 3'UTR in HEK293 cells. We used the same wild-type and mutagenized Blimp1 3'UTR constructs described above. We transiently transfected either reporter construct along with a scramble miRNA, miR290-5p or miR292-5p into HEK293 cells. We then used lysates from these cells, 24 hours post-transfection, to perform luciferase assays for both the renilla reporter and the firefly transfection control. Intriguingly, we observed a consistent decrease in luciferase expression in the wild-type Blimp1 3'UTR reporter co-transfected with miR292-5p (Fig. 4.39). This decrease was not observed in the mutagenized Blimp1 3'UTR reporter co-transfected with miR292-5p (Fig. 4.39). This result indicates that the miR290-5p/292-5p binding site in the Blimp1 3'UTR is required for miR290-5p/292-5p to exert its mode of regulation on the target transcript Blimp1. However, it also indicates that depending on the cell-type, the specific mode of regulation by miR290-5p/292-5p on the Blimp1 3'UTR can differ.

Pim1 as a Potential Direct Target by miR290-5p/miR292-5p

As mentioned above, our group previously described the change in expression of several B cell-lineage genes in AMuLV cells treated with STI by microarray (Muljo et al. 2003). In order to identify potential targets of miR290-5p/292-5p that conform to the canonical miRNA-mediated repression, we examined that data set for transcripts that were downregulated and had predicted miR290-5p/292-5p binding sites. One such gene, Pim1, conformed to this criteria. Pim1 has a predicted binding site for miR290-5p/292-5p in the 3'UTR as predicted by the algorithm RNA22.

As described above, the IL-7 signal at the pro-B stage promotes proliferation and survival. Pim1 is a factor that promotes survival at the pro-B stage through IL-7 signaling (Bednarski et al. 2012). Upon attenuation of that signal, Pim1 transcripts decrease and proliferation ceases, to prepare the cells for further recombination at the light chain loci. We observed that the Pim1 pattern of expression conforms to conventional miRNA mode of regulation, repression. We therefore sought to determine if Pim1 is repressed by miR290-5p/292-5p either indirectly or directly.

To address if Pim1 is regulated by miR290-5p/292-5p, we harvested RNA from the E2A+/+ cell lines stably over-expressing either miR129-2_3p, miR290-5p, or miR292-5p. We then generated cDNA to perform qPCR analysis for Pim1 and observed that miR290-5p/miR292-5p over-expression alone represses Pim1 expression in the AMuLV cells (Figure 4.40). These results indicate that Pim1 expression is regulated by the STI571-induced miR290-5p/292-5p pathway at the pre-B-like stage.

We then wanted to determine if the Pim1 transcript decrease observed from the pro-B to pre-B transition can be attributed to the miR290-5p/292-5p induction observed at the same transition. To answer this question, we examined Pim1 transcript expression in E2A+/+ AMuLV cells stably expressing knockdown sponges against miR129-2_3p, miR290-5p, miR292-5p. Upon addition of STI571, with miR129-2_3p knockdown, we observed a decrease in Pim1 expression by qPCR as expected (Figure 4.41). However, in the miR290-5p or miR292-5p knockdown cells, upon addition of STI571, we no longer observed a decrease in Pim1 expression (Figure 4.41). These data indicate that Pim1 expression is regulated by miR290-5p/292-5p induction in STI-treated AMuLV cells lines.

In order to determine if the same is true in primary B cells, we quantified Pim1 expression by qPCR from cDNA from sorted pro-B (B220+CD43+IgM-), large pre-B (B220+CD43-IgM-FSChi), and small pre-B cells (B220+CD43-IgM-FSClo) from wild-type and miR290 cluster knockout mice. In the wild-type sorted large pre-B and small pre-B populations, we observed a decrease in Pim1 expression as expected (Figure 4.42). However, from miR290 cluster knock-out large pre-B to small pre-B populations, we observed an increase in Pim1 expression (Figure 4.42). The increase in Pim1 expression

at the small pre-B stage in the absence of the miR290 cluster indicated a misregulation of the Pim1 transcript.

We used the Targetscan and RNA22 algorithms to map predicted binding sites for miR290-5p/292-5p in the Pim1 3'UTR. The RNA22 algorithm determined that there was a single miR290-5p/292-5p binding site in the Pim1 3'UTR. We mutagenized the wild-type Pim1 3'UTR for the predicted binding sites to conduct dual-luciferase assays. We transiently transfected either reporter construct along with a scramble miRNA, miR290-5p or miR292-5p into HEK293 cells. We then used lysates from these cells, 24 hours post-transfection, to perform luciferase assays for both the renilla reporter and the firefly transfection control. We observed a modest repression (~20%) on the Pim1 3'UTR by miR290-5p or miR292-5p (Figure 4.43), as measured by renilla luciferase activity.

Taken together, these data support that Pim1 is in the miR290-5p/292-5p pathway of regulation at the small pre-B stage of B cell development. It also indicates that Pim1 may be directly targeted by miR290-5p/292-5-, causing its repression.

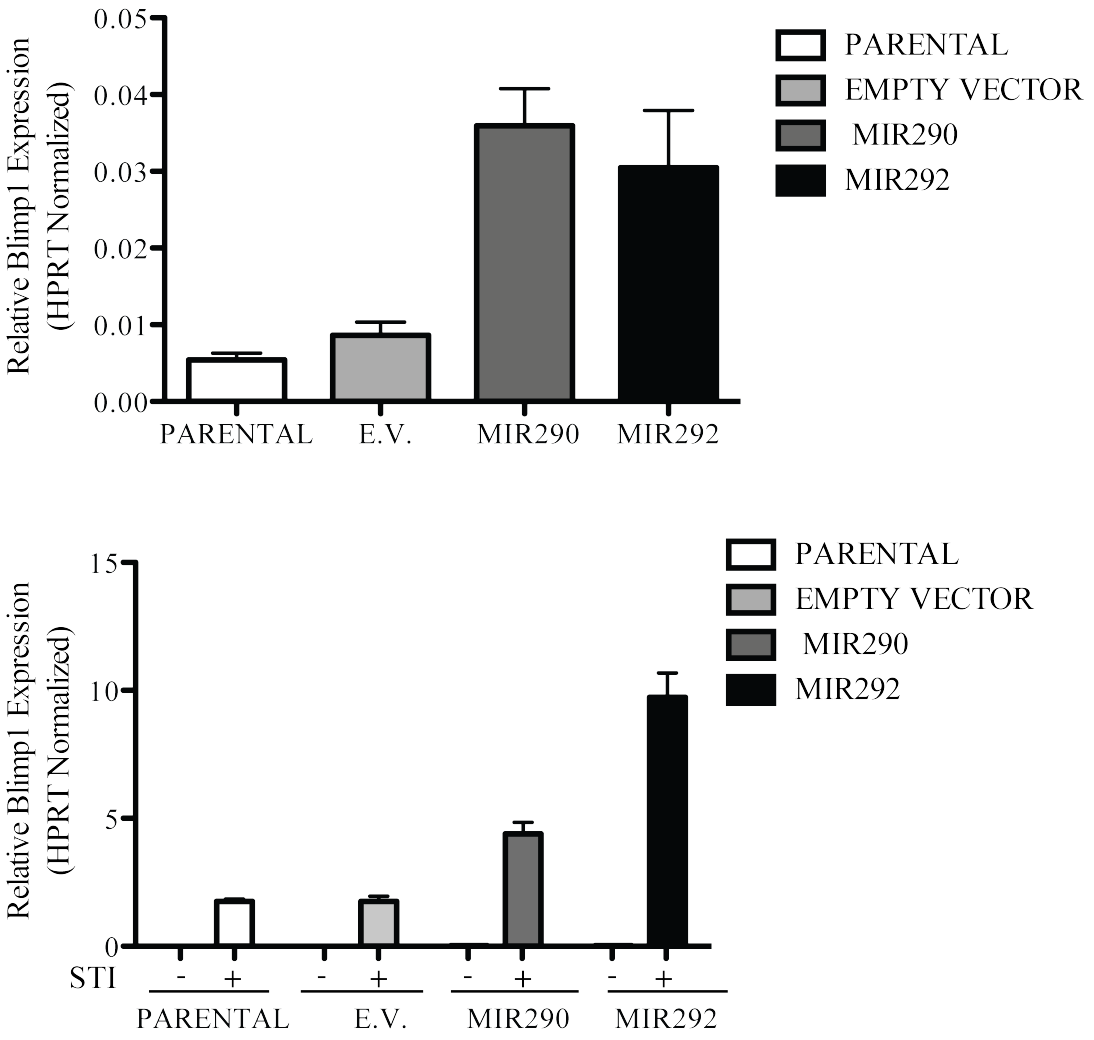

Figure 4.34. **Over-expression of miR290-5p or miR292-5p induces Blimp1 expression in AMuLV cells.** qPCR analysis of Blimp1 expression in RNA purified from E2A+/+ AMuLV cells over-expressing either an empty vector control, miR290-5p or miR292-5p, cultured in the absence or presence of STI571 (2.5μM, 12hr). Data was normalized to the expression of HPRT. Error bars represent range for replicate qPCR reactions. Data represents at least four individual experiments.

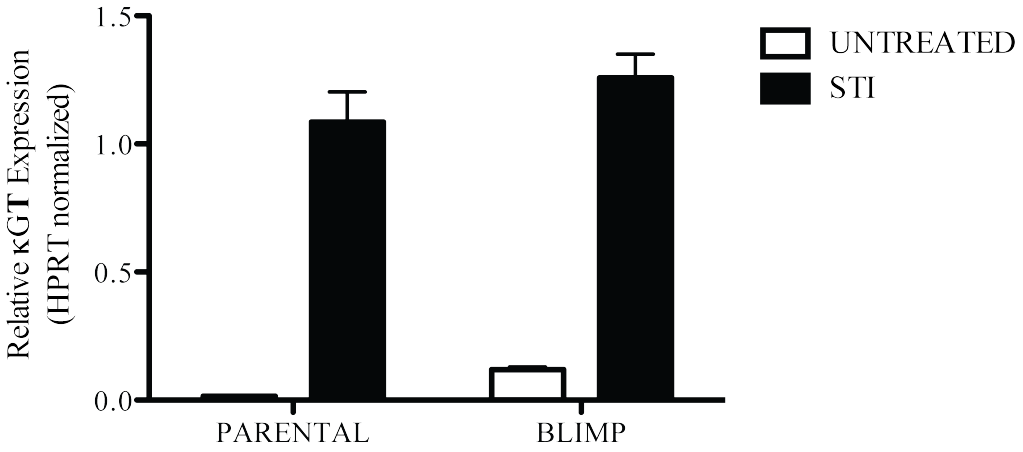

Figure 4.35. **Over-expression of Blimp1 induces κGT expression in AMuLV cells.** qPCR analysis of κGT expression in RNA purified from E2A+/+ AMuLV cells over-expressing either an empty vector control, miR290-5p or miR292-5p, cultured in the absence or presence of STI571 (2.5μM, 12hr). Data was normalized to the expression of HPRT. Error bars represent range for replicate qPCR reactions. Data represents at least four individual experiments.

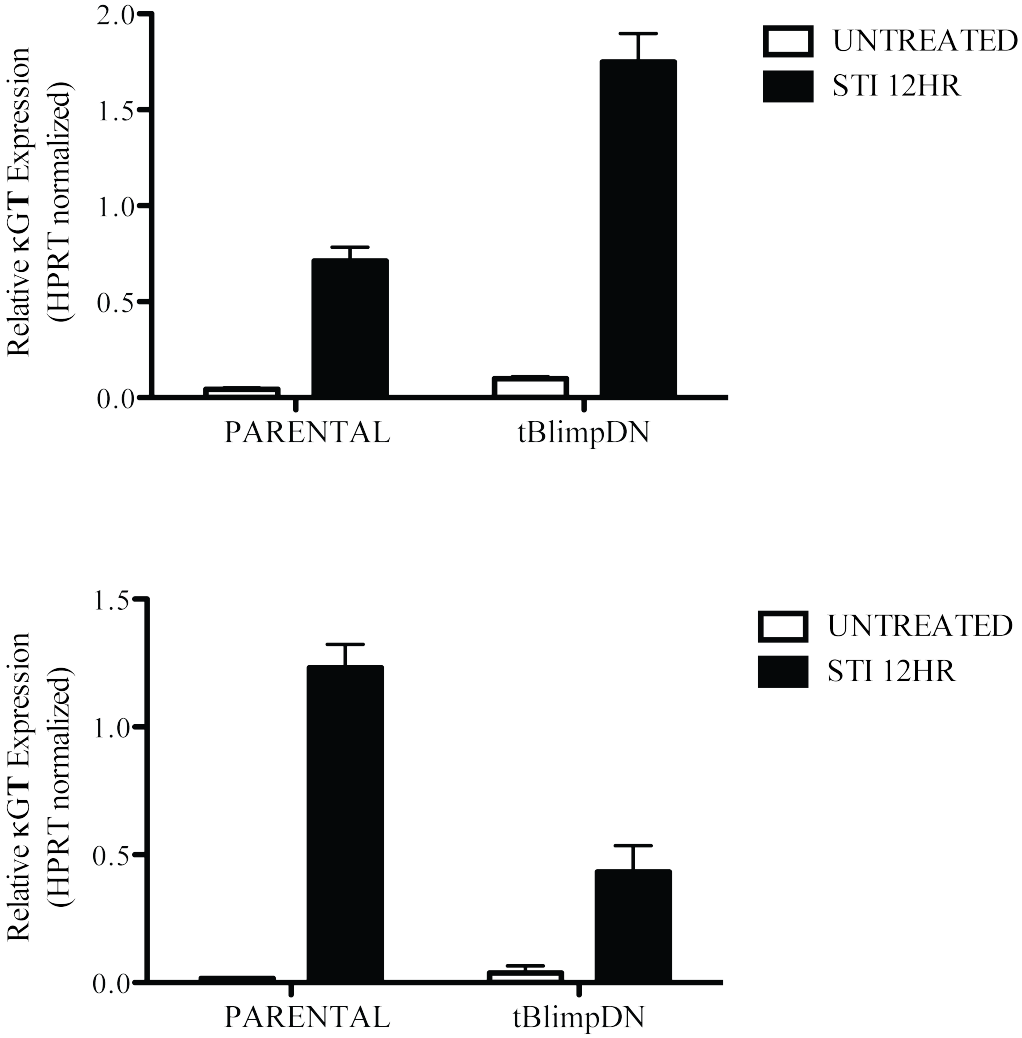

Figure 4.36. **Blimp1 dominant-negative expression inconsistently repressed κGT expression.** qPCR analysis of κGT expression in RNA purified from E2A+/+ AMuLV cells stably expressing a dominant-negative Blimp1, cultured in the absence or presence of STI571 (2.5μM, 12hr). Data was normalized to the expression of HPRT. Top panel represents an example of normal κGT induction upon STI treatment. Bottom panel represents an example of κGT repression. Error bars represent range for replicate qPCR reactions. Data represents at least three individual experiments.

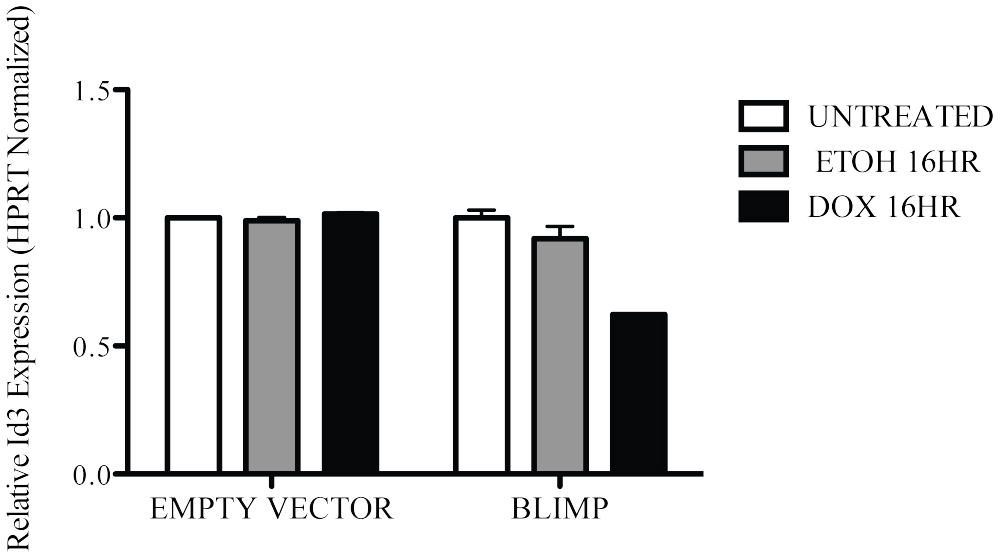

Figure 4.37. **Id3 expression is repressed upon induction of Blimp1 expression.** qPCR analysis of Id3 expression in RNA purified from E2A+/+ AMuLV cells stably expressing an empty vector control or Doxycycline-inducible Blimp1 cDNA, cultured in the absence or presence of ethanol or Doxycycline (1:5000, 16hr). Data was normalized to the expression of HPRT. Error bars represent range for replicate qPCR reactions. Data represents at least two individual experiments.

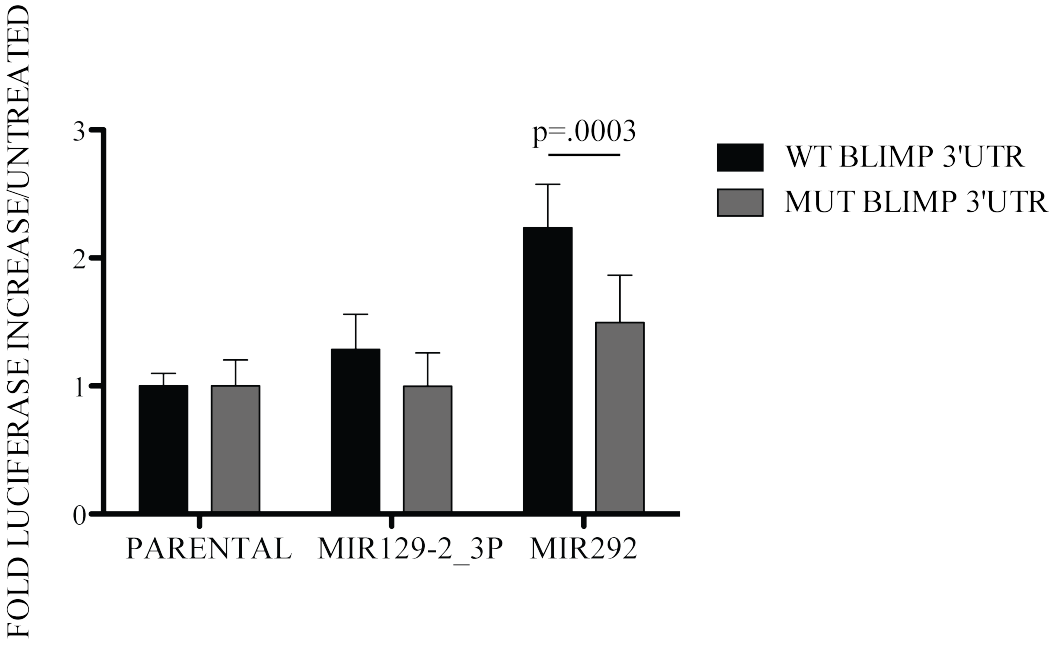

Figure 4.38. **miR292-5p directly activates Blimp1 by the Blimp1 3'UTR.** Luciferase assay of total cell lysates from E2A+/+ cells stably over-expression miR129-2_3p or miR292-5p and transiently transfected with either a wild-type Blimp1 3'UTR reporter or a mutant Blimp1 3'UTR reporter. Error bars represent range for biological replicate luciferase reactions. Data represents at least five independent experiments.

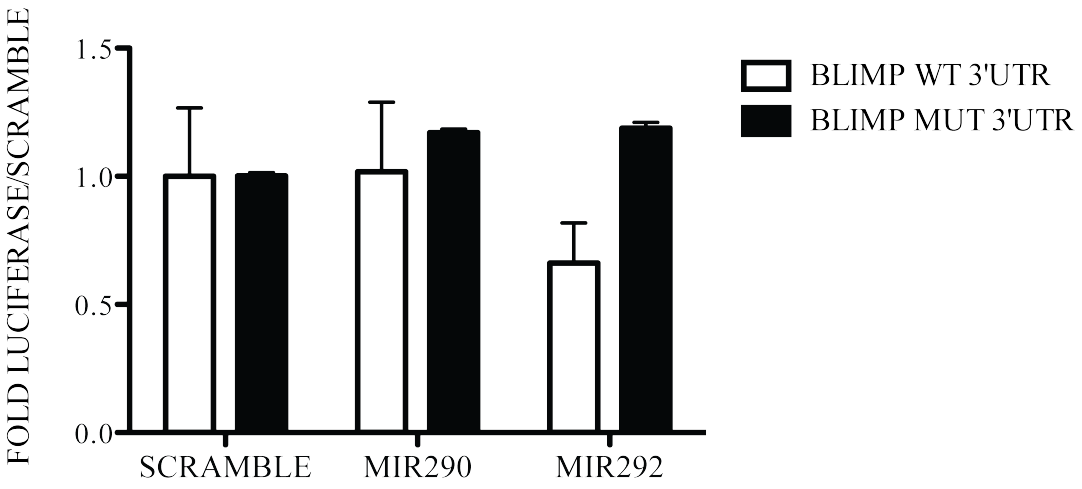

Figure 4.39. **miR292-5p directly represses the Blimp1 3'UTR in HEK293 cells.** Luciferase assay of total cell lysates from HEK293 cells transiently transfected with either a wild-type Blimp1 3'UTR reporter or a mutant Blimp1 3'UTR reporter along with a scramble miRNA, mir290-5p or miR292-5p. Error bars represent range for biological replicate luciferase reactions. Data represents at least three independent experiments.

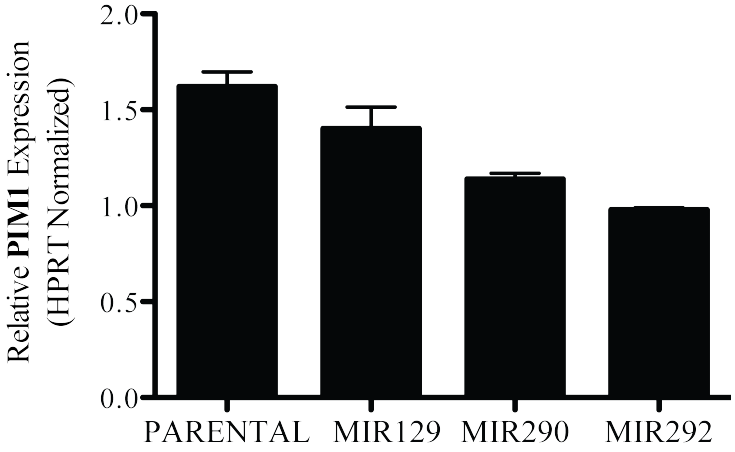

Figure 4.40. **miR290-5p and miR292-5p over-expression represses Pim1 expression.** qPCR analysis of Pim1 expression in RNA purified from E2A+/+ AMuLV cells over-expressing either miR129-2_3p, miR290-5p or miR292-5p. Data was normalized to the expression of HPRT. Error bars represent range for replicate qPCR reactions. Data represents at least two individual experiments.

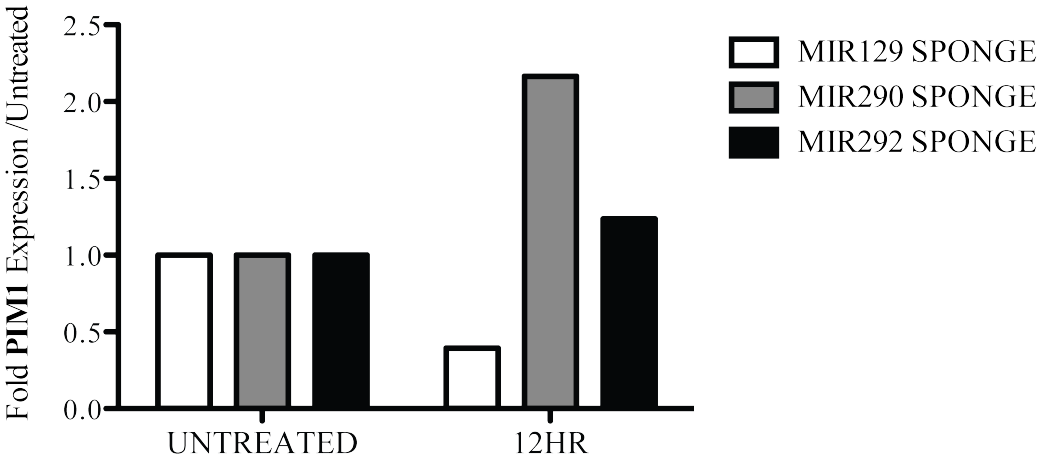

Figure 4.41. **Pim expression is induced upon STI571 treatment with miR290-5p or miR292-5p knockdown.** qPCR analysis of Pim1 expression in RNA purified from E2A+/+ AMuLV cells expressing a miR290-5p or miR292-5p sponge knockdown construct, and cultured in the presence of STI571 (2.5μM) for 12hr. Data was normalized to the expression of HPRT. These data represent at least two independently performed experiments.

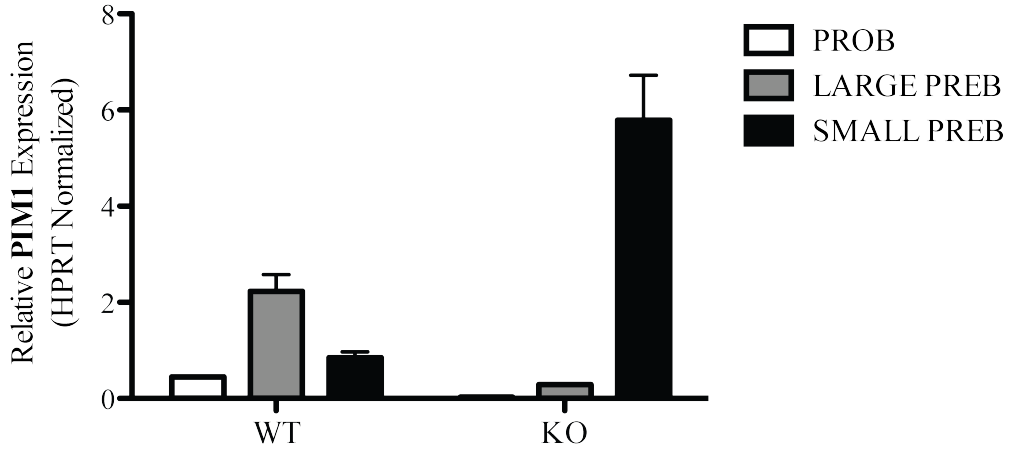

Figure 4.42. **Pim1 expression is induced at small pre-B in the miR290 cluster knockout mouse.** qPCR analysis of Pim1 levels in RNA purified from flow-sorted pro-B (B220+, CD43+, IgM-), large pre-B (B220+, CD43-, IgM-, FSC-Hi), and small pre-B (B220+, CD43-, IgM-, FSC-Lo) cells. Mice were 6 week old miR290 cluster knockout or wild-type mice. The data was normalized to HPRT expression. Error bars represent range for replicate qPCR reactions. This experiment is representative of one experiment.

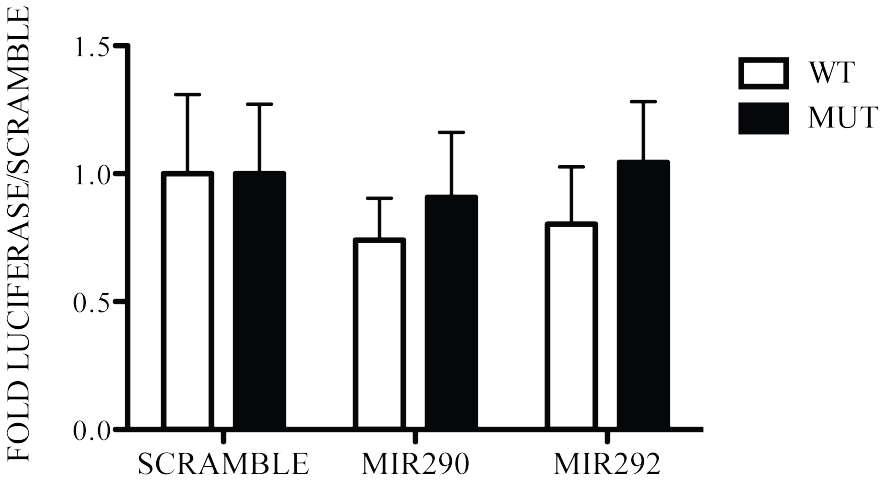

Figure 4.43. **miR290-5p and miR292-5p directly repress the Pim1 3'UTR in HEK293 cells.** Luciferase assay of total cell lysates from HEK293 cells transiently transfected with either a wild-type Pim1 3'UTR reporter or a mutant Pim1 3'UTR reporter along with a scramble miRNA, mir290-5p or miR292-5p. Error bars represent range for biological replicate luciferase reactions. Data represents at least two independent experiments.

Discussion:

miR290-5p/292-5p share the seed sequence CUCAAA and in our study are thought to be similar in function. The miR290 cluster members that share the seed sequence AAGUCC are expressed under different contexts. The differential expression of the CUCAAA and AAGUCC members in B cells may be attributed to differential maturation of the miRNAs in the miR290 cluster. Differential maturation may be due to pri-miRNA accessibility to Drosha, determined by the miR290 cluster tertiary structure, as is the case with the miR17~92 cluster (Chaulk et al. 2011), among other possibilities. Despite differential expression of the miR290 cluster miRNAs in B cells, these miRNAs are robustly expressed together in eutherian embryonic stem cells and have therefore been called the Early Embryonic microRNA Cluster (EEmiRC) (Houbaviy et al. 2005). Generally these two sets of miR290 cluster members are not thought to overlap functionally.

Most recently, a role for the AAGUCC but not CUCAAA miRNAs, was described in regulating DNA methyltransferases including the Dnmt3 genes (Sinkkonen et al. 2008). Those microRNAs have also been implicated in regulating genes involved in apoptosis. In Dicer deletion studies of ESC (Zheng et al. 2011), Caspase 2 and Ei24 were both identified as direct targets of the AAGUCC but not CUCAAA miR290 cluster members. Additionally, the AAGUCC miRNAs have been implicated in the regulation of the G1/S transition of the cell cycle in ESC. Therefore, the AAGUCC miRNAs are characterized as proliferation-regulating miRNAs (Wang et al. 2008). It is worth noting that in the ESC, the miR290 cluster AAGUCC members play the role of master regulators and strongly regulate proliferation. In our study we observe a more modulatory role for the CUCAAA members of this cluster, miR290-5p and miR292-5p. Interestingly, the AAGUCC miRNAs, including miR* counterparts miR290-3p and miR292-3p, are not detected in our system (Fig 2.5). There are few validated targets for miR290-5p or miR292-5p, but this group may include p16 (Rizzo et al. 2011) and Lats1, two genes implicated in cell cycling.

Conventional miRNA regulation occurs by repression of mRNA targets (Filipowicz et al. 2008; He et al. 2004). However, recently there have been a handful of reports that imply that miRNA regulation may occur by mRNA activation rather than repression under certain cellular contexts (Mortensen et al. 2011; Vasudevan et al. 2007). Specifically, Vasudevan et al have proposed that mRNA target activation by miRNAs may occur in cells that have undergone cell-cycle arrest. They have shown that this may occur in both drug-induced cell-cycle arrested mammalian cell lines (Vasudevan et al. 2007), as well as physiologically arrested primary cells, such as in Xenopus oocytes (Mortensen et al. 2011). In addition, they go on to show that AU-rich elements in the 3'UTR are responsible for the miRNA-mediated activation of targets.

Developing B cells that have rearranged a functional pre-BCR go through a proliferative burst prior to arresting at a G0-like state (Geier et al. 2006). Cell-cycle arrest at the pre-B stage is necessary for the cells to continue immunoglobulin rearrangements of the light

chain loci. Our studies show that miR290-5p/292-5p are induced at this stage of B cell development. Therefore, it was important for us to consider the possibility that miR290-5p/292-5p may be regulating their targets by a similar mRNA activation mechanism observed in other cell-cycle arrested systems.

The transcription factor Blimp1 has not previously been described as playing a role at the pro-B to pre-B transition of B cell development. As mentioned above, it had first been described as being an essential developmental regulator of terminal mature B cells (Shaffer et al. 2002). However, roles for Blimp1 have expanded to other immune developmental systems, including T cells (Ji et al. 2011). Therefore, we considered that Blimp1 may play a developmental role at the pro-B to pre-B stages of B cell development. In these studies, we found that Blimp1 may be involved in regulating κGT expression and have further found that it may do so by regulating the E2A-Id axis through inhibition of Id3 expression.

The observation that the Blimp1 3'UTR has four predicted binding sites for miR290-5p/292-5p led us to consider that perhaps Blimp1 may be a direct target of miR290-5p/292-5p in G0-like pre-B cells. Surprisingly, in dual-luciferase studies with a wild-type Blimp1 3'UTR, in E2A+/+ AMuLV cell lines, we observed an increase in luciferase reporter expression with miR292-5p over-expression. We did not observe this when we performed the dual-luciferase experiment with the mutant Blimp1 3'UTR. It is important to note that the AMuLV cells used in the luciferase studies were not treated with STI and were therefore not arrested in a G0-like state. Interestingly, we performed a similar dual-luciferase study with the wild-type and mutant Blimp1 3'UTR reporter in HEK293 cells co-transfected with mimic miRNAs and observed the opposite effect. In HEK293 cells the wild-type Blimp1 3'UTR luciferase reporter was repressed upon co-transfection with miR292-5p. The repression was relieved in the mutant Blimp1 3'UTR or with the scramble miRNA mimic.

The difference in miR292-5p-directed regulation of the Blimp1 3'UTR, between E2A+/+ AMuLV cell lines and HEK293 cells, indicates that it is a context dependent regulation. We examined the Blimp1 3'UTR for AREs neighboring the predicted miR290-5p/292-5p binding sites, but did not identify any to which to attribute our observation. This leads us to conclude that factors that lead to miRNA-directed activation of Blimp1 must exist in the physiological context of AMuLV pro-B cells and not in HEK293 cells. This would allow for conventional miRNA-mediated repression of Blimp1 in HEK293 cells, and miRNA-mediated activation of Blimp1 in AMuLV cell lines. However, regardless of the mode of miRNA regulation, we propose that Blimp1 may be directly targeted by miR292-5p in its 3'UTR.

The survival factor Pim1 may also be a direct target of miR290-5p/292-5p at the pre-B stage of B cell development. We first observed that in the absence of miR290-5p/292-5p Pim1 expression is no longer repressed upon STI571 treatment or at the small pre-B stage of B cell cevelopment. In dual-luciferase studies with a wild-type Pim1 3'UTR in HEK293 cells, the Pim1 3'UTR luciferase reporter was modestly repressed upon co-

transfection with miR290-5p/292-5p. The repression was relieved in the mutant Pim1 3'UTR or with the scramble miRNA mimic. Together these data indicate that miR290-5p/292-5p directly regulate Pim1 by a conventional repression mechanism. It is important to note that we did not perform the dual-luciferase experiments with the Pim1 3'UTR reporters in AMuLV cell lines. Further studies are needed to determine if Pim1 is also repressed by miR290-5p/292-5p in the AMuLV cell lines.

Our observations here show that miR290-5p/292-5p regulate various components of the B cell development pathways at the pre-B stage. We propose that miR290-5p/292-5p directly regulate both Pim1 and Blimp1. However, we hypothesize that Blimp1 miRNA-directed reguation is cell-context specific. We further hypothesize that this differential regulation may be due to Blimp1 3'UTR-specific features. Further studies are needed to identify what specifically leads to these differences in regulation.

Concluding Remarks:

miRNAs have been shown to be robust regulators of a multitude of developmental processes. However, miRNAs with modest effects or a modulatory role in regulating development has been underappreciated. In these studies we have shown an example of miRNAs regulating a critical stage of B cell development in a more modulatory or modest manner. Activation of the light chain loci, including the *kappa* locus, is a critical step at the pre-B stage of B cell development. A defect in activation of this locus can lead to a block in the transition to the immature stage of B cell development. We have shown that miRNAs from the miR290 cluster family can modulate the amount of *kappa* locus induction at the pre-B stage of B cell development. This highlights the importance and potential roles of modulatory miRNAs in various other systems. We would like to stress that these modulatory miRNAs and their roles must not be ignored and must be considered as important factors in the regulation of developmental pathways. Further studies are needed to elucidate their roles in various developmental systems.

References:

Amin, R. H., D. Cado, H. Nolla, D. Huang, S. A. Shinton, Y. Zhou, R. R. Hardy, and M. S. Schlissel. 2009. Biallelic, ubiquitous transcription from the distal germline Ig{kappa} locus promoter during B cell development. *Proc. Natl. Acad. Sci. U. S. A.* 106: 522-527.

Amin, R. H. and M. S. Schlissel. 2008. Foxo1 directly regulates the transcription of recombination-activating genes during B cell development. *Nat. Immunol.* 9: 613-622.

Bartel, D. P. 2009. MicroRNAs: target recognition and regulatory functions. *Cell* 136: 215-233.

Bates, J. G., J. Salzman, D. May, P. B. Garcia, G. J. Hogan, M. Wilson, M. McIntosh, M. S. Schlissel, and P. O. Brown. 2012. Extensive Gene-specific Translational Reprogramming in a Model of B cell Differentiation and Abl-dependent Transformation. *PLoS One.*

Bednarski, J. J., A. Nickless, D. Bhattacharya, R. H. Amin, M. S. Schlissel, and B. P. Sleckman. 2012. RAG-induced DNA double-strand breaks signal through Pim2 to promote pre-B cell survival and limit proliferation. *J. Exp. Med.* 209: 11-17.

Boldin, M. P. and D. Baltimore. 2012. MicroRNAs, new effectors and regulators of NF-kappaB. *Immunol. Rev.* 246: 205-220.

Cadera, E. J., F. Wan, R. H. Amin, H. Nolla, M. J. Lenardo, and M. S. Schlissel. 2009. NF-kappaB activity marks cells engaged in receptor editing. *J. Exp. Med.* 206: 1803-1816.

Carrington, J. C. and V. Ambros. 2003. Role of microRNAs in plant and animal development. *Science* 301: 336-338.

Chaulk, S. G., G. L. Thede, O. A. Kent, Z. Xu, E. M. Gesner, R. A. Veldhoen, S. K. Khanna, I. S. Goping, A. M. MacMillan, J. T. Mendell, H. S. Young, R. P. Fahlman, and J. N. Glover. 2011. Role of pri-miRNA tertiary structure in miR-17~92 miRNA biogenesis. *RNA Biol.* 8: 1105-1114.

Chen, C., D. A. Ridzon, A. J. Broomer, Z. Zhou, D. H. Lee, J. T. Nguyen, M. Barbisin, N. L. Xu, V. R. Mahuvakar, M. R. Andersen, K. Q. Lao, K. J. Livak, and K. J. Guegler. 2005. Real-time quantification of microRNAs by stem-loop RT-PCR. *Nucleic Acids Res.* 33: e179.

Chen, Y. Y., L. C. Wang, M. S. Huang, and N. Rosenberg. 1994. An active v-abl protein tyrosine kinase blocks immunoglobulin light-chain gene rearrangement. *Genes Dev.* 8: 688-697.

Chiao, P. J., S. Miyamoto, and I. M. Verma. 1994. Autoregulation of I kappa B alpha activity. *Proc. Natl. Acad. Sci. U. S. A.* 91: 28-32.

Constantinescu, A. and M. S. Schlissel. 1997. Changes in locus-specific V(D)J recombinase activity induced by immunoglobulin gene products during B cell development. *J. Exp. Med.* 185: 609-620.

Cooper, M. D. and M. N. Alder. 2006. The evolution of adaptive immune systems. *Cell* 124: 815-822.

Czech, B. and G. J. Hannon. 2011. Small RNA sorting: matchmaking for Argonautes. *Nat. Rev. Genet.* 12: 19-31.

Derudder, E., E. J. Cadera, J. C. Vahl, J. Wang, C. J. Fox, S. Zha, G. van Loo, M. Pasparakis, M. S. Schlissel, M. Schmidt-Supprian, and K. Rajewsky. 2009. Development of immunoglobulin lambda-chain-positive B cells, but not editing of immunoglobulin kappa-chain, depends on NF-kappaB signals. *Nat. Immunol.* 10: 647-654.

Ebert, M. S., J. R. Neilson, and P. A. Sharp. 2007. MicroRNA sponges: competitive inhibitors of small RNAs in mammalian cells. *Nat. Methods* 4: 721-726.

Filipowicz, W., S. N. Bhattacharyya, and N. Sonenberg. 2008. Mechanisms of post-transcriptional regulation by microRNAs: are the answers in sight? *Nat. Rev. Genet.* 9: 102-114.

Geier, J. K. and M. S. Schlissel. 2006. Pre-BCR signals and the control of Ig gene rearrangements. *Semin. Immunol.* 18: 31-39.

Greenbaum, S. and Y. Zhuang. 2002. Identification of E2A target genes in B lymphocyte development by using a gene tagging-based chromatin immunoprecipitation system. *Proc. Natl. Acad. Sci. U. S. A.* 99: 15030-15035.

Hardy, R. R., P. W. Kincade, and K. Dorshkind. 2007. The protean nature of cells in the B lymphocyte lineage. *Immunity* 26: 703-714.

He, L. and G. J. Hannon. 2004. MicroRNAs: small RNAs with a big role in gene regulation. *Nat. Rev. Genet.* 5: 522-531.

He, L., J. M. Thomson, M. T. Hemann, E. Hernando-Monge, D. Mu, S. Goodson, S. Powers, C. Cordon-Cardo, S. W. Lowe, G. J. Hannon, and S. M. Hammond. 2005. A microRNA polycistron as a potential human oncogene. *Nature* 435: 828-833.

Hendrickson, D. G., D. J. Hogan, H. L. McCullough, J. W. Myers, D. Herschlag, J. E. Ferrell, and P. O. Brown. 2009. Concordant regulation of translation and mRNA abundance for hundreds of targets of a human microRNA. *PLoS Biol.* 7: e1000238.

Hewitt, S. L., D. Farmer, K. Marszalek, E. Cadera, H. E. Liang, Y. Xu, M. S. Schlissel, and J. A. Skok. 2008. Association between the Igk and Igh immunoglobulin loci mediated by the 3' Igk enhancer induces 'decontraction' of the Igh locus in pre-B cells. *Nat. Immunol.* 9: 396-404.

Houbaviy, H. B., L. Dennis, R. Jaenisch, and P. A. Sharp. 2005. Characterization of a highly variable eutherian microRNA gene. *RNA* 11: 1245-1257.

Inlay, M., F. W. Alt, D. Baltimore, and Y. Xu. 2002. Essential roles of the kappa light chain intronic enhancer and 3' enhancer in kappa rearrangement and demethylation. *Nat. Immunol.* 3: 463-468.

Inlay, M. A., H. Tian, T. Lin, and Y. Xu. 2004. Important roles for E protein binding sites within the immunoglobulin kappa chain intronic enhancer in activating Vkappa Jkappa rearrangement. *J. Exp. Med.* 200: 1205-1211.

Ji, Y., Z. Pos, M. Rao, C. A. Klebanoff, Z. Yu, M. Sukumar, R. N. Reger, D. C. Palmer, Z. A. Borman, P. Muranski, E. Wang, D. S. Schrump, F. M. Marincola, N. P. Restifo, and L. Gattinoni. 2011. Repression of the DNA-binding inhibitor Id3 by Blimp-1 limits the formation of memory CD8+ T cells. *Nat. Immunol.* 12: 1230-1237.

Johnson, K., T. Hashimshony, C. M. Sawai, J. M. Pongubala, J. A. Skok, I. Aifantis, and H. Singh. 2008. Regulation of immunoglobulin light-chain recombination by the transcription factor IRF-4 and the attenuation of interleukin-7 signaling. *Immunity* 28: 335-345.

Kee, B. L. 2009. E and ID proteins branch out. *Nat. Rev. Immunol.* 9: 175-184.

Klug, C. A., S. J. Gerety, P. C. Shah, Y. Y. Chen, N. R. Rice, N. Rosenberg, and H. Singh. 1994. The v-abl tyrosine kinase negatively regulates NF-kappa B/Rel factors and blocks kappa gene transcription in pre-B lymphocytes. *Genes Dev.* 8: 678-687.

Koralov, S. B., S. A. Muljo, G. R. Galler, A. Krek, T. Chakraborty, C. Kanellopoulou, K. Jensen, B. S. Cobb, M. Merkenschlager, N. Rajewsky, and K. Rajewsky. 2008. Dicer ablation affects antibody diversity and cell survival in the B lymphocyte lineage. *Cell* 132: 860-874.

Kuchen, S., W. Resch, A. Yamane, N. Kuo, Z. Li, T. Chakraborty, L. Wei, A. Laurence, T. Yasuda, S. Peng, J. Hu-Li, K. Lu, W. Dubois, Y. Kitamura, N. Charles, H. W. Sun, S. Muljo, P. L. Schwartzberg, W. E. Paul, J. O'Shea, K. Rajewsky, and R. Casellas. 2010. Regulation of microRNA expression and abundance during lymphopoiesis. *Immunity* 32: 828-839.

Kuo, T. C., J. E. Chavarria-Smith, D. Huang, and M. S. Schlissel. 2011. Forced expression of cyclin-dependent kinase 6 confers resistance of pro-B acute lymphocytic leukemia to Gleevec treatment. *Mol. Cell. Biol.* 31: 2566-2576.

Lam, K. P., R. Kuhn, and K. Rajewsky. 1997. In vivo ablation of surface immunoglobulin on mature B cells by inducible gene targeting results in rapid cell death. *Cell* 90: 1073-1083.

Lin, K. I., C. Angelin-Duclos, T. C. Kuo, and K. Calame. 2002. Blimp-1-dependent repression of Pax-5 is required for differentiation of B cells to immunoglobulin M-secreting plasma cells. *Mol. Cell. Biol.* 22: 4771-4780.

Lin, K. I., Y. Lin, and K. Calame. 2000. Repression of c-myc is necessary but not sufficient for terminal differentiation of B lymphocytes in vitro. *Mol. Cell. Biol.* 20: 8684-8695.

Mandal, M., S. E. Powers, M. Maienschein-Cline, E. T. Bartom, K. M. Hamel, B. L. Kee, A. R. Dinner, and M. R. Clark. 2011. Epigenetic repression of the Igk locus by STAT5-mediated recruitment of the histone methyltransferase Ezh2. *Nat. Immunol.* 12: 1212-1220.

Mandal, M., S. E. Powers, K. Ochiai, K. Georgopoulos, B. L. Kee, H. Singh, and M. R. Clark. 2009. Ras orchestrates exit from the cell cycle and light-chain recombination during early B cell development. *Nat. Immunol.* 10: 1110-1117.

McDevit, D. C., L. Perkins, M. L. Atchison, and B. S. Nikolajczyk. 2005. The Ig kappa 3' enhancer is activated by gradients of chromatin accessibility and protein association. *J. Immunol.* 174: 2834-2842.

Medeiros, L. A., L. M. Dennis, M. E. Gill, H. Houbaviy, S. Markoulaki, D. Fu, A. C. White, O. Kirak, P. A. Sharp, D. C. Page, and R. Jaenisch. 2011. Mir-290-295 deficiency in mice results in partially penetrant embryonic lethality and germ cell defects. *Proc. Natl. Acad. Sci. U. S. A.* 108: 14163-14168.

Milne, C. D., H. E. Fleming, and C. J. Paige. 2004. IL-7 does not prevent pro-B/pre-B cell maturation to the immature/sIgM(+) stage. *Eur. J. Immunol.* 34: 2647-2655.

Mortensen, R. D., M. Serra, J. A. Steitz, and S. Vasudevan. 2011. Posttranscriptional activation of gene expression in Xenopus laevis oocytes by microRNA-protein complexes (microRNPs). *Proc. Natl. Acad. Sci. U. S. A.* 108: 8281-8286.

Muljo, S. A. and M. S. Schlissel. 2003. A small molecule Abl kinase inhibitor induces differentiation of Abelson virus-transformed pre-B cell lines. *Nat. Immunol.* 4: 31-37.

Nutt, S. L. and B. L. Kee. 2007. The transcriptional regulation of B cell lineage commitment. *Immunity* 26: 715-725.

Ochiai, K., M. Maienschein-Cline, M. Mandal, J. R. Triggs, E. Bertolino, R. Sciammas, A. R. Dinner, M. R. Clark, and H. Singh. 2012. A self-reinforcing regulatory network triggered by limiting IL-7 activates pre-BCR signaling and differentiation. *Nat. Immunol.* 13: 300-307.

Rizzo, M., M. Evangelista, L. Mariani, M. Simili, G. Rainaldi, and L. Pitto. 2011. Immortalized mouse embryo fibroblasts are resistant to miR-290-induced senescence regardless of p53 status. *Physiol. Genomics* 43: 1153-1159.

Schatz, D. G. and P. C. Swanson. 2011. V(D)J recombination: mechanisms of initiation. *Annu. Rev. Genet.* 45: 167-202.

Scherer, D. C., J. A. Brockman, H. H. Bendall, G. M. Zhang, D. W. Ballard, and E. M. Oltz. 1996. Corepression of RelA and c-rel inhibits immunoglobulin kappa gene transcription and rearrangement in precursor B lymphocytes. *Immunity* 5: 563-574.

Schlissel, M. S. and D. Baltimore. 1989. Activation of immunoglobulin kappa gene rearrangement correlates with induction of germline kappa gene transcription. *Cell* 58: 1001-1007.

Schlissel, M. S. and T. Morrow. 1994. Ig heavy chain protein controls B cell development by regulating germ-line transcription and retargeting V(D)J recombination. *J. Immunol.* 153: 1645-1657.

Sciammas, R. and M. M. Davis. 2004. Modular nature of Blimp-1 in the regulation of gene expression during B cell maturation. *J. Immunol.* 172: 5427-5440.

Sen, R. and D. Baltimore. 1986. Multiple nuclear factors interact with the immunoglobulin enhancer sequences. *Cell* 46: 705-716.

Shaffer, A. L., K. I. Lin, T. C. Kuo, X. Yu, E. M. Hurt, A. Rosenwald, J. M. Giltnane, L. Yang, H. Zhao, K. Calame, and L. M. Staudt. 2002. Blimp-1 orchestrates plasma cell differentiation by extinguishing the mature B cell gene expression program. *Immunity* 17: 51-62.

Shaffer, A. L., A. Peng, and M. S. Schlissel. 1997. In vivo occupancy of the kappa light chain enhancers in primary pro- and pre-B cells: a model for kappa locus activation. *Immunity* 6: 131-143.

Sinkkonen, L., T. Hugenschmidt, P. Berninger, D. Gaidatzis, F. Mohn, C. G. Artus-Revel, M. Zavolan, P. Svoboda, and W. Filipowicz. 2008. MicroRNAs control de novo DNA methylation through regulation of transcriptional repressors in mouse embryonic stem cells. *Nat. Struct. Mol. Biol.* 15: 259-267.

Swift, S., J. Lorens, P. Achacoso, and G. P. Nolan. 2001. Rapid production of retroviruses for efficient gene delivery to mammalian cells using 293T cell-based systems. *Curr. Protoc. Immunol.* Chapter 10: Unit 10.17C.

Vasudevan, S., Y. Tong, and J. A. Steitz. 2007. Switching from repression to activation: microRNAs can up-regulate translation. *Science* 318: 1931-1934.

Ventura, A., A. G. Young, M. M. Winslow, L. Lintault, A. Meissner, S. J. Erkeland, J. Newman, R. T. Bronson, D. Crowley, J. R. Stone, R. Jaenisch, P. A. Sharp, and T. Jacks. 2008. Targeted deletion reveals essential and overlapping functions of the miR-17 through 92 family of miRNA clusters. *Cell* 132: 875-886.

Wang, Y., S. Baskerville, A. Shenoy, J. E. Babiarz, L. Baehner, and R. Blelloch. 2008. Embryonic stem cell-specific microRNAs regulate the G1-S transition and promote rapid proliferation. *Nat. Genet.* 40: 1478-1483.

Xiao, C., D. P. Calado, G. Galler, T. H. Thai, H. C. Patterson, J. Wang, N. Rajewsky, T. P. Bender, and K. Rajewsky. 2007. MiR-150 controls B cell differentiation by targeting the transcription factor c-Myb. *Cell* 131: 146-159.

Xiao, C., L. Srinivasan, D. P. Calado, H. C. Patterson, B. Zhang, J. Wang, J. M. Henderson, J. L. Kutok, and K. Rajewsky. 2008. Lymphoproliferative disease and autoimmunity in mice with increased miR-17-92 expression in lymphocytes. *Nat. Immunol.* 9: 405-414.

Yigit, E., P. J. Batista, Y. Bei, K. M. Pang, C. C. Chen, N. H. Tolia, L. Joshua-Tor, S. Mitani, M. J. Simard, and C. C. Mello. 2006. Analysis of the C. elegans Argonaute family reveals that distinct Argonautes act sequentially during RNAi. *Cell* 127: 747-757.

Zheng, G. X., A. Ravi, J. M. Calabrese, L. A. Medeiros, O. Kirak, L. M. Dennis, R. Jaenisch, C. B. Burge, and P. A. Sharp. 2011. A latent pro-survival function for the mir-290-295 cluster in mouse embryonic stem cells. *PLoS Genet.* 7: e1002054.

Zhou, B., S. Wang, C. Mayr, D. P. Bartel, and H. F. Lodish. 2007. miR-150, a microRNA expressed in mature B and T cells, blocks early B cell development when expressed prematurely. *Proc. Natl. Acad. Sci. U. S. A.* 104: 7080-7085.

Appendix:

Background:

miRNA-mediated repression is conferred by either target transcript degradation or translational repression (Filipowicz et al. 2008). To identify target transcripts that are repressed upon miRNA expression, a common assay used is microarray profiling (Koralov et al. 2009) in the presence or absence of the miRNA of interest. In this way, miRNA-repressed targets that are degraded can potentially be identified, as the abundance of transcripts decreases upon expression of the miRNA of interest.

Another approach to examine miRNA-repressed targets is to identify transcripts that are translationally repressed. A method used by the Brown Laboratory at Stanford University, uses the gradient encoding method. This is a method to do polysome profiling on a genome wide scale (Hendrickson et al. 2009). From this method you can obtain information about the average ribosome density of each mRNA by sucrose density fractionation, followed by microarray analysis. Since changes in ribosome density are believed to correspond to changes in translation rates (Hendrickson et al. 2009), we can use this method to determine translation rate changes upon stable miRNA over-expression.

In these studies we attempt to elucidate the targets by which miR290-5p and miR292-5p act to regulate *kappa* locus activation, in collaboration with the Brown Laboratory. We observed Blimp1 translationally activated in the gradient encoding assay performed in AMuLV cells treated with STI, as previously described. We also observed that NF-κB predicted targets are upregulated upon miR290-5p over-expression in AMuLV cells. This indicates that miR290-5p/292-5p possibly turn on the NF-κB program in this system. By performing an abundance array on the miR290 cluster knock-out mice (Medeiros et al. 2011), described above, we identified pre-BCR signaling pathway components to be deregulated in the absence of the miR290 cluster.

Materials and Methods:

Preparation of Cell Extracts for Translation Profiling
E2A+/+ AMuLV cells (60-100 X 10>6) in the absence or presence of STI (12hr, 2.5μM) were harvested by resuspension in ice-cold buffer A (20 mM Tris pH 8.0, 140 mM KCl, 5 mM $MgCl_2$, 0.1 mg/ml cycloheximide (Calbiochem Cat# 239764). After the second wash, cells were resuspended in lysis buffer which was buffer A containing 0.22 mg/ml of heparin, 1× protease inhibitor cocktail (Pierce Cat# 78437), 100 U/ml SUPERASin, and 0.5 mM DTT, 0.1% Brij 58 (Sigma Aldrich Cat# P5884-100G) and 0.1% sodium deoxycholate (Sigma Aldrich Cat# D6750-100G). Cells were kept on ice for 15 min with intermittent inversion and then spun at 9,500 rpm in a microcentrifuge for 5 min at 4°C yielding ~6-10 A260 units. Supernatant was collected, flash frozen in liquid nitrogen, and then stored at −80°C until use.

Gradient Encoding
Sucrose gradient preparation and gradient encoding were performed as described in Bates et al (Bates et al. 2012) and Hendrickson et al (Hendrickson et al. 2009).

Flow Cytometry and FACS Sorting Analysis
Total bone marrow was harvested from mice and red blood cells were depleted with EryLyse Buffer (0.14M NH4Cl, 20mM Hepes). Cells were stained with anti-CD19 MACS microbeads (Miltenyi Biotec) and were CD19+ enriched using MACS MS columns (Miltenyi Biotec). CD19+ cells were then stained using the following antibodies: B220-PeCy5 (clone RA3-6B2, BD), CD43-Pe (clone S7, BD), IgM-FITC (clone II/41, eBiosciences), IgD-Biotin (clone 11-26, eBiosciences), Streptavidin-PeCy7 (BD). Stained cells were resuspended in FACS buffer (5% BSA, 10mM Hepes) for cell sorting.

Preparation of RNA for Microarray Experiments
Total RNA was harvested from cells using the Qiagen RNeasy Kit as per manufacturer protocol (Qiagen, 74104). RNA was then flash frozen in liquid nitrogen, and stored at −80°C until use.

Microarray
Microarray preparation and data processing were performed as described in Bates et al (Bates et al. 2012).

Results:

miR290-5p and miR292-5p Abundance Arrays

In an effort to identify the targets of miR290-5p/miR292-5p we performed transcript abundance arrays in collaboration with the Brown Laboratory at Stanford University. We harvested total RNA from the untreated E2A+/+ AMuLV parental cell line, or from E2A+/+ AMuLV cells stably over-expressing either miR290-5p or miR292-5p. The samples were harvested and processed in triplicates. The samples were processed on a MEEBO microarray platform by the Brown Laboratory. Data processing were performed as described in Bates et al (Bates et al. 2012).

To determine change in abundance upon miR290-5p or miR292-5p over-expression as compared to the untreated sample, array data was expressed as log2(untreated/mir290) and log2(untreated/miR292). In this manner, a positive value results from a large ratio, indicating a decrease in abundance upon miRNA over-expression. To identify potential miR290-5p/292-5p targets we overlapped the microarray data to the list of miR292-5p predicted targets from the miRanda website (microrna.sanger.ac.uk/targets/v4/) and asked what the log2 values are of those genes.

We ordered the log2(untreated/mir290) list to determine which genes were most repressed upon miR290 over-expression (Table A.2). Those genes with a positive value indicate repression upon miR290-5p over-expression. A few interesting top targets that were repressed upon miR290-5p over-expression include: Tnfrsf18, expressed normally in T cell activation; Lat2, involved in pre-BCR signaling; and IgH-V, the immunoglobulin heavy V gene.

We also decided to order the log2(untreated/mir290) list to determine which genes were most upregulated upon miR290 over-expression (Table A.3). Those genes with a negative value indicate activation upon miR290-5p over-expression. A few interesting top hits that were activated upon miR290-5p over-expression include several B and T-cell lineage genes: Btla, MybL2, Nfkbiz, Aid, Blimp1, Klf4, Zap70, Card11, MapK8. When we examined the promoters of these genes for predicted transcription factor binding sites using the Qiagen website (http://www.sabiosciences.com/chipqpcrsearch.php), interestingly, we found that of the aforementioned genes, Klf4, Blimp1, and Nfkbiz, had predicted binding sites for NF-κB, the pathway we had previously determined to be activated by miR290-5p/miR292-5p expression.

It is interesting to point out that there was almost no change in Rag1 expression upon miR290-5 over-expression (Table A.2). Also, out of three Igk-V1 probes on the MEEBO array, two probes indicated an increase in abundance upon miR290-5p over-expression. However, we did observe that for Igk-V4 and Igk-V5, there may be a slight decrease in expression upon miR290-5p over-expression.

Gradient Encoding

As described above, one model for miRNA-mediated repression is translational repression (Filipowicz et al. 2008). Therefore, in an effort to identify miR290-5p/292-5p targets that are translationally repressed, we collaborated with the Brown Laboratory at Stanford University to perform the gradient encoding method. This is a method to do polysome profiling on a genome wide scale (Hendrickson et al. 2009). From this method you can obtain information about the average ribosome density of each mRNA by sucrose density fractionation, followed by microarray analysis. Since changes in ribosome density are believed to correspond to changes in translation rates (Hendrickson et al. 2009), we can use this method to determine translation rate changes upon stable miRNA over-expression.

We prepared total cell lysates in duplicate from STI-treated (12hr, 2.5μM) E2A+/+ AMuLV cell lines stably over-expressing either an empty vector or miR292-5p. By comparing these two samples we expect to identify transcripts that have greater translational repression in combined STI-miR292-5p over-expression samples than in combined STI-empty vector samples. Total cell lysates were processed on a sucrose gradient and prepared for gradient encoding by the Brown Laboratory, as described in Bates et al (Bates et al. 2012). The samples were processed on a MEEBO microarray platform by the Brown Laboratory. Data processing were performed as described in Bates et al (Bates et al. 2012).

Using SAM (significance analysis of microarrays) analysis, we determined which genes changed significantly between the STI-empty vector and the STI-miR292-5p sample. SAM scored the genes and a positive score indicates an increased mRNA abundance in the combined STI-miR292-5p sample as compared to the STI-empty vector sample. A negative score indicates a decrease in mRNA abundance in the combined STI-miR292-5p sample as compared to the STI-empty vector sample. We compiled a list of the genes that had a decrease in translation in the STI-miR292-5p sample as compared to the STI-empty vector sample, and that also had a low False Discovery Rate (FDR) (Bates et al. 2012), a measure of the ratio of false positives (Table A.4.). The top gene that was translationally repressed, as measured by two probes, was Tnfrsf18. This gene was also one of our top hits in the mir290-5p abundance arrays, described above. Gramd3 is another gene that was both translationally repressed by STI-miR292-5p as well as had decreased abundance in the miR290-5p arrays. Interestingly, Casp4 was translationally repressed by STI-miR292-5p, but the miR290-5p abundance array indicated that it increased in abundance. Id2 and IκBα appeared to be translationally repressed as well, however they had a higher FDR(~35%), indicating a lower confidence.

We also compiled a list of the genes that had an increase in translation in the STI-miR292-5p sample as compared to the STI-empty vector sample, and that also had a low FDR (Table A.5). It is interesting to point out that Blimp1 (Prdm1) increased translationally in the STI-miR292-5p sample as compared to the STI-empty vector sample. The Blimp1 FDR of 17% is around the ~15% FDR threshold.

miR290 Cluster Knockout Abundance Array

In an effort to identifty miRNA targets for miR290-5p and miR292-5p, in collaboration with the Brown Laboratory, we performed abundance arrays on RNA from sorted large pre-B (B220+, CD43-, IgM-, FSChi) and small pre-B (B220+, CD43-, IgM-, FSClo) cells from wild-type and miR290 cluster knockout mice. The samples were processed on a MEEBO microarray platform by the Brown Laboratory. Data processing were performed as in Bates et al (Bates et al. 2012). We performed the sort on one mouse per genotype.

In order to determine which genes are potential targets of miR290-5p/292-5p we considered that at the small pre-B stage, when miRNA expression is induced, the target would be repressed. Therefore, in the absence of miR290-5p/292-5p in the miR290 cluster knockout mice, the target would be "less repressed." We therefore generated a list of genes that were "less repressed" in the miR290 cluster knockout mouse as compared to the wild-type mouse. To do this, we first determined the change in abundance from large pre-B to small pre-B in both the wild-type and knock-out mice. To identify transcripts repressed at the small pre-B stage. We then determined the log2(Δwildtype/Δknockout) value and further determined by SAM analysis if that change was significant from the wild-type to the knock-out mouse. We observed several genes that are normally decreased at the small-preB stage, that are no longer repressed at the same stage in the miR290 cluster knock-out mouse (Table A.6). Some of these genes include: IgL1, Syk, Vpre-B, IL7-R, and Id3. We note that this experiment was not performed in multiplicate. Further studies are needed to validate the results of the array.

GENE SYMBOI	log2(untreated/miR290transd)	GENE SYMBC	log2(untreated/miR290transd)
CAPN2	3.905	**LAT2**	1.896
COL6A1	3.414	CTH	1.838
MTAP6	3.399	SELL	1.82
CARD10	2.917	H2-DMB2	1.799
CIITA	2.674	**SLC7A7**	1.791
H2-AA	2.622	TCAM1	1.785
NCF1	2.506	CD74	1.752
H2-EB1	2.465	**IGH-V**	1.744
MYO10	2.464	CD74	1.72
SLC45A3	2.431	MAPKAPK5	1.666
LUZP2	2.421	GALM	1.637
TNFRSF18	2.346	**GRAMD3**	1.627
TNFRSF18	2.294	LY6A	1.608
1700013F07RIK	2.233	MTAP7	1.602
H2-DMB1	2.205	SLC39A8	1.591
CTH	2.201	NFIL3	1.587
H2-DMA	2.117	**PCDHB5**	1.552
CCNY	2.093	RTN2	1.532
BTBD6	2.044	MYO1D	1.526
EN2	2.042	SLC39A8	1.525
NUPR1	2.039	LST1	1.486
CSF2	2.03	CNR2	1.463
GRAMD3	1.998	CTNND1	1.459
PSTPIP2	1.982	LSP1	1.419
LTBP3	1.954	COX6A2	1.414
		RAG1	**-0.037**

Table A.2. **Genes repressed upon miR290-5p over-expression.** Top hits for genes with most decrease in abundance upon miR290-5p over-expression as measured by abundance array. Array performed on E2A+/+ parental cell line and E2A+/+ stably over-expressing miR290-5p. Value is from log2(untreated/mir290). The smaller the number indicates repression upon miR290-5p overexpression as compared to the untreated E2A+/+ AMuLV cell line. Genes in bold are lymphocyte lineage genes.

gene symbol	log2(untreated/miR290transduced)	gene symbol,	log2(untreated/miR290transduced)
ICA1	-6.467	FHIT	-2.592
ELOVL4	-5.622	NAP1L3	-2.574
PFN2	-4.75	ZHX2	-2.538
GFRA2	-4.593	AIF1L	-2.521
GKAP1	-4.405	KLRA12	-2.449
ZFP623	-3.918	KLRA20	-2.402
TUSC1	-3.907	KLRA16	-2.381
MEGF10	-3.865	RBP1	-2.371
SLAMF7	-3.835	WASF1	-2.339
ATP1B1	-3.76	CAV1	-2.307
Tmsb15l	-3.756	**LIFR**	-2.284
Radil	-3.646	PTPN22	-2.266
NME7	-3.509	UACA	-2.228
Sel1l3	-3.36	CLGN	-2.2
CAMK4	-3.275	2310031A18	-2.144
SLC30A4	-3.195	ROBO2	-2.14
Tmsb15l	-3.109	IGH-V10	-2.112
Ninl	-3.014	**BCR**	-2.094
TFPT	-2.868	KLF9	-2.019
EIF5A2	-2.86	**IGK-V1**	-1.607
ATP1B1	-2.842	**BTLA**	-1.208
KLRA22	-2.827	**MYBL2**	-1.044
KIF13A	-2.749	**NFKBIZ**	-1.019
PTPN22	-2.714	**AICDA**	-0.995
EGFL7	-2.688	**PRDM1**	-0.936
ANGPT1	-2.66	**KLF4**	-0.916
PROS1	-2.64	**ZAP70**	-0.882
CASP4	-2.638	**CARD11**	-0.86
2010204N08	-2.619	**MAPK8**	-0.672
		IGK-V1	-0.275
		IGK-V1	-1.607
		IGK-V1	0.356
		IGK-V4	0.364
		IGK-V5	0.183

Table A.3. **Genes induced upon miR290-5p over-expression.** Top hits for genes with most increase in abundance upon miR290-5p over-expression as measured by abundance array. Array performed on E2A+/+ parental cell line and E2A+/+ stably over-expressing miR290-5p. Value is from log2(untreated/mir290). The larger the number indicates increase in abundance upon miR290-5p overexpression as compared to the untreated E2A+/+ AMuLV cell line.

Gene ID	Score(d)	localfdr(%)	Gene ID	Score(d)	localfdr(%)
Tnfrsf18	-9.54476961	0.209770502	Ptpla	-4.82792401	0
Tnfrsf18	-8.94720887	0.205954893	Tfpi	-4.8159265	0
Satb2	-8.4770295	0.188433364	Nanos1	-4.79653899	0
Gramd3	-8.065224	0.150951316	Prodh	-4.78740895	0
Tnni2	-7.3529377	0.021259328	Hist1h2bg	-4.77332067	0
Maged1	-7.134707	0	Tsc22d3	-4.7602549	0
Ly6a	-6.94780733	0	H2-Q8	-4.70112465	0
Mapk11	-6.87407724	0	Nanos1	-4.66803666	0
Casp4	-6.21777312	0	**Casp4**	-4.60266942	0
Ly6d	-6.19398717	0	Slc7a7	-4.55412307	0
Ly6f	-6.07574888	0	Rbpms	-4.53166872	0
Vrk1	-5.80032533	0	Fam158a	-4.50274283	0
Tal1	-5.61627232	0	Polr3a	-4.47477328	0
C1qtnf6	-5.53413814	0	Cybb	-4.46814575	0
2210409B22Rik	-5.36110945	0	Slc44a1	-4.41386057	0
Phlpp1	-5.21823295	0	Nedd4l	-4.32714123	0
Gramd3	-5.15360367	0	Ephx1	-4.32232446	0
9130223C08Rik	-5.13034556	0	Slc22a17	-4.28900839	0
Tsc22d3	-5.09875322	0	Papola	-4.17604014	0
Rbpms	-5.0356206	0	Tnnt3	-4.14674558	0
Ptpla	-5.02702829	0	Hoxc6	-4.12030703	0
Amigo1	-5.02074993	0	Cybb	-4.08547253	0
Elavl2	-4.95431164	0	Ms4a6d	-4.08404892	0
Morn2	-4.87334235	0	Ms4a6d	-4.0654828	0
Dnahc8	-4.83792694	0	Apob48r	-4.05274797	0
			Id2	-0.15411376	35.16579692
			Nfkbia	-0.1976681	35.00869596

Table A.4. **Genes translationally repressed upon combined STI-miR292-5p over-expression.** Top hits of genes with most translational repression upon combined STI-miR292-5p over-expression as compared to STI-empty vector in E2A+/+ cells in a gradient encoding experiment. Score is the SAM value to determine significant change. A negative score indicates translational repression upon miR292-5p overexpression as compared to the empty vector. FDR determines rate of false positives. Genes in bold are lymphocyte lineage genes.

Gene ID	Score(d)	localfdr(%)	Gene ID	Score(d)	localfdr(%)
Litaf	14.93408212	0	Slc30a4	7.380366483	0
Gkap1	13.00583066	0	Ampd3	7.231801987	0
Cdyl	12.28574261	0	Gng12	7.134179636	0
Pfn2	10.46307261	0.022302491	Fhit	7.069134529	0
Gcat	9.746506132	0.042413943	Ak3	7.030131855	0
Frmd4b	9.611850744	0.046369024	1500011B03Ri	6.847965087	0
Olfml2b	9.503550272	0.049457464	Cd1d1	6.596531433	0
Slc40a	9.23266878	0.056457256	Slc29a3	6.581398196	0
Rhoq	9.169664253	0.057855624	Chpt1	6.580552057	0
Cdyl	8.931332445	0.061879054	9430080K19R	6.539017958	0
Klhl7	8.725426573	0.063131568	Sdc1	6.445736889	0
Map4k4	8.433877449	0.059833061	Tctex1d2	6.397481219	0
Afp	8.24030061	0.053173265	Ski	6.31381307	0
Rabl2a	8.181246905	0.050261073	Aldh1b1	6.197411388	0
Snn	8.018204728	0.039759145	Evi5	6.108940283	0
9230111I22Rik	7.995266434	0.037969085	Hmox1	6.096053356	0
Prkar2b	7.79043554	0.018134214	Ercc5	6.034146813	0
Tm6sf1	7.679077162	0.004143534	Aifm2	6.02256464	0
Frat2	7.644782377	0	Renbp	6.021385232	0
Creld1	7.608432145	0	Ercc5	5.957283127	0
Zhx2	7.455847998	0	**Prdm1**	1.446300223	17.80796246

Table A.5. **Genes translationally activated upon combined STI-miR292-5p over-expression.** Top hits of genes with most translational activation upon combined STI-miR292-5p over-expression as compared to STI-empty vector in E2A+/+ cells in a gradient encoding experiment. Score is the SAM value to determine significant change. A positive score indicates translational activation upon miR292-5p overexpression as compared to the empty vector. FDR determines rate of false positives. Genes in bold are lymphocyte lineage genes.

Gene	diff	Gene	diff
Mxd3	0.621126938	**Syk**	0.408462958
Igll1	0.578256897	Ftsj1	0.393409469
Car2	0.551872004	Rrm2	0.391668777
Ttk	0.502033663	Cdkn2c	0.390674387
Ramp1	0.48710434	**Vpreb1**	0.389087025
Ncapd2	0.48453472	Jakmip1	0.388625783
Ankle1	0.484271549	Smc1a	0.384304762
Usf2	0.473966041	Hist2h2be	0.384204628
Gsg2	0.473489189	Chaf1a	0.38259078
Nrgn	0.463824	Uhrf1	0.382479722
Incenp	0.459699688	**Il7r**	0.381376349
Cd93	0.459614153	Mdm1	0.380641386
Mcm6	0.447452116	4930534B04Ri	0.379842162
Rrm1	0.444742607	Smc2	0.373648124
Hist3h2ba	0.43993365	Hist1h4i	0.373258143
Ilf3(NF90)	0.43970379	Mcm3	0.365646719
Ccne1	0.436776552	Dtymk	0.365045248
Nusap1	0.435589993	Perq1	0.364815612
Pold3	0.433065734	Rad51ap1	0.36318389
Rpo1-3	0.428234744	Cenpf	0.361677963
Sgol1	0.419677455	Dot1l	0.361246229
Neil3	0.416232235	Srm	0.36113474
Ccnb1	0.410713331	**Id3**	0.297235672

Table A.6. **Genes "less reduced" from large pre-B to small pre-B in miR290 knockout mice.** Top hits of genes with smaller decrease in abundance at the small pre-B stage in miR290 knockout mouse as compared to the wild-type mouse. Diff. is the log2 value of the ratio from wild-type to knockout mouse. Genes in bold are lymphocyte lineage genes.